The Properties Improvement of Rice Starch Films by Cooperated with Cellulose and Crystalline Cellulose from Palm Pressed Fiber

Phattaraporn Thongsane

A Thesis Submitted in Partial Fulfillment of the Requirements
for the Degree of Master of Science in Packaging Technology
Prince of Songkla University
2009

Thesis Title	The Properties Improvement of Rice Starch Films by Cooperated with Cellulose and Crystalline Cellulose from Palm Pressed Fiber
Author	Miss Phattaraporn Thongsane
Major Program	Packaging Technology

Major Advisor

…….....
(Dr. Thawien Bourtoom)

Co-Advisor

…….....
(Dr. Waranyou Sridach)

Examining Committee

……..Chairperson
(Dr. Piyarat Sirivongpaisal)

…….....
(Dr. Thanachan Mahawanich)

…….....
(Dr. Thawien Bourtoom)

…….....
(Dr. Waranyou Sridach)

The Graduate School, Prince of Songkla University, has approved this thesis as partial fulfillment of the requirements for the Degree of Master of Science in Packaging Technology.

..……..……
(Assoc. Prof. Dr. Krerkchai Thongnoo)
Dean of Graduate School

ชื่อวิทยานิพนธ์	การปรับปรุงสมบัติฟิล์มสตาร์ชข้าวเจ้าด้วยเซลลูโลสและคริสตัลไลน์เซลลูโลสจากเส้นใยปาล์ม
ผู้เขียน	นางสาวภัทรพร ทองเสน
สาขาวิชา	เทคโนโลยีบรรจุภัณฑ์
ปีการศึกษา	2551

บทคัดย่อ

จากการศึกษาผลของขนาด (125, 177, 250 และ 420 ไมโครเมตร) และปริมาณเส้นใยปาล์ม (ร้อยละ 10, 20, 30 และ 40) ต่อสมบัติของฟิล์มจากสตาร์ชข้าวเจ้า พบว่าเมื่อปริมาณเส้นใยเพิ่มขึ้นส่งผลให้ค่าความต้านทานแรงดึง (Tensile strength) ค่าการซึมผ่านไอน้ำ (Water vapor permeability, WVP) และสมบัติทางความร้อน (Thermal properties) มีแนวโน้มเพิ่มขึ้น ขณะที่ค่าการยืดตัวเมื่อขาด (Elongation at break) ค่าการดูดซับน้ำ (Water uptake) และค่าความใสลดลงในทุกขนาดของเส้นใยที่เติม เมื่อพิจารณาผลของขนาดเส้นใยต่อสมบัติของฟิล์มสตาร์ชข้าวเจ้า พบว่าเมื่อขนาดของเส้นใยใหญ่ขึ้นส่งผลให้ค่าความต้านทานแรงดึงและสมบัติทางความร้อนของฟิล์มสตาร์ชข้าวเจ้ามีแนวโน้มเพิ่มขึ้น ส่วนค่าการซึมผ่านไอน้ำมีแนวโน้มลดลง จากผลการทดลองดังกล่าวอาจกล่าวได้ว่าเส้นใยปาล์มสามารถใช้เป็นสารเสริมแรงและปรับปรุงสมบัติของฟิล์มสตาร์ชข้าวเจ้าได้ โดยการใช้เส้นใยปาล์มที่มีขนาด 420 ไมโครเมตร ในปริมาณร้อยละ 40 ของฟิล์มสตาร์ชข้าวเจ้าให้ฟิล์มดังกล่าวมีสมบัติดีที่สุด เมื่อพิจารณาการปรับปรุงพื้นผิวเส้นใยต่อสมบัติของฟิล์มสตาร์ชข้าวเจ้า โดยทำการปรับปรุงพื้นผิวเส้นใยด้วยวิธี Alkaline treatment (2% NaOH) และ Silane treatment (10-40% glysidoxypropyltrimethoxy silane) พบว่าฟิล์มสตาร์ชข้าวเจ้าที่เสริมแรงด้วยเส้นใยที่ผ่านการปรับปรุงผิวทั้ง 2 ชนิด มีสมบัติเชิงกลและสมบัติทางความร้อนสูงกว่าฟิล์มสตาร์ชข้าวเจ้าที่เสริมแรงด้วยเส้นใยที่ไม่ผ่านการปรับปรุงผิว เมื่อทำการเปรียบเทียบวิธีการปรับปรุงพื้นผิวเส้นใยต่อสมบัติของฟิล์มจากสตาร์ชข้าวเจ้า พบว่าฟิล์มสตาร์ชข้าวเจ้าที่เสริมแรงด้วยเส้นใยที่ผ่านการปรับปรุงผิวด้วยวิธี Alkaline treatment มีค่าความต้านทานแรงดึงสูงกว่าฟิล์มสตาร์ชข้าวเจ้าที่เสริมแรงด้วยเส้นใยที่ผ่านการปรับปรุงผิวด้วยวิธี Silane treatment ขณะที่ค่าการซึมผ่านไอน้ำ ค่าการดูดซับน้ำและสมบัติทางความร้อนต่ำกว่า นอกจากนี้พบว่าเมื่อความเข้มข้นของสาร Silane coupling agent ที่ใช้ในการปรับปรุงพื้นผิวเส้นใยและปริมาณเส้นใยเพิ่มขึ้นส่งผลให้ค่าความต้านทานแรงดึง ค่าการซึมผ่านไอน้ำ ค่าการดูดซับน้ำและสมบัติทางความร้อนเพิ่มขึ้น ส่วนค่าการยืดตัวเมื่อขาดลดลง ดังนั้นการใช้เส้นใยที่ทำการปรับปรุงพื้นผิวด้วยสาร Silane coupling agent ความเข้มข้นร้อยละ 40 เป็นสารเสริมแรง สามารถปรับปรุงสมบัติของฟิล์มสตาร์ชข้าวเจ้าได้ดีที่สุด

เมื่อทำการเตรียมคริสตัลไลน์เซลลูโลสจากเส้นใยปาล์มด้วยวิธี acid hydrolysis จะได้คริสตัลไลน์เซลลูโลสที่มีขนาด 90±0.051 นาโนเมตรและมีปริมาณผลึกร้อยละ 94.60 จากนั้นจึงทำการศึกษาผลของปริมาณคริสตัลไลน์เซลลูโลสต่อสมบัติของฟิล์มสตาร์ชข้าวเจ้า พบว่าเมื่อปริมาณคริสตัลไลน์เซลลูโลสเพิ่มขึ้น ส่งผลให้ค่าปริมาณผลึก ค่าความต้านทานแรงดึงและสมบัติทางความร้อนเพิ่มขึ้น ขณะที่ค่าการซึมผ่านไอน้ำ ค่าการดูดซับน้ำและค่าการยืดตัวเมื่อขาดมีแนวโน้มลดลง ทั้งนี้เนื่องจากคริสตัลไลน์เซลลูโลสมีลักษณะโครงสร้างที่เป็นผลึกสูงซึ่งมีความแข็งแรงและมีการจัดเรียงตัวของโมเลกุลอย่างเป็นระเบียบ อย่างไรก็ตามเมื่อปริมาณคริสตัลไลน์เซลลูโลสมากเกินไปส่งผลให้ฟิล์มสตาร์ชข้าวเจ้ามีค่าความต้านทานแรงดึงลดลง เนื่องจากเกิดการรวมกลุ่มกันเองของคริสตัลไลน์เซลลูโลส ซึ่งผลที่ได้สอดคล้องกับลักษณะการกระจายตัวของคริสตัลไลน์เซลลูโลสของฟิล์มสตาร์ชข้าวเจ้าเมื่อทำการศึกษาโดยใช้กล้องจุลทรรศน์อิเล็กตรอนชนิดส่องกราด สำหรับการศึกษาผลการดูดซับความชื้นที่อุณหภูมิคงที่ พบว่าที่ปริมาณความชื้นคงที่ (EMC) ฟิล์มสตาร์ชข้าวเจ้าที่ไม่มีการเสริมแรงด้วยเส้นใยปาล์มมีค่าการดูดซับความชื้นสูงที่สุด และเมื่อทำการเสริมแรงด้วยเส้นใยปาล์มส่งผลให้ฟิล์มสตาร์ชข้าวเจ้ามีการดูดซับความชื้นลดลง นอกจากนี้พบว่าที่ระดับความชื้นสัมพัทธ์สูงขึ้นส่งผลให้ฟิล์มสตาร์ชข้าวเจ้ามีค่าความต้านทานแรงดึงลดลง

Thesis Title	The Properties Improvement of Rice Starch Films by Cooperated with Cellulose and Crystalline Cellulose from Palm Pressed Fiber.
Author	Miss Phattaraporn Thongsane
Major Program	Packaging Technology
Academic Year	2008

ABSTRACT

The native rice starch (RS) (Thai Flower brand) films were prepared by casting on leveled trays. The mechanical properties and water vapor permeability as well as thermal properties of RS films reinforced with 125, 177, 250 and 420 µm at 10 20 30 and 40 wt. % of starch were investigated. The tensile strength (TS), water vapor permeability (WVP) and thermal properties of RS films increased with increasing palm pressed fibers (PPF) content whereas elongation at break (ε) and transparent decreased. Comparing with the same amount of PPF reinforced the RS films, the results demonstrated that addition of 420 µm of PPF showed better properties including mechanical and thermal properties as well as physical properties than 125, 177 and 250 µm. The RS films reinforced with different fiber surface treatments and content of treated PPF were investigated. Higher TS, WVP, water uptake and thermal properties of RS films were obtained as treated fiber was applied. Comparing between the alkaline treatment and silane treatment for the fiber on RS films properties, the TS of RS film reinforced with alkaline treated PPF showed higher than RS film reinforced with silane treated but lower in WVP, water uptake and thermal properties. Increasing concentration of silane coupling agents and content of treated PPF resulted in increased TS, WVP and water uptake but decreased ε. The thermal properties behavior of RS films reinforced with treated and untreated PPF were investigated by means of dynamic mechanical thermal analyzer (DMTA), differential scanning calorimeter (DSC) and thermo gravimetric analyzer (TGA). The glass transition temperature (T_g) shifted towards higher temperatures with increasing concentration of silane coupling agents, which can be restriction of the mobility of starch chain due to the establishment of strong interactions between RS and treated PPF. The maximum improvement in the mechanical and thermal properties obtained

for at 40% of glysidoxy propyltrimethoxy silane treated PPF/RS films. These results pointed out that the interfacial interactions improved the filler compatibility, mechanical and thermal properties.

Crystalline cellulose (CC) was prepared by acid hydrolysis and having an average length about 90 ± 0.051 nm, the crystallinity value was estimated as 94.60%. The TS, thermal properties and crystallinity value (X_c) of the RS films increased but decreased in ε, WVP and water uptake when increasing the CC fillers content. The morphology of the existence of CC in the rice starch film can be easily observed in the composite films. When more than 20% of CC was used, the larger agglomerates were observed. The EMC of the pure RS film showed the highest moisture content. When the fillers were added into the RS films, the moisture content at EMC was decreased. The TS of the RS films decreased as the relative humidity increased, by the reason of the starch is strongly sensitive to the moisture content.

CONTENTS

LIST OF TABLES

LIST OF FIGURES

LIST OF FIGURES (CONTINUED)

LIST OF FIGURES (CONTINUED)

CHAPTER 1

INTRODUCTION

The improper disposition of the enormous volume of petroleum-derived plastics in the environmental has led to environment pollution and raised much interest in edible and biodegradable films from nature polymers, the biodegradable and renewable resources (Lawton, 1996; Fishman *et al*., 2000). Usually biodegradable and edible films include lipids, proteins and carbohydrates such as cellulose, starch and there derivatives in their formulation (Rodriguez *et al.,* 2006). Starch is one of the most studied and promising raw materials for the production of biodegradable plastics, which is a natural renewable carbohydrate polymer obtained from a great variety of crops. Starch is a low cost material in comparison to most synthetic plastics and is readily available. Starch has been investigated widely for the potential manufacture of products such as water-soluble pouches for detergents and insecticides, flushable liners and bags, and medical delivery systems and devices (Fishman *et al.,* 2000).

Rice is the most widely consumed basic food in the world. Each year over 500 million tons of rice is harvested, providing sustenance to many countries and people throughout the world. The unique properties of rice starches are found in its many varieties (Bourtoom and Chinnan, 2008). Rice starch and its major components, amylose and amylopectin are biopolymers, which are attractive raw materials for used as barriers in packaging materials. They have been used to produce biodegradable films to partially or entirely replace plastic polymers because of its low cost and renewability, as well as possessing good mechanical properties (Xu *et al.,* 2005). However, compared to the common thermoplastics, biodegradable products based on starch (Lourdin *et al.,* 1995; Arvanitoyannis and Biliaderis, 1997; Garcia *et al.,* 1999; Mali and Grossmann, 2003), unfortunately, still reveal many disadvantages such as low mechanical properties and efficient barrier against low polarity compounds (Kester and Fennema, 1986). The disadvantages mainly attributed to the highly hydrophilic character of starch polymers (Santayanon and Wootthikanokkhan, 2003). To cope with these problems while preservering the biodegradability of the materials,

one approach is the use of fibers as reinforcement for starch (Ma *et al.,* 2008). Natural fiber-reinforced composites have many advantages such as light weight, reasonable strength and stiffness, renewable and biodegradable (Demir *et al.,* 2006; Kunanopparat *et al.,* 2008). Various types of fillers have been tested such as potato pulp based microfibrils (Dufresne and Vignon, 1998; Dufresne *et al.,* 2000), bleached leaf wood fibers (Funke *et al.,* 1998; Averous and Boquillon, 2004), bleached eucalyptus pulp fibers (Curvelo *et al.,* 2001), wood pulp (De Carvalho *et al.,* 2002), softwood aspen (Low *et al.,* 2007), Jute, Hemp and flax fibers (Wollerdorfer and Bader, 1998; Soykeabkaew *et al.,* 2004; Park *et al.,* 2006) tunicin whiskers (Angles and Dufresne, 2000; Angles and Dufresne, 2001) and oil palm fibers (Sreekala and Thomas, 2003).

Oil palm empty fruit bunches are obtained after the extraction of oil from the seeds. Many million tons of empty fruit bunches are produced annually throughout the world, as an industrial waste by the oil mills, and left unutilized. This creates a good habitat for insects and pests, thereby causing severe environmental problems. Therefore, the utilization of this fiber as reinforcement in plastics has economical as well as ecological importance (Rozman *et al.,* 1996; Agrawal *et al.,* 2000).

New natural fiber or wood-based composites are being developed that could benefit from a thorough and fundamental understanding of the fiber surface. These products may require new adhesive systems to reach their full commercial potential. A better understanding of natural or wood fiber surface and adhesive bonding is necessary. The natural fiber or wood surface is a complex heterogeneous polymer composed of cellulose, hemicellulose and lignin. The surface is influenced by polymer morphology, extractive chemicals and processing conditions (Bledzki and Gassan, 1999). Chemical treatment of cellulosic materials usually changes the physical and chemical structure of the fiber by reacting with the OH group of the cellulose. There are reports that chemically treated palm fibers are more stable and can withstand heat to a greater extent compared with untreated fibers (Sreekala and Thomas, 2003) during the course of thermal cycling. Moreover, advances development of biocomposites by micro or nano cellulose crystallites from natural fiber was interesting. It is known that native celluloses, when subjected to strong acid

hydrolysis, readily break down into “micro- or nano- crystalline cellulose” (whisker) with almost no weight loss (Battista, 1975). Due to it high aspect ratio and a high modulus (Ishikawa *et al.,* 1997), the use of cellulose crystallites for preparation of high performance composite materials has been, therefore, explored extensively (Dufresne *et al.,* 1997; Angles *et al.,* 2000; Eichhorn *et al.,* 2001; Noishiki *et al.,* 2002). When the cellulose crystallites were homogeneously dispersed into polymer matrices, they gave a remarkable reinforcing effect, even at concentrations of a few percent (Favier *et al.,* 1996). In previous work (Bourtoom and Chinnan, 2008) a rice starch edible film was developed. It has been observed that the functional properties e.g., the film ductility and the barrier properties of rice starch film are generally poor. The objective of this work was to investigate the properties of rice starch films reinforced with palm pressed fibre. The effects of fiber content and fiber size, fiber surface treatment and the crystalline cellulose content on physical, mechanical and thermal properties were investigated.

Review of Literature

1. Edible film

Edible films are defined as thin layer of material which can be eaten by the consumer and provide a barrier to moisture, oxygen and solute movement for the food. The material can complete food coating or can be disposed as a continuous layer between food components (Guilbert, 1986). Edible films can be formed as food coatings and free-standing films, and have potential to be used with food as gas aroma barrier (Kester and Fennema, 1986). However, the technical information is still needed to develop films for food application (Donhowe and Fennema, 1993). The edible films and coatings have received a consideration attention in the recent years because of their advantage over the synthetic films. The advantages of edible films over other traditional synthetic films are summarized below:

1. They can be consumed with the package products. This is obviously of critical importance since it represents the environmentally ideal package.

2. There is no package to dispose of even if the films are not consumed they could still contribute to the reduction of environmental pollution.

3. The films are produced exclusively from renewable, edible ingredients and therefore are anticipated to degrade more readily than polymeric materials.

4. The films can enhance the organoleptic properties of packaged foods provided that various components (flavorings, colorings, sweeteners)

5. The films can supplement the nutrition value of the foods. This is particular true for films made from proteins.

6. The films can be used for individual packaging of small portion of food, particularly products that currently are not individually packaged for practical reasons such as pears, beans, nuts and strawberries.

7. The films can be applied inside heterogeneous foods at the interfaces between different layers of components. They can be tailored to prevent deteriorative inter-component moisture and solute migration in foods such as pizzas, pies and candies.

8. The films can function as carriers for antimicrobial and antioxidant agents. In a similar application they also can be used at the surface of food to control the diffusion rate of preservative substances from the surface to the interior of the food.

9. The films can be very conveniently used for micro encapsulation of food flavoring and leavening agents to efficiently control their addition and release into the interior of foods.

10. Another possible application for edible films could be their use in multilayer food packaging materials together with non edible films. In this case, the edible films would be the internal layers in direct contact with food materials.

Production of edible films causes less waste and pollution, however, their permeability and mechanical properties are generally poorer than synthetic films (Kester and Fennema, 1986). Extensive research is needed on the development of new materials, methods of films formation, methods to improve film properties and the potential applications.

1.1 Classification of edible films

Edible films can be produced from materials with film forming ability. During manufacturing, film materials must be dispersed and dissolved in the solvent such as water, alcohol or mixture of water and alcohol or mixture other solvents. Plasticizer, antimicrobial agent, colors or flavor can be added in this process. Adjusting pH and/or heating the solutions may be done for the specific polymer to facilitate the dispersion. Film solution is then casted and dried at desired temperature and relative humidity to obtain free-standing films. In the food application, film solutions could be applied to food by several methods such as dipping, spraying, brushing and panning followed by a drying step. Kester and Fennema (1986) classified the edible films based on the nature of material as polysaccharide, protein, lipid and composite films.

1.1.1 Polysaccharides

Polysaccharides used for edible films or coatings include cellulose and derivatives starch and derivatives pectin, seaweed extracts, exudate gums, microbial fermentation gums, chitosan (Krochta and Mulder-Johnson, 1997). Polysaccharides are generally very hydrophilic resulting in poor water vapor and gas barrier properties. Although coating by polysaccharide polymers may not provide a good water vapor barrier, these coating can act as sacrificing agent retarding moisture loss from food products (Kester and Fennema, 1986).

1.1.1.1 Cellulose and derivatives

Cellulose is composed of repeating D-glucose units linked through ß-1, 4 glycosidic bonds. In its native state, the hydroxymethyl groups of anhydroglucose residues are alternatively located above and below the plan of the polymer backbone. This results in very tight packing of polymer chains and a highly crystalline structure that resists salvation in aqueous media. Water solubility can be increased by treating cellulose with alkali to swell the structure, followed by reaction with chloroacetic acid, methyl chloride or propylene oxide to yield carboxy methyl cellulose (CMC), methyl cellulose (MC), hydroxy propyl cellulose (HPMC) or hydroxyl propyl cellulose (HPC). Placement of bulky substituents along the cellulose molecule, in the form of ether linkages at reactive hydroxyls, separates the polymer chains and interferes with formation of the crystalline unit cell, thereby enhancing aqueous

solubility (Krumel and Lindsay, 1976). MC, HPMC, HPC and CMC film possess good film-forming characteristic; films are generally odorless and tasteless, flexible and are of moderate strength, transparent, resistance to oil and fats, water-soluble, moderate to moisture and oxygen transmission (Krochta and Mulder-Johnson, 1997). MC is the most resistant to water and it is the lowest hydrophilic cellulose derivatives (Kester and Fennema, 1986). However, the water vapor permeability of cellulose ether film is still relatively high. MC and HPMC have ability to form thermally induced gelatinous coating; they have been used to retard oil absorption in deep frying food product (Kester and Fennema, 1986; Balasubramanium *et al*., 1995). MC could be applied as coating on confectionery products as barrier to lipid migration (Nelson and Fennema, 1991). A number of groups have investigated composite films composed of MC or HPMC and various kinds of solids, such as beeswax and fatty acids (Kamper and Fennema, 1984; Greener and Fennema, 1989; Kester and Fennema, 1989; Koelsch and Labuza, 1992; Debeaufort *et al*., 1993; Park *et al*., 1994). Many of these have water vapor permeability as low as low density polyethylene (LDPE). These composite films were all polymer-lipid bilayer formed either in one step from aqueous ethanolic solutions of cellulose ether fatty acids.

Cellulose can also be chemically modified to ether, ethyl cellulose (EC), which is biodegradable but not edible. EC films can either be cast from non-aqueous solutions or extruded. Like the other cellulose ethers. EC films are poor moisture barrier, but they have been reported to be good oil and fat barriers (Hanlon, 1992).

1.1.1.2 Starch

Starch consists of amylose and amylopectin, the ratio of amylose and amylopectin depends on the type and variety of raw material. Amylose is a linear chain of D-glucose residues linked through α-1,4 glycosidic bonds. Amylopectin is a branched molecule consisting of glucose units connected by α-1,4 and α-1,6 linkages. High amylose starch as cornstarch is a good source for films formation; free-standing films can be produced from aqueous solution of gelatinized amylose and drying. Normal cornstarch consists of approximately 25% amylose and 75% amylopectin. Mutant varies of corn are produced which contain starch with up to 85% amylose. Wolf *et al*. (1951) produced self-supporting films by casting aqueous solutions of

gelatinized amylose, followed by solvent evaporation. The films were transparent and had very low permeability to oxygen at low RH (Rankin *et al*., 1958). Mark *et al*. (1966) reported that films produced from high amylose corn starch (71% amylose) had no detectable oxygen permeability at RH levels less than 100%. This was true for both unplasticized and plasticized (16% glycerol) films. This result is surprising in light of the fact that addition of plasticizers and absorption of water molecules by hydrophilic polymers increase polymer chain mobility and generally lead to increased gas permeability (Banker, 1966). Partial etherification of high-amylose starch with propylene oxide, to yield the hydroxypropylated derivative, improves water solubility. As expected, films produced from hydroxypropylated starch possess virtually no resistance to the passage of water vapor. However, as with the pure amylose films, resistance to oxygen transport is substantial (Jokay *et al*., 1967). Oxygen permeation through plasticized and unplasticized films was not detectable at 25^{o}C and RH up to 78% (Roth and Mehltretter, 1967). At the high RH, films became distorted due to the moisture absorption and were not tested for oxygen permeability. However, it is likely that oxygen transport increased greatly as the film became hydrated. Jokay *et al*. (1967) applied hydroxylpropylated starch films almond nutmeats, and organoleptic evaluation revealed that the film retarded development of oxidative rancidity during storage. Starch hydrolysates (dextrin) of low dextrose equivalent (DE) have been suggested for use as protective coatings. Although hydrophilic in nature, starch hydrolyses do provide a limited resistance to transport of water vapor. Allen *et al*. (1963) evaluated the relative barrier properties of edible film materials by coating them onto a cellulose acetate support. Starch films displayed minimal resistance to water transport, while films of low-DE dextrin and corn syrup were approximately 2- and 3-fold more resistant, respectively. Murray and Luft (1973) coated almond nutmeats with a 50% solution of a 10-DE starch hydrolysate. Sensory evaluation indicated that the coated nuts maintained a more desirable texture than uncoated controls during storage. Presumably, this was attributation to a reduction in the rate of moisture absorption by coated almonds. Films of starch hydrolysates may exhibit some resistance to oxygen transmission. Dipping of fresh sliced apples in a 40% solution of a 15-DE hydrolysate prior to dehydration prevented browning of the tissue, probably by retarding the entrance of oxygen (Murray and Luft, 1973).

1.1.2 Lipid Films

Lipid compounds utilized as protective coating consist of acetylated monoglycerides, nutural wax, and surfactants. The most effective lipid substances are paraffin wax and beeswax. The primarily function of lipid coating is to block transport of moisture due to their relative low polarity. In contrast, the hydrophobic characteristic of lipid forms thicker and more brittle films. Consequently, they must be associated with film forming agents such as proteins or cellulose derivatives (Park *et al*., 1994). Generally, water vapor permeability decrease when the concentration of hydrophobicity phase increases. Lipid-based films are often supported on a polymer structure matrix, usually a polysaccharide, to provide mechanical strength.

1.1.2.1 Waxes and Paraffin

Paraffin wax is derived from distillate fraction of crude petroleum and consists of mixture of solid hydrocarbon resulting from ethylene catalytic polymerization. Paraffin wax is permitted for use on raw fruit and vegetable and cheese. Carnauba wax is exudates from palm tree leaves (*Copoernica cerifera*). Beewax (white wax) is produced from honeybees. Candelilla is obtained from candelilla plant. Mineral oil consists of a mixture of liquid paraffin and naphtheric hydrocarbon (Hernandez, 1994). Waxes are used as barrier films to gas and moisture (skin on fresh fruits) and to improve the surface appearance of various foods (e.g., the sheen on sweet). Applied in a thick layer, they must be removed before consumption (certain cheese); when used in thin layers, they are considered edible. Waxes (notably paraffin, carnauba, candellila and beewax) are the most efficient edible compounds providing a humidity barrier.

1.1.2.2. Acetoglyceride

Acetylation of glycerol monosterate by its reaction with acetic anhydride yields 1-stearodiacetin. This acetylated monoglyceride displays the unique characteristic of solidifying from the molten state into a flexible, wax-like solid (Feuge *et al*., 1953). Most lipids in the solid state can be stretched to only about 102% of their original length before fracturing. Acetylated glycerol monostearate, however, can be stretch up to 800% of its original length (Jackson and Lutton, 1952), water vapor permeability of this film is much less than that of polysaccharide film with the exception of methyl cellulose or ethyl cellulose (Kester and Fennema, 1986).

Acetylated monoglyceride coating have been used on poultry and meat cuts to retard the moisture loss during storage (Kester and Fennema, 1986).

1.1.3 Protein Films

In their native states, proteins generally exist as either fibrous proteins, which are water insoluble and serve as the main structural materials of animal tissues, or globular proteins, which are soluble in water or aqueous solutions of acids bases or salts and function widely in living system (Morrison and Boyd, 1959). The fibrous proteins are fully extended and associated closely with each other in parallel structures, generally through hydrogen bonding, to form fibers. The globular proteins fold into complicated spherical structures held together by a combination of hydrogen, ionic, hydrophobic and covalent (disulfide) bonds (Bushuk and Wrigley, 1974). The chemical and physical properties of these proteins depend on the relative amounts of the component amino acid residues and their placement along the protein polymer chain. Of the fibrous proteins, collagen has received the most attention in the production of edible films. Several globular proteins, including wheat gluten, corn zein, soy protein, and whey protein, have been investigated for their film properties. Protein films are generally formed from solutions or dispersions of the protein as the solvent/carrier evaporates. The solvent/carrier is generally limited to water, ethanol or ethanol-water mixtures (Kester and Fennema, 1986). Generally, proteins must be denatured by heat, acid, base, and/or solvent in order to form the more extended structures that are required for film formation. Once extended, protein chains can associate through hydrogen, ionic, hydrophobic and covalent bonding. The chain-to-chain interaction that produces a cohesive films are affected by the degree of chain extension and the nature and sequence of amino acid residues. Uniform distribution of polar, hydrophobic, and/or thiol groups along the polymer chain increases the likelihood of the respective interactions. Increased polymer chain-to-chain interaction results in films that are stronger but less flexible and less permeable to gases, vapors and liquids (Kester and Fennema, 1986). Polymers containing groups that can associate through hydrogen or ionic bonding result in films that are excellent oxygen barrier but that are susceptible to moisture (Salame, 1986). Thus, protein films are expected to be good oxygen barriers at low relative humidities. Polymers containing a preponderance of hydrophobic groups are poor oxygen barriers but excellent moisture

barriers. The more hydrophobic, water-insoluble proteins. However, the fact that they are not totally hydrophobic and contain predominantly hydrophillic amino acid residues limits their moisture-barrier properties. Creation of protein-versed edible films with low water vapor permeability requires addition of lipid components. This is analogous to the situation with synthetic polymers where moisture- sensitive oxygen-barrier polymers must be either co-polymerized with a hydrophobic polymer or sandwiched between hydrophobic polymer layers to limit the ability of water to reduce barrier properties. Various types of protein have been used as edible films. These include collagen, casein, whey protein, corn zein, wheat gluten, soy protein, mung bean protein, and peanut protein (Gennadois *et al*., 1993; Bourtoom and Chinnan, 2008).

Several approaches can be used to form edible films (Kester and Fennema, 1986) as follows:

1. Simple coacervation: A single hydrocolloids is driven from aqueous suspension or caused to undergo a phase change by evaporation of solvent, addition of a water-miscible nonelectrolyte in which the hydrocolloids is not soluble (e.g., alcohol), addition of an electrolyte to cause salting out or crosslinking, or alteration of pH.

2. Complex coacervation: Two solutions of oppositely charged hydrocolloids are combined, causing interaction and precipitation of the polymer complex.

3. Thermal gelation or precipitation: A sol-gel transformation can occur by heating of a protein to cause denaturation followed by gelation (e.g., egg albumin) or precipitation, or simple cooling of a warm hydrocolloid suspension.

2. Starch

In nature starch is available in an abundance surpassed only by cellulose as naturally occurring organic compound. It is found in all forms of green leafed plants, located in their roots, stems, seeds or fruits. Starch serves the plant as food for energy during dormancy and germination. It serves similar purposes for man and animal as well as lower forms of life. Man, however, has found uses for starch that extend far beyond its original design as a source of biological energy. Practically

every industry in existence uses starch or its derivatives in one form or another. In foods and pharmaceuticals starch is used to influence or control such characteristics as texture, aesthetics, moisture, consistency and shelf stability. It can be used to bind or to disintegrate; to expand or to density; to clarify or to opacity; to attract moisture or to inhibit moisture; to produce short texture or stringy texture, smooth texture or pulpy texture, soft coatings or crisp coatings. It can be used to stabilize emulsions or to form oil resistant films. Starch can be used to aid processing, packaging, lubrication or moisture equilibration.

2.1 Starch molecule

The glucose polymers that make up starch come in two molecular forms, linear and branched. The former is referred to as amylose and the latter as amylopectin. The basic glucose building block is a ring-shaped molecular with six atoms in the ring, see Figure 1. Although for simplicity often drawn as a flat structure, the ring is, in fact, mobile and can take many shapes through “puckering”. Of these many shapes or conformations one- known as the chair form- is favoured. Moreover, the chair form comes in two varieties (stereoisomers): α-D-glucose and β-D-glucose. The two are interconvertible using heat and one is transformed into the other by a series of twists around the six-membered ring which cause the groups to “wag” sequentially in a molecular-scale “Mexican wave” around the “arena” of the glucose ring. It is the α-D-glucose that is used in natural to form the starch polymers. Once polymerized into starch, α-D-glucose is locked into this chair form. When the ring atoms are numbered as in Figure 1, it is clear that the links (glucosidic links) between carbons 1 and 4 of neighbouring units give rise to amylose, while occasional branches from this linear chain between carbons 1 and 6 give rise to the larger, more highly branched amylopectin.

In fact, the “linear” amylose has a small degree of branching but it is predominantly regarded as a single chain. The chain length can very with the botanical origin of the starch but will be of the order of 500 to 6000 glucose units. Because of its more simple polymeric structure, amylose has a greater propensity to deposit in a regular manner forming crystals. In nature, three crystalline forms of amylose, A, B and C exist, depending upon the source: cereals (A), tuber (B) and

certain pea and bean varieties (C). Precipitated starch complexes (with iodine, long-chain alcohols and fatty acids) are found in the V form. The so-called linearity of the amylose of further complicated by a twisting of the polymer into a helix. It is different degrees of hydration of the helix that gives rise to the A, B and C forms.

In contrast to amylose, each branched chain of amylopectin contains only up to 30 glucose units. However, the multitude of branching in amylopectin gives it a molecular weight that is 1000 times that of amylose. Indeed, amylopectin is a titan of a molecule from nature: one of the largest with a molecular weight of 400 million. The ratio of amylose and amylopectin in any native starch is dependent not only on its source, Table 1, but also on selective crop breeding, a process known as hybridization.

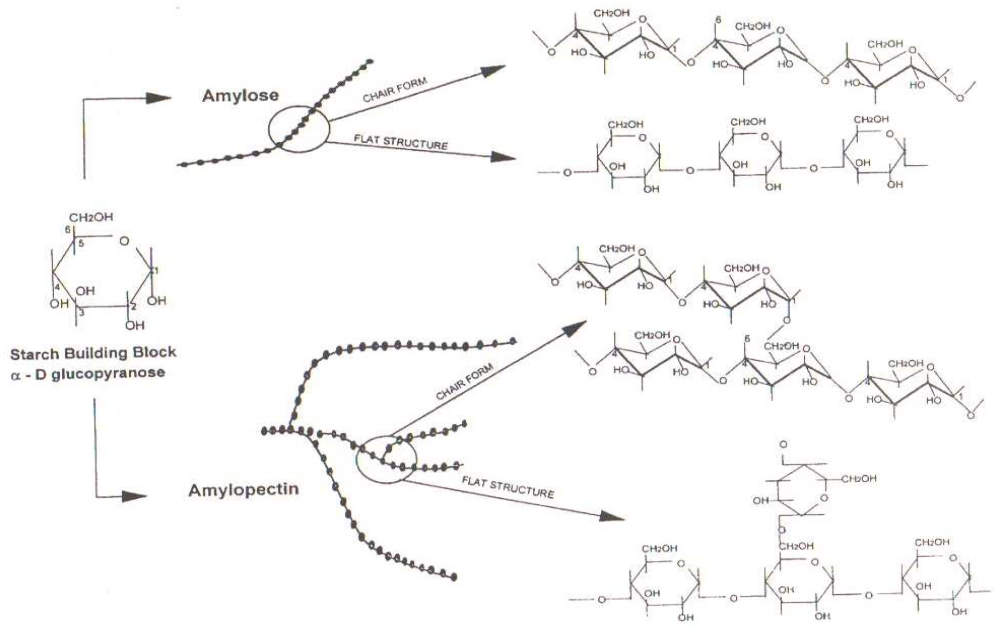

Figure 1. Linear and branched starch polymers.

Source : Murphy (1999)

Table 1. Starch granule characteristic.

Starch	Diameter (μm)	Gelatinization temp. °C	Pasting temp. °C	Amylose content
Maize	5-30	62-72	80	25
Waxy Maize	5-30	63-72	74	<1
Tapioca	4-35	62-73	17	17
Potato	5-1000	59-68	64	20
Wheat	1-45	58-64	77	25
Rice	3-8	68-78	81	19
Sago	15-65	69-74	74	26

Source : Murphy (1999)

2.2 Hydrogen bonding

Hydroxyl groups are the very same groups that make up water- the usual medium for starch in the food industry. There is consequently a strong interaction (hydration) and affinity, through hydrogen bonding, between the colossal starch and the diminutive water molecules. Hydration, when brought about by cooking, produces an irreversible change in the structure of the starch granule whereby the starch-starch interactions are “unzipped” and replaced by starch-water interactions. This forces the chains apart and the granule swells. Eventually the granule ruptures and starch polymers are dispersed in solution producing a viscous colloidal state. This is a form of water management that controls structure. “Gelatinization” and “pasting” are, respectively, the technical descriptions of the hydration within the granule and the irreversible granule swelling that builds viscosity.

Dispersal of the simpler and more linear form of starch, amylose, allows for greater mobility which can result in the molecules self-assembling into a more ordered structure. Aligning themselves parallel to each other, the hydrogen bonding that previously may have involved water, can be reduced and replaced by hydrogen bonding between the aligned chains.

3. Lignocellulosic fibers / natural fibers

Natural fibers are subdivided based on their origins, coming from plants, animals or minerals. All plant fibers are composed of cellulose while animals fibers consist of proteins (hair, silk and wool). Plant fibers include bast (or stem or soft sclerenchyma) fibers, leaf or hard fibers, seed, fruit, wood, cereal straw and other grass fibers. Over the last few years, a number of researchers have been involved in investigating the exploitation of natural fibers as load bearing constituents in composite materials. The use of such materials in composites has increased due to their relative cheapness, their ability to recycle and for the fact that they can compete well in terms of strength per weight of material. Natural fibers can be considered as naturally occurring composites consisting mainly of cellulose fibrils embedded in lignin matrix. The cellulose fibrils are aligned along the length of the fiber, which render maximum tensile and flexural strengths, in addition to providing rigidity. The reinforcing efficiency of natural fiber is related to the nature of cellulose and its crystallinity. In recent years, prices for natural fibers have not been stable, especially for flax fibers. Flax fibers show the highest values of strength, but they are about 30% more expensive than glass-fibers. Further the price depends on the extent of fiber preparation and pretreatment, e.g. size-finishing including a coupling agent and other surfactants, which are well-established for glass-fibers. For such applications, natural fibers have to be pretreated in similar way. In most cases, the substitution of glass-fibers by natural fibers is precluded first of all by economic reasons. But, natural fibers offer several advantages over glass-fibers:

- Plant fibers are a renewable raw material and their availability is more or less unlimited.
- When natural reinforced plastics were subjected, at the end of their life cycle, to a combustion process or landfill, the released amount of CO_2 of the fibers is neutral with respect to the assimilated amount during there growth.
- The abrasive nature of natural fibers is much lower compared to that of glass-fibers, which leads to advantages with regard to

technical, material recycling or process of composite materials in general.

- Natural fiber reinforced plastics by using biodegradable polymers as matrix are the most environmental friendly materials which can be composted at the end of their life cycle. Unfortunately, the overall physical properties of those composites are far away from glass-fiber reinforced thermoplastics. Further, a balance between life performance and biodegradable has to be developed.

3.1 Mechanical properties of natural fibers

Natural fiber are in general suitable to reinforce materials due to their relative high strength and stiffness and low density. Natural fibers can be processed in different ways to yield reinforcing elements having different mechanical properties. The elements and their elastic modulus are shown in Figure 2. The elastic modulus of bulk natural fibers such as wood is about 10 GPa. Cellulose fiber with modulus up to 40 GPa can be separated from wood, for instance, by chemical pulping processes. Such fibers can be further subdivided by hydrolysis followed by mechanical disintegration into microfibrils with an elastic modulus of 70 GPa. Theoretical calculations of the elastic modulus of cellulose chains have given values of up to 250 GPa, however, there is no technology available to separate these from microfibrils.

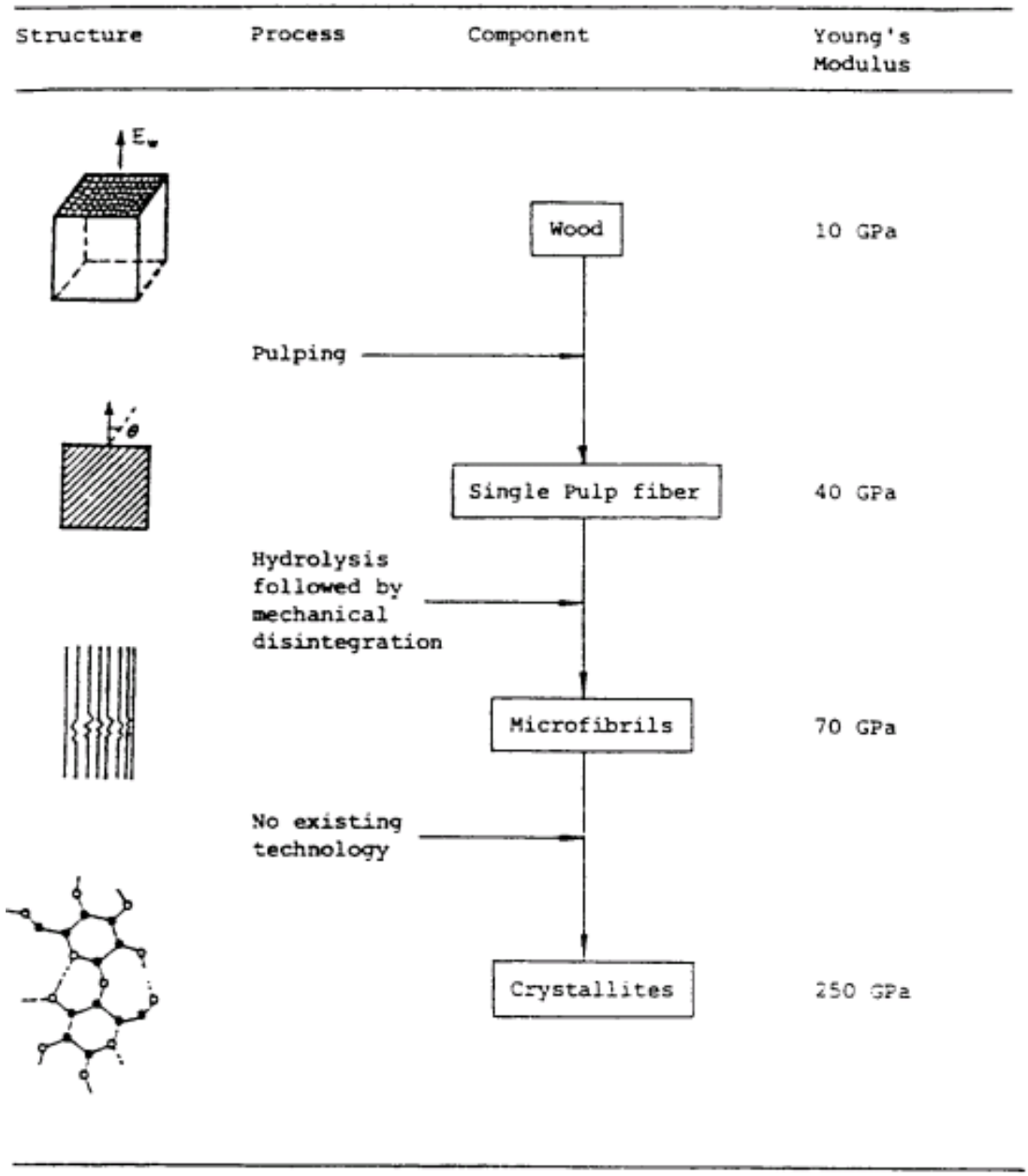

Figure 2. Correlation between structure, who to process, resulting component and modulus.

Source : Michell (1989).

3.2 Natural fibers and their chemical compositions

Climatic conditions, age and the digestion process influences not only the structure of fibers but also the chemical composition. The main components of natural fibers are cellulose (α-cellulose), hemicellulose, lignin, pectins and waxes. These components with regard to the physical properties of the fibers.

3.2.1 Cellulose

Cellulose is a natural polymer consisting of D-anhydroglucose ($C_6H_{11}O_5$) repeating units jointed by 1,4-β-D-glycosidic linkages at C_1 and C_4 position (Nevell and Zeronian, 1985). The degree of polymerization (DP) is around 10,000. Each repeating unit contains three hydroxyl groups. These hydroxyl groups and their ability to hydrogen bond play a major role in directing the crystalline packing and also govern the physical properties of cellulose. Solid cellulose forms a microcrystalline structure with regions of high order i.e. crystalline regions and regions of low order i.e. amorphous regions. Cellulose is also formed of slender rod like crystalline microfibrils. The crystal nature (monoclinic sphenodic) of naturally occurring cellulose is known as cellulose I. Cellulose is resistant to strong alkali (17.5 wt%) but easily hydrolyzed by acid to water-soluble sugars. Cellulose is relatively resistant to oxidizing agents.

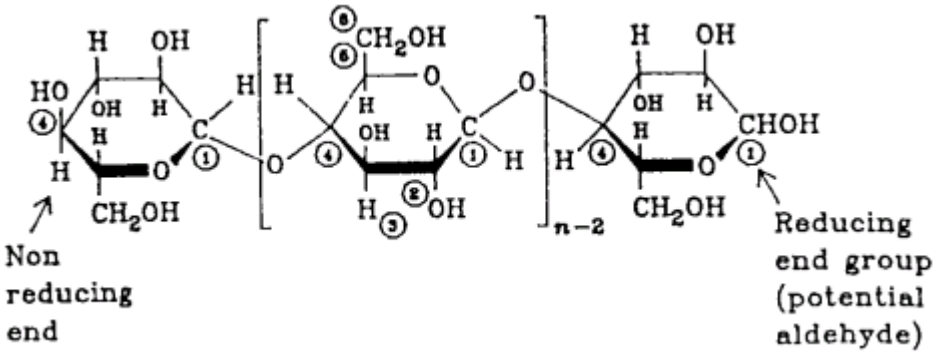

Figure 3. Chemical structure of cellulose
Source : Nevell and Zeronian (1985).

3.2.2 Hemicellulose

Hemicellulose is not a form of cellulose and the name is a misnomer. They comprise a group of polysaccharides composed of a combination of 5- and 6-carbon ring sugars. Hemicellulose differs from cellulose in three aspects. Firtsly, they contain several different sugar units whereas cellulose contains only 1,4-β-D-glucopyranose units. Secondary, they exhibit a considerable degree of chain branching containing pendant side groups giving rise to its non crystalline nature,

whereas cellulose is linear polymer. Thirdly, the degree of polymerization (DP) of native cellulose is 10-100 times higher than that of hemicellulose. The DP of hemicellulose is around 50-300. Hemicellulose form the supportive matrix for cellulose microfibrils. Hemicellulose is very hydrophilic, soluble in alkali and easily hydrolyzed in acids.

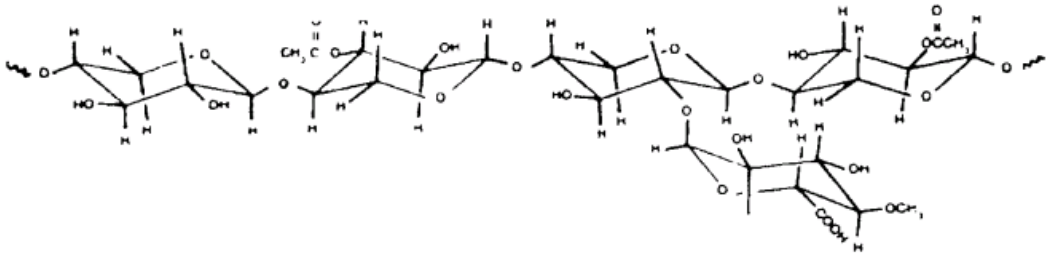

Figure 4. Chemical structure of hemicellulose
Source : Nevell and Zeronian (1985).

3.2.3 Lignin

Lignin is a complex hydrocarbon polymer with both aliphatic and aromatic constituents. They are totally insoluble in most solvents and cannot be broken down to monomeric units. Lignin is totally amorphous and hydrophobic in nature. It is the compound that gives rigidity to the plants. It is thought to be a complex, three-dimensional copolymer of aliphatic and aromatic constituents with very high molecular weight. Hydroxyl, ethoxyl and carbonyl groups have been identified. Lignin has been found to contain five hydroxyl and five methoxyl groups per building unit. It is believed that the structural units of lignin molecule are derivatives of 4-hydroxy-3-methoxy phenylpropane. The main difficulty in lignin chemistry is that no method has been established by which it is isolate lignin in its native state from the fiber. Lignin is considered to be a thermoplastic polymer exhibiting glass transition temperature of around 90°C and temperature of around 170°C (Olesen and Plackett, 1999). It is not hydrolyzed by acids, but soluble in hot alkali, readily oxidized and easily condensable with phenol (Bismarck *et al.*, 2005).

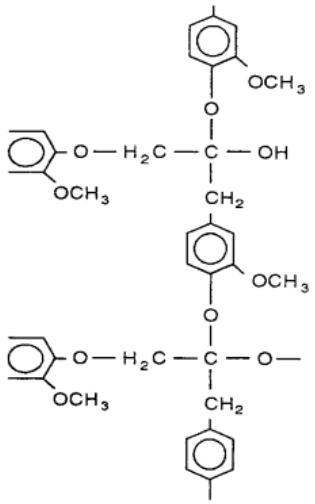

Figure 5. Chemical structure of lignin.
Source : Nevell and Zeronian (1985).

3.2.4 Pectin and wax

Pectins are a collective name for heteropolysaccharides. They give plants flexibility. Waxes make up the last part of fibers and they consist of different types of alcohols.

Biofibers can be considered to be composites of hollow cellulose fibrils held together by a lignin and hemicellulose matrix (Jayaraman, 2003). The cell wall in a fiber is not a homogenous membrane (Figure 6). Each fibril has a complex, layered structure consisting of a thin primary wall that is the first layer deposited during cell growth encircling a secondary wall. The secondary wall is made up of three layers and the thick middle layer determines the mechanical properties of the fiber. The middle layer consists of a series of helically wound cellular microfibrils formed from long chain cellulose molecules. The angle between the fiber axis and the microfibrils is call the microfibrillar angle. The characteristic value for this parameter varies from one fiber to another.

Such microfibrils have typically a diameter of about 10-30 nm and are made up of 30-100 cellulose molecules in extended chain conformation and provide mechanical strength to the fiber. The amorphous matrix phase (Figure 7) in a cell wall is very complex and consists of hemicellulose, lignin and in some cases pectin. The hemicellulose molecules are hydrogen bonded to cellulose and act as cementing

matrix between the cellulose microfibrils, froming the cellulose-hemicellulose network, which is thought to be the main structural component of the fiber cell. The hydrophobic lignin network affects the properties of other network in a way that it acts as a coupling agent and increases the stiffness of the cellulose/hemicellulose composite.

The structure, microfibrillar angle, cell dimensions, defects and the chemical composition of fibers are the most important variables that determine the overall properties of the fibers (Satyanarayana *et al.*, 1986). Generally, tensile strength and Young's modulus of fibers increases with increasing cellulose content. The microfibrillar angle determines the stiffness of the fibers. Plant fibers are more ductile if the microfibrils have a spiral orientation to the fiber axis. If the microfibrils are oriented parallel to the fiber axis, the fibers will be rigid, inflexible and have high tensile strength.

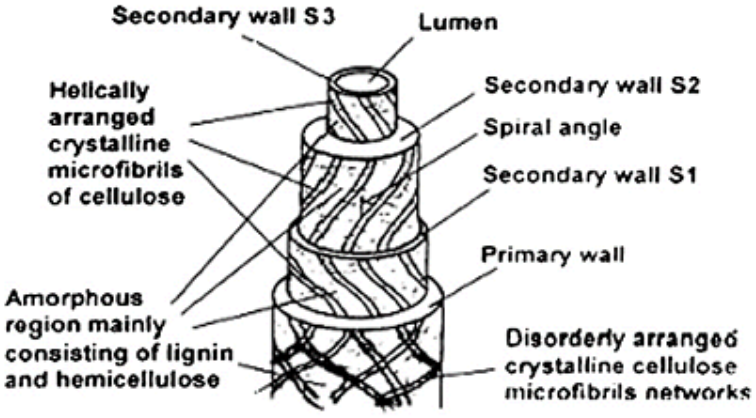

Figure 6. Structure of biofiber.
Source : John and Thomas (2008)

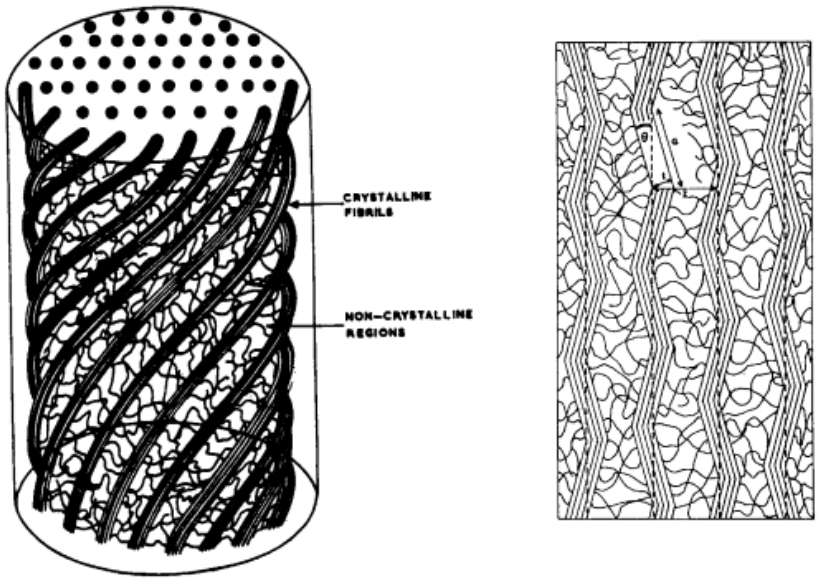

Figure 7. Crystalline and amorphous structure of the fiber
Source : Satyanarayana *et al.* (1986)

3.3 Methods for surface modification of natural fibers

The quality of the fiber-matrix interface is significant for the application of natural fibers as reinforcement fiber for polymer. Physical and chemical methods can be used to optimize this interface. These modification methods are of different efficiency for the adhesion between matrix and fiber (Bladzki and Gassan, 1999).

3.3.1 Physical methods

Reinforcing fibers can be modified by physical and chemical methods. Physical methods, such as stretching, calendaring, thermotreatment and the production of hybrid yarns do not change the chemical composition of the fibers. Physical treatments change structure and surface properties of the fiber and thereby influence the mechanical bondings to polymers.

Electric discharge (corona, cold plasma) is another way of physical treatment. Corona treatment is one of the most interesting techniques for surface oxidation activation. This process changes the surface energy of the cellulose fibers and in case of wood surface activation increases the amount of aldehyde groups.

The same effects are reached by cold plasma treatment. Depending on type and nature of the used gasses, a variety of surface modification could be achieved. Surface crosslinkings could be introduced, surface energy could be increased or decreased, reactive free radicals and groups could be produced.

Electric discharge methods are known to be very effective for “non-active” polymer substrates as polystyrene, polyethylene, polypropylene, etc.

3.3.2 Chemical methods

Strongly polarized cellulose fibers are inherently incompatible with hydrophobic polymers. When two materials are incompatible, it is often possible to bring about compatibility by introducing a third material, that has properties intermediate between those of the other two. There are several mechanisms of coupling in materials:

- Weak boundary layers - coupling agents eliminate weak boundary layers,
- Deformable layers – coupling agents produce a tough, flexible layer,
- Restrained layers – coupling agents develop a highly crosslinked interphase region, with a modulus intermediate between that of substrate and of the polymer,
- Chemical bonding – coupling agents form covalent bonds with both materials, and
- Acid – base effect – coupling agents alter acidity of substrate surface.

The development of a definitive theory for the mechanism of bonding by coupling agents in composites is a complex problem. The main chemical bonding theory alone is not sufficient. So the consideration of other concepts appears to be necessary, which include the morphology of the interphase, the acid – base reactions at the interface, surface energy and the wetting phenomena.

3.3.2.1 Organosilanes as coupling agents

Organosilanes are the main group of coupling agents. They have been developed to couple virtually any polymer to the minerals, which are used in reinforced composites. Most of the silane coupling agents can be represented by the following formula:

$$R - (CH_2)_n - Si(OR')_3$$

Where n = 0-3, OR' is the coupling agent causes the reaction with the polymer. This could be a co-polymerization, and/or the formation of an interpenetrating network. The curing reaction of a silane treated substrate enhances the wetting by the resin.

The general mechanism of how alkoxysilanes form bonds with the fiber surface which contains hydroxyl group is as follows:

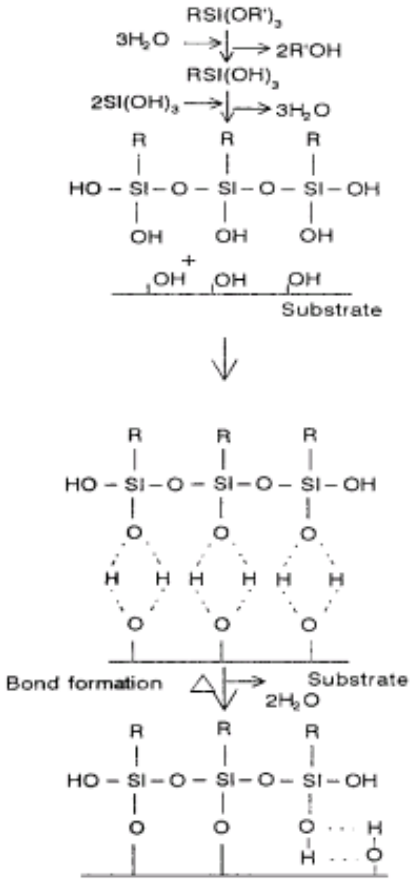

Figure 8. Reaction of silane coupling agents

Source : Bledzki and Gassan (1999)

Alkoxysilanes undergo hydrolysis, condensation (Catalysts for alkoxysilane hydrolysis are usually catalysts for condensation.) and the bond formation stage, under base as well as under acid catalyzed mechanisms. In addition to this reactions of silanols with hydroxyls of the fiber surface, the formation of polysiloxane structures can take place.

Analogous to glass-fibers, silanes are used as coupling agents for natural-fiber-polymer composites. For example, Lee and Wang (2006) investigated the effects of lysine-based diisocyanate (LDI) as a coupling agent on the properties of biocomposites from poly(lactic acid) (PLA), poly(butylene succinate) (PBS) and bamboo fiber (BF). They observed that the tensile properties, water resistance, and interfacial adhesion of both PLA/BF and PBS/BF composites were improved by the addition of LDI, but thermal flow (Ohkita and Lee, 2006) was hindered due to cross-linking between polymer matrix and BF.

Researchers have also developed green composites from jute fabric and Biopol composites (Mohanty *et al.,* 2000). Chemical modification of the fabric was carried out to improve interfacial properties. A significant amount of research has been done at the German Aerospace Centre (DLR) in Braunschweg on biodegradable plastics and composites (Plackett *et al.,* 2003).

Herrera-Franco and Valadez-Gonzalez (2005) investigated the properties of short natural-fiber reinforced composites as a function of chemical modification. Short natural fibers were subjected to alkali treatment (NaOH) and silane treatment (vinyltris or 2-methoxy-ethoxy silane). The authors observed that the increase in the mechanical properties ranged between 3 and 30%, for the tensile and flexural properties. The shear strength of this composite, such increase was of the order of 25%. From the micrographs, obtained from failure surfaces from the SEM, it was observed that with increasing fiber-matrix interaction the failure mode changed from interfacial failure to matrix failure. The interface failure was mainly a frictional type failure, and only for the pre-impregnated and silane treated fibers, matrix tearing and shearing was observed. The silane surface treated fibers also showed a layer of polymer covering the fibers even after failure.

Shih (2006) has also developed epoxy composites from waste water bamboo husk fiber. The fibers were chemically modified by coupling agents and untreated fibers were added to epoxy resin to form novel reinforced composites. The results shows that the morphology analysis reveals that the fibers modified by coupling agent exhibited better compatibility with the polymer matrices than the untreated fiber did. In addition, the mechanical properties were also enhanced due to the addition of coupling agent treated fibers and untreated fibers. The increment of storage modulus of epoxy were about 16.4 and 36.1% with the addition of 10% coupling agent treated fibers and untreated fibers, respectively.

As a continuation to above study the mechanical, morphological and water sorption properties of polypropylene-luffa fiber composites. Three different types of coupling agents, 3-aminopropyl-triethoxysilane (AS), 3-trimethoxysilyl-1-propanethiol (MS) and maleic anhydride grafted polypropylene (MAPP) were used. Tensile strength and Young's modulus increased with employment of the coupling agents accompanied by a decrease in water absorption with treatment due to the better adhesion between the fiber and the matrix. The maximum improvement in the mechanical properties was obtained for the MS treated luffa composites. The interfacial interactions improved the filler compatibility, mechanical properties, and water resistance of composites. Morphological studied demonstrated that better adhesion between the fiber and the matrix was achieved especially for the MS and AS treated luffa composites. Atomic force microscope (AFM) studies also showed that the surface roughness of luffa composites decreased with the employment of silane-coupling agents (Demir *et al.,* 2006).

Pothan and Thomas (2003) have also explored the dynamic mechanical behaviour of chemically modified banana fiber reinforced polyester composites. The results of the dynamic mechanical analysis that the storage modulus value was found to be the highest for the silane (2-methoxy-ethoxy silane) treated fibers composites.

3.3.2.2 Alkaline treatment

The effects of mercerization on the suitability to mechanical treatment, notable tensile strength, of cotton fibers have been extensively studied. The standard definition of mercerization proposed by ASTM D 1965 is a process of subjecting a vegetable fiber to an interaction with a fairly concentrated aqueous solution of a

strong base, to produce great swelling with resultant changes in the fine structure, dimension, morphology and mechanical properties.

Cellulose forms the main structural component of vegetable natural fiber, the non-cellulosic components, e.g. lignin and hemicellulose, also play an important part in the characteristic properties of the fiber. Hemicellulose, which is thought to consist principally of xylan, polyuronide and hexosan, has shown to be very sensitive to the action of caustic soda, which exerts only a slight effect on lignin or a-cellulose. Later studies about the alkali treatment of jute-fiber, for instance, reports about the removal of lignin and hemicellulose which affects the tensile characteristics of the fiber (Bledzki and Gassan, 1999). When the hemicelluloses are removed, the interfibrillar region is likely to be less dense and less rigid and thereby makes the fibrils more capable of rearranging themselves along the direction of tensile deformation. When natural fibers are stretched, such rearrangements amongst the fibrils would result in better load sharing by them and hence result in higher stress development in the fiber. In contrast, softening of the inter-fibrillar matrix adversely affects the stress transfer between the fibril and, thereby, the overall stress development in the fiber under tensile deformation. As lignin is removed gradually, the middle lamella joining the ultimate cells is expected to be more plastic as well as homogeneous due to the gradual elimination of microvoids, while the ultimate cells themselves are affected only slightly.

Further, some authors reported about changes in the crystallinity through alkaline treatment on flax fibers (Bledzki and Gassan, 1999). The increase in the percentage crystallinity index of alkali treated fiber occurs because of the removal on the cementing materials, which leads to a better packing of cellulose chains. Additionally, treatment with NaOH leads to a decrease in the spiral angle, i.e. closer to fiber axis, and increase in molecular orientation. A fair amount of randomness is introduced in the orientation of the crystallites due to the removal of non-cellulosic matter. The elastic modulus of fibers, for instance, are expected to increase with increasing degree of molecular orientation. Well oriented cellulosic fibers such as flax have much higher Young’s modulus than fibers with medium orientation, such as cotton. In addition to the modification of orientation and the consolidation of weak points, other important factors with regard to the mechanical properties could be the

crystallite length and degree of crystallinity as well as the removal of fractions of cellulose at a very low degree of polymerization (Sharma *et al.*, 1995 cited by Bledzki and Gassan, 1999). Tests made by Prasad *et al.* (1983 cited by Bledzki and Gassan, 1999) on leather fibers, and by Chand *et al.* (1986 cited by Bledzki and Gassan, 1999) on sisal fibers showed distinct index changes achieved by an alkalization process in an 8% NaOH solution. An increase of 25% in tensile strength was reached in leather fibers and of 100% in sisal fibers, also depending on the respective soaking time. Additional to the increase of the mechanical properties through alkalization, an increase of composite quality are to be expected of laminates due to the improved fiber–matrix adheshion. In the fiber extraction (pull-out test), the cohesion of polyester resin alkalized coconut-and sisal fibers were characterized by Prasad *et al.* (1983 cited by Bledzki and Gassan, 1999) and by Chand *et al.* (1986 cited by Bledzki and Gassan, 1999). The pull-out load of alkalized sisal fibers went from 10 to 15.5 N, and the adhesion increased correspondingly up to an alkalizing time of 90 h. After that, the pull out load as well as the adhesion decreased distinctly.

3.4 Crystalline cellulose

Crystalline cellulose is obtained by hydrolysis of the amorphous portion of cellulose until a level-off degree of polymerization (LODP) product is obtained. Crystalline cellulose comprises of highly crystalline regions of cellulose. Crystalline cellulose is useful for a number of different applications. Pieces of crystalline cellulose easily bond together without the use of an adhesive. Furthermore, crystalline cellulose can be mixed with other substances so as to hold an additive while bonding to itself. It can be made into pharmaceutical-grade tablets, such as vitamins, pain relievers and other medicines. It also may be used as a substitute for starch where starch is used as a smoothener, such as in suntan lotion. It is known that native celluloses, when subjected to strong acid hydrolysis, readily break down into “micro- or nano- crystalline cellulose” (whisker) with almost no weight loss (Battista, 1975; Ebeling *et al.*, 1999). Due to it high aspect ratio and a high modulus (Ishikawa *et al.*, 1997), the use of cellulose crystallites for preparation of high performance composite materials has been, therefore, explored extensively (Dufresne *et al.*, 1997; Angles *et al.*, 2000; Eichhorn *et al.*, 2001; Noishiki *et al.*, 2002). When the cellulose

crystallites were homogeneously dispersed into polymer matrices, they gave a remarkable reinforcing effect, even at concentrations of a few percent (Favier *et al.*, 1996).

The hydrolysis of cellulose to obtain crystalline cellulose can be accomplished using mineral acid, enzymes or microorganisms. Although methods are desirable because glucose, a useful by-product, in created, these methods are more expensive and create crystalline cellulose products having a lower crystallinity. Thus, acid hydrolysis is the conventional method of choice for manufacturing crystalline cellulose. Acid that can be used in this process include hydrochloric acid, sulfuric acid and phosphoric acid. At higher temperatures, sulfuric acid and phosphoric acid can peptize and surface modified crystalline cellulose. However, such crystalline cellulose is difficult to purify and does not have the same visual and functional properties as underutilized cellulose produced with hydrochloric acid.

Lu *et al.* (2006) investigated the morphological and mechanical properties of ramie crystallites (RN) reinforced plasticized starch (PS) biocomposites. The ramie cellulose nanocrystallites, having lengths of 538.5 ± 125.3 nm and diameters of 85.4 ± 25.3 nm on average, were prepared from ramie fibers by acid hydrolysis. The results indicate that the synergistic interactions between fillers and between filler and matrix play a key role in reinforcing the composites. The PS/RN composites, composites, conditioned at 50% relative humidity, increases, respectively, in tensile strength and Young's modulus from 2.8 MPa for PS film to 6.9 MPa and from 56 MPa for PS film to 480 MPa with increasing RN content from 0 to 40 wt%. Further, incorporating RN fillers into PS matrix also leads to a decrease in water sensitivity for the PS based biocomposites.

Alemdar and Sain (2007) studied the morphology, thermal and mechanical properties of wheat straw nanofibers reinforced starch biocomposites. The nanocomposites from the wheat straw nanofibers and the thermoplastic starch were prepared by the solution casting method. They founded that the tensile strength and modulus of the nanocomposite films revealed significantly enhanced properties compared to the pure thermoplastic starch. The glass transition of the nanocomposites was shifted to higher temperatures with respect to the pure thermoplastic starch.

Ma *et al.* (2008) investigated the morphological, thermal, mechanical properties and water vapor permeability (WVP) of thermoplastic pea starch (TPS) reinforced with microcrystalline cellulose (MC). Scanning electron microscope (SEM) showed that there was good adhesion between starch and MC, but these superfluous cellulose resulted in the conglomeration in TPS matrix. MC increased the thermal stability. DMTA revealed that the addition of MC enhanced the storage modulus and the glass transition temperature of the composites. Increasing MC contents resulted the tensile strength of the composites were increased and WVP of the composites were decreased.

Effect of orientation of nano sized reinforcements on properties is reported (Kvien and Oksman, 2007) in a solution cast cellulose whiskers reinforced polyvinyl alcohol (PVA) nano composite. With the application of a magnetic field of 7 Tesla to orient the whiskers while the water was evaporated after the casting of the composite, higher dynamic modulus of about 2GPa was observed in the direction of orientation over that in the transverse direction of the composite. Similarly, significant increases in Young`s modulus (674.5 times) and tensile strength (3.5 times) by increasing reinforcement content from 0 to 30wt. % are reported (Xiaodong *et al.*, 2007) recently in a nanocomposite of nanocrystals of flax cellulose reinforcement in water borne polyurethane. Observed increases are attributed to the uniform distribution of nanocrystals and improved morphology showing separation of soft and hard segments of matrix. More studies on this topic may be worth pursuing considering the advantages nanocomposites would offer in general. It is worth mentioning here that the concept of nanocomposites for load bearing applications being new, challenges will be high for the commercialization of nanostructured reinforcements such as cellulose microfibrils due to their disintegration while extracting them from plant cell walls and in also in polymer matrices, while high cost involved in the former (John and Thomas, 2008).

4. Palm pressed fiber

Oil palm press fiber, or mesocarp fiber, is the fiber obtained after expressing oil from the fruit mesocarp. On average, for every tone of fresh fruit bunches (FFB) processed, 200 kg empty fruit bunches (EFB), 670 kg palm oil mill effluent, 120 kg mesocarp fiber, 70 kg shell and 30 kg palm kernel cake are produced. In 1993, an estimated 4.74 million tones of FFB and 1.68 million tones of EFB were produced (Gurmit, 1994). Oil palm press fiber contains, on a dry weight basis, approximately 40% cellulose, 21% lignin, 24% pentosan and 5% ash. Cellulose, a polymer of β-D-1,4-linked anhydrous glucose units $(C_6H_{11}O_5)_n$, constitutes 40% - 60% of the cell walls of woody plants. Basically, the individual cellulose molecules are linked together to form elementary microfibrils, which, in turn are aggregated by intermolecular hydrogen bonding into larger subunits called fibrils. The microfibrils contain alternating phases of highly ordered (crystalline) and randomly oriented (amorphous) cellulose embedded in a matrix of hemicellulose. This latter carbohydrate (also known as pentosan), constituting 20%-50% of the plant dry weight, is a branched polymer of pentose sugars, $(C_5H_{10}O_4)_n$. The cellulosic and hemicellulose fractions are encrusted in an amorphous layer of lignin. Lignin, which constitutes 15%-25% of the plant material, is a complex three-dimensional polymer formed by carbon-carbon or ether bonding between phenyl-propane units (Aziz *et al.*,2002).

Figure 9. Illustrative pictures of palm pressed fibers

5. Biocomposites

Since biocomposites are considered “marginal” structural materials, the addition of lignocellulosic fibers to improve their chemical, physical and mechanical properties, including their durability, is seen as necessary. Even with the limited experience so far, they are expected to be useful for a wide range of applications in mass-produced consumer products for short-time uses (e.g. packaging), as well as for long-term indoor applications (e.g. furniture), leading to an exciting and promising future for these new generations of composites (Mohanty *et al.*, 2002). One of the major hurdles for commercialization of lignocellulosic fiber composites till recently is reported to be non-recognition of research and development carried out by the researchers in developing countries where these fibers are available in plenty. This has been overcome with many of the industrialized countries particularly in Europe taking the lead in this area in recent years. But these materials also pose challenges to material scientists particularly with the acceptance criteria for these composites being their performance and cost, despite the renewability and recyclability of the matrix and the reinforcements used. Accordingly, some of the critical issues/developments required and the hurdles to be overcome are mentioned below:

5.1 Raw materials

5.1.1 Reinforcement

1. One of the prominent barriers for the large scale manufacture lignocellulosic based composites has been their widely dispersed resources and variable properties. Possibility of producing quality fibers suitable for different applications through better cultivation including use of genetic engineering and treatment methods to get uniform properties is one such step. Another important aspect is the quality assurance for these fibers and development of optimized fibers for specific sectors such as automotive sector (Mohanty *et al.*, 2002), availability of fibers with minimum range of variation in their properties will continue to be the real challenge.

2. Selection of cost effective and suitable fiber for particular applications is another critical area to be considered. This may call for looking into other less used but potential fibers such as curaua or development of other reinforcement sources as recently reported (Panthpulakkal and Sain, 2007; Beakou *et al.*, 2008).

3. Since synergism of properties is observed in biodegradable polymer-lignocellulosic fiber composite, development of component-dependent and non-dependent blending system is another area of development while blending the fibers.

4. Development of appropriate reinforcement form is essential particularly to fabricate hybrid biocomposites by using lignocellulosic fibers either in the fiber form or in other forms, with a view to manipulate the biodegradable composite properties particularly to obtain optimum balance in mechanical properties. In the latter case, the hurdle will be to determine the type of fibers for use as warp and weft using textile engineering concepts, considering the dependence of use of appropriate fiber on their properties. Of course, this can be overcome by the use of an interesting concept of “engineered natural fibers” where in proper blend of bast and leaf fibers are reported to provide proper balance of stiffness-toughness in the composites (Mohanty, 2002). Also, for balanced bi-directional properties, the ratio of warp to weft should be determined based on the type of fibers used. For example, in jute-cotton fabric, 60/40 warp/weft gives better properties, while 70/30 of the same is better in unidirectional composites (Joseph and Carvalho, 2000).

5.1.2 Matrix

1. Consistent properties of biodegradable composites along with affordable cost, their stability during storage and shipment and recyclability are of primary concern for their large scale use in many application sectors. These call for future critical areas of developments of suitable inexpensive biopolymers (mostly thermoplastics since lower priced synthetic plastics constitute about 70% of thermoplastics consumed by the plastics industry) to use lower processing temperature to avoid degradation and / or volatile emissions, which may affect the final properties of composite. This should also take care of cost, which should not far outweigh the use the inexpensive fibers.

2. Similarly, processing and design of new polymers with much improved mechanical properties and thermal stability than those reported so far and appropriate barrier properties and heat resistance characteristics will be another area for future development. Non-improvement of these properties will be greater hurdles for the applications of their composites such as packaging and structural components. Probably, this may call for new pathways for producing natural polymers even using nanotechnology to make biodegradable plastics by matrix hybridization or blending with suitable natural polymers.

5.2 Interface between the reinforcement and matrix

1. As in the case of synthetic polymers based composites, possibility of loading of very high filler/reinforcement (may be above 60 wt. %) should be achieved possibly to reduce the final cost of the product. This requires development of improved compounding technology and new coupling agents as critical areas of future research. This can have a tremendous impact in lowering the usage of petroleum-based plastics as well beneficial effects in terms of the environment and also in socio-economic sectors.

2. Of course, some of the limitations for the use of lignocellulosic fibers in composites such as low processing temperatures($<170^{o}C$) and moisture absorption have to be seriously looked into, while developing end use applications of these composites particularly in the automotive, building, appliance and other applications, which have in fact, dramatically increased in recent times (Satyanarayana *et al.*, 2007)

3. Since it is difficult to completely eliminate moisture absorption of the lignocellulosic fibers, it is necessary to develop suitable low cost coating or encapsulation methods to minimize the moisture absorption by the fibers, which normally results in swelling of the fibers, leading to the dimensional stability of lignocellulosic fiber composites. One of methods suggested is the use of acetylation of some of the hydroxyl groups present (Beldzki and Gassan, 1999; Mohanty *et al.*, 2001; Mohanty *et al.*, 2002) in the fiber, which may increase the cost of the fiber, though may provide good matrix-matrix bonding. This can also decrease the rate and amount of water absorbed by the composite.

4. In addition to reducing the moisture absorption by the fibers, some times tensile properties also show increase by the surface modification of fibers. Even mechanical loading during chemical modification of fibers has been found to improve the tensile properties significantly due to the structure changes (change in microfibrillar angle) occurred by the loading (Milewski, 1992). This could be another area for future development to increase the strength properties of biodegradable composites keeping in mind the composition and structure of lignocellulosic fibers.

5. It is well known fiber related parameters such as their dispersion and length as well as their orientation along with their adhesion with the matrix determine properties of their composite particularly with short fibers. Including these, there are various reasons for the lower properties of composites compared to the potential of the reinforcing agents (Goda *et al.,* 2006). In the case of lignocellulosic fiber–biopolymer composites though some of these such as adhesion between the fibers and matrix and dispersion of fibers can be overcome due to both of them being hydrophilic and breakage being the least for cellulose fibers, clumping (mostly with long fibers leading to either fiber-rich or the matrix-rich regions) and agglomeration of fibers may still have to be overcome. To minimize these or to get improved fiber dispersion without agglomeration, development and/or selection of suitable surface modifiers or dispersion aids/coupling agents for the fibers is another critical area for future development.

5.3 Processing

1. Limitation of low processing temperatures suggests importance of appropriate processing technique as another critical area of development. It is well known that high processing temperatures that reduce melt viscosity and facilitates good mixing cannot be used (except for short periods) and hence other routes are needed to facilitate mixing of the fibers and matrix to produce these composites.

2. Further, to achieve good efficiency of composite by appropriate stress transfer from the matrix to the fiber along with retaining the maximum length of fiber, improvement of interaction and adhesion between the fiber and matrix should be maximized (Bigg *et al.,* 1988). It is also known that the stress transfer efficiency of the composite is dependent on the properties of the interphase zone, which includes

the physical or chemical interactions between two different interfaces. Hence, good efficiency of composite is another critical area to be addressed to make acceptable biodegradable composites for many applications. Selection of a suitable processing technique to take care of these parameters including matrix attrition (breaking down of the long chain polymers to shorter chain lengths) thus becomes relevant despite availability of several types of batch and continuous compounding equipment for blending of fibers and matrices. This underlines that the properties of lignocellulosic fiber based composites particularly with thermoplastics is process dependent. For example, it has been reported that the level of fiber attrition depended on the screw configuration and the processing temperature during the blending of wood fibers with high density polyethylene (HDPE) in a twin-screw extruder (Yam *et al.,* 1990).

5.4 Design and Performance

1. Development of appropriate design of composite, which is dictated by the application, with a high degree of variability, should be looked into. Similarly, there is need for product standards to back up product performance.

2. Despite conceptual development, exploring manufacturing, short term experimental and analysis of characterization of innovative designs incorporating lab-scale concepts and some long term performance and durability under indoor and outdoor environments is another critical area of development for increased application of these special composites.

3. More studies are required on product development and performance evaluation, including the effect of environmental aging on the relationship between the damage caused in the thermo-mechanical-chemical processes of biodegradable composites, including their hybrids.

4. Development of degradation models for natural fibers similar to those developed for glass fibers is another critical area for future.

5. Understanding the aging of these composites exposed to different environments such as hygrothermal ageing and loading as well as prediction of effects on the lifetimes of these composites through modeling as recently done for glass fibers are other areas of interest for development to enhance possibility of their utilization in structural applications.

6. Despite increasing interest in research and development of lignocellulosic fiber based composites as seen from increasing publications, greater challenge lies in making them structurally and functionally stable during storage and use but easily degradable on disposal, which still remain as major hurdles. This calls for paradigm shift in design such as ‘tricorner approach’ in designing such high performance biodegradable composites. This approach involves some crucial steps as mentioned earlier such as efficient and cost effective modification of both the reinforcements and the matrix materials through proper functionalizing and blending followed by efficient processing technique for a variety of product development.

5.5 Others

1. Many obstacles in terms of low strength, production costs, product quality and supplier-user relations may have to be looked into with a view to increase their use and hence their market. It is also worthwhile to point out that till such time that development of high strength in these composites is achieved they may be used for non-critical, but large volume applications where moderate strength is desirable.

2. Continuous research and development in biodegradable composites in terms of various aspects mentioned above should be carried out as has been done in the case of non-biodegradable composites, whose performance is improved along with increasing their demand and utilization resulting in their low cost and hence enlarging the market (Mohanty, 2000).

3. In the case of use of nanoscience in biodegradable composites, it may make the products cheaper through more efficient production, with the added advantages of producing less waste and use of less energy. But, one has to be careful while using nano-filler materials, particularly if their products are used in food packaging, since it involves legal and ethical aspects in view of their effect on human health and the environment. Hence, regulations for their use are needed (Satyanarayana *et al.*, 2008).

Objectives

1. To prepare fibers and crystalline cellulose from palm pressed fibers.
2. To analyze the characteristics of fibers and crystalline cellulose from palm pressed fibers.
3. To study the effect of size and content of palm pressed fiber on the properties of rice starch films.
4. To study the effect of fiber surface treatment of palm pressed fiber on the properties of rice starch films.
5. To study the effect of content of crystalline cellulose from palm pressed fiber on the properties of rice starch films.

CHAPTER 2

MATERIAL AND METHODS

1. Materials

1.1 Raw materials

Native rice starch (Thai Flower brand) used was obtained from Bangkok Starch Industrial Co. Ltd. and contained a moisture content of about 14% (determined in triplicate by vacuum drying at 70 ^{o}C and < 1 mmHg pressure for 24 h, EYELA^{TM}, Model VOS-300VD, Japan) and peak viscosity (8% sample solid) of 500 BU (Brabender unit, Model VISKOGRAPH, Germany). Palm pressed fiber was obtained from local community in Songkhla province. Commercial grade sorbitol was obtained from Vidyasom Co. Ltd. (Thailand).

1.2 Chemical reagents

The coupling agents (glysidoxypropyl trimethoxy silane) were supplied by Sigma-Aldrich Chemie, Damstadt, Germany. Analytical grade (AR) magnesium chloride, magnesium nitrate, sodium chloride, potassium nitrate and sodium sulfate for saturated salt solutions (at 33% RH, 50% RH, 75% RH, 90% RH and 98% RH, respectively), nitric acid 10%, sodium hypochlorite 10%, sulfuric acid 64%, sodium hydroxide 2%, acetone and acetic acid were purchased from High Science Co. Ltd. (Thailand).

2. Instruments

Instruments	Model	Company/City/Country
Magnetic stirrer	RO 10 power	IKA LABORTECHNIK, Stanfen, Germany
stirrer	RW 20n	IKA LABORTECHNIK, Stanfen, Germany
Homogenizer	T 25	Ultra Turrax, Malaysia
Water bath	W 350	Memmert, Schwabach, Germany
Blender	MX-T700GN	National, Japan
Scanning electron microscope	JSM-5800 LV	JEOL, Tokyo, Japan
Universal testing machine	LR 30K	Lloyd Instruments Ltd, Hampshire, UK
Spectrophotometer	UV-1601	Shimadzu, Kyoto, Japan
Differential scanning calorimeters	Perkin-Elmer DSC-7	Norwalk, Conn., U. S.
Thermogravimetric analyzer	Perkin-Elmer TGA-7	USA
Dynamic mechanical thermal analyzer	DMTA-V	Rheometric Scientific, US
FTIR spectrometer	Equinox 55	Bruker, Japan
Laser particle size analyzer	LS-230	Coulter, U.S.
X-ray diffractometer	X'Pert MPD	Philips, Netherland
Hunter associates laboratory	Inc., VA.	USA

3. Preparation of palm pressed fiber (PPF)

Palm pressed fiber (PPF) were washed with water for carried out of oil and dirts, dried at 70 ^{o}C in an oven for 12 h. PPF were prepared by acid treatment (10% HNO_3) on dry base of palm pressed fiber at 90 ℃ for 1 h, and bleaching the produced pulp using the sodium hypochlorite bleaching method (Browning, 1967). Bleached palm pressed fiber was then size reduction and screened at 40 (420 μm), 60 (250 μm), 80 (177 μm) and 120 mesh (125 μm).

4. Effect of size and content of palm pressed fiber (PPF) on properties of rice starch films

4.1 Film preparation

Starch solution with concentration of 3% (w/v) was prepared by dispersing rice starch in distilled water and heating the mixtures with stirring until it gelatinized (85 ℃ for 5 min), and then cooling to 45± 2 ℃. The solution was filtered through a polyester screen (mesh no.140 with mesh opening of 106 μm) by vacuum aspiration to remove any small lumps in the solution. Sorbitol was added 50% of starch solution. Subsequently, the PPF (at 125, 177, 250 and 420 μm) dispersion was added at 10, 20, 30 and 40% of sorbitol and stirred for 20 min. After mixing, the mixer was degassed under vacuum then casting onto flat, leveled non-stick tray to set. Once set, the tray were held at 55 ℃ for 10 h undisturbed, and then cooled to ambient temperature before peeling the films off the trays. All treatments were made in triplicate. The resulted films were tested as followed;

- Tensile strength and elongation at break by ASTM D882-91 (ASTM, 1995)
- Water vapor permeability (McHugh *et al*.,1993)
- Water uptake (Sreekala and Thomas, 2003)
- Film colour by CIELAB system
- Film transparency
- Degradation Temperature, Td by Thermogravimetric Analysis (TGA)*

- Glass Transition Temperature, Tg of films by Differential Scanning Calorimetry (DSC)*
- Dynamic Mechanical Thermal Analysis (DMTA)*
- Morphological properties*

* Remark, selected samples

5. Effect of fiber surface treatment of palm pressed fiber (PPF) on properties of rice starch films

5.1 Fiber surface treatment

5.1.1 Alkaline treatment (application by Herrera-Franco and Valadez-Gonzalez, 2005)

After received the suitable size of PPF from item 4, the PPF were treated with a NaOH aqueous solution (2% w/v) for 1 h at room temperature, then, they were washed with distilled water until all the sodium hydroxide was eliminated, that is, until the water no longer indicated any alkalinity reaction. Subsequently, the PPF were dried at 70 ^{o}C for 24 h.

5.1.2 Silane treatment (application by Shih, 2006)

After received the suitable size of PPF from item 4, surface treatments of dried fibers were carried out in the acetone solution of silane. Fibers (5 g) and silane (0.5 g) were put in flask with the proper volume of acetone. After agitation for half and hour, the flask was sealed with a parafin film and kept for 12 h at room temperature. Then the samples were first washed with acetone to remove compound, and dried at 70 ^{o}C in an oven to constant weight.

5.2 Film preparation

Starch solution with concentration of 3% (w/v) was prepared by dispersing rice starch in distilled water and heating the mixtures with stirring until it gelatinized (85 ℃ for 5 min), and then cooling to 45± 2 ℃. The solution was filtered through a polyester screen (mesh no.140 with mesh opening of 106 μm) by vacuum aspiration to remove any small lumps in the solution. Sorbitol was added 50% of starch solution. Subsequently, both of the treated PPF dispersion was added at 10, 20, 30 and 40% of sorbitol and stirred for 20 min. After mixing, the mixer was degassed

under vacuum cast onto flat, leveled non-stick tray to set. Once set, the tray were held at 55℃ for 10 h undisturbed, and then cooled to ambient temperature before peeling the films off the trays. All treatments were made in triplicate. The resulted films were tested as followed;

- Fourier Transform Infrared Spectrometer (FTIR) of the untreated PPF and silane treated PPF
- Tensile strength and elongation at break by ASTM D882-91 (ASTM, 1995)
- Water vapor permeability (McHugh *et al*, 1993)
- Water uptake (Sreekala and Thomas, 2003)
- Film colour by CIELAB system
- Film transparency
- Degradation Temperature, T_d by Thermogravimetric Analysis (TGA)*
- Glass Transition Temperature, T_g of films by Differential Scanning Calorimetry (DSC)*
- Dynamic Mechanical Thermal Analysis (DMTA)*
- Morphological properties*

* Remark, selected samples

6. Effect of content of crystalline cellulose (CC) on properties of rice starch films

6.1 Preparation of crystalline cellulose (CC) (application by Lu and Cao, 2005)

The suspensions of crystalline cellulose were prepared by acid-catalyzed hydrolysis of palm pressed fiber similar to the method as described by Lu and Cao (2005). Briefly, the bleached palm pressed fiber (20 g) was mixed with sulfuric acid (175 ml, 64%) and stirred vigorously at 45 ℃ for 4 h, and then a dispersion of CC was obtained. After sonication of 15 min, the suspension was neutralized with 0.5 N NaOH.

6.2 Film preparation

Starch solution with concentration of 3% (w/v) was prepared by dispersing rice starch in distilled water and heating the mixtures with stirring until it gelatinized (85 ℃ for 5 min), and then cooling to 45± 2 ℃. The solution was filtered through a polyester screen (mesh no.140 with mesh opening of 106 μm) by vacuum aspiration to remove any small lumps in the solution. Sorbitol was added 50% of starch solution. Subsequently, the CC dispersion was added at 10, 20, 30 and 40% of sorbitol and stirred for 20 min. After mixing, the mixer was degassed under vacuum cast onto flat, leveled non-stick tray to set. Once set, the tray were held at 55 ℃ for 10 h undisturbed, and then cooled to ambient temperature before peeling the films off the trays. All treatments were made in triplicate. The resulted films were tested as followed;

- X-Ray Diffraction
- Tensile strength and elongation at break by ASTM D882-91 (ASTM, 1995)
- Water vapor permeability (McHugh *et al*., 1993)
- Water uptake (Sreekala and Thomas, 2003)
- Film colour by CIELAB system
- Film transparency
- Degradation Temperature, Td by Thermogravimetric Analysis (TGA)*
- Glass Transition Temperature, T_g of films by Differential Scanning Calorimetry (DSC)*
- Dynamic Mechanical Thermal Analysis (DMTA)*
- Morphological properties*

* Remark, selected samples

7. Effect of moisture sorption on properties of rice starch film

Water sorption isotherms were determined by placing rice starch films into a controlled humidity environment at a constant temperature until equilibrium. After drying at 75 ℃ and < 1 mmHg pressure for 24 h (EYELA^{TM}, Model VOS-300VD, Japan), the films were placed into environments of various relative

humidities above salt solutions and constant temperature at 27±2°C in desiccators. The relative humidities were 33% RH (magnesium chloride), 50% RH (magnesium nitrate), 75% RH (sodium chloride) and 90% RH (potassium nitrate). The sorption experiments were carried out by keeping approximately 1,000 mg of films (2 cm x 2 cm for weighing and 2.54 cm x 12 cm for Tensile Strength) in desiccators, removing at frequent intervals and weighing until they reach constant weight (within ± 5%), after that, the films were tested by tensile strength and water activity (a_w).

8. Determination of RS films properties

8.1 Conditioning

All films were conditioned prior to subjecting them to permeability and mechanical tests according to the Standard method, D618-61 (ASTM, 1993a). Films used for testing water vapor permeability (WVP), tensile strength (TS), and elongation at break (ε) were conditioned at 50% RH and 27±2^{o}C by placing them in desiccators over a saturated solution of $Mg(NO_3)_2$ for 72 h or more. For other tests, film samples were transferred to plastic bags after peeling and placed in desiccators.

8.2 Film thickness

The thickness of the films was measured with a precision digital micrometer (Digimatic Indicator, Mitutoyo Corporation, Japan) to the nearest 0.0001 mm (±5%) at five random locations on the film. Mean thickness values for each sample were calculated and used in water vapor permeability (WVP) and tensile strength (TS) calculations.

8.3 Water vapor permeability (WVP)

The gravimetric modified cup method based on ASTM E96-92 (McHugh, 1993) was used to determine the WVP of films. The test cups were filled with 20 g of Silica gel (desiccant) to produce a 0% RH below the film. A sample was placed in between the cup and the ring cover of each cup coated with silicone sealant (high vacuum grease, Lithelin, Hannau, Germany) and held with four screws around the cup's circumference. The air gap was at approximately 1.5 cm between the films surface and desiccant. The water vapor transmission rate (WVTR) of each film was

measured at 60±2% RH and 25±2^{o}C. After taking the initial weight of the test cup, it was placed into a growth chamber with an air velocity rate of 125 m/min (Model KBF115, Contherm Scientific, Lower Hutt, New Zealand). Weight gain measurements were taken by weighing the test cup to the nearest 0.0001 g with an electronic scale (Sartorious Corp.) every 3 h for 18 h. A plot of weight gained versus time was used to determine the WVTR. The slope of the linear portion of this plot represented the steady state amount of water vapor diffusing through the film per unit time (g/h). The WVTR was expressed in grams per square meter per day. Steady state over time (slope) yielded a regression coefficient of 0.99 or greater. Six samples per treatment were tested. The WVP of film was calculated by multiplying the steady WVTR by the film thickness and dividing that by the water vapor pressure difference across the films.

8.4 Mechanical properties

Tensile strength (TS) was measured with a LLOYD Instrument (Model LR30K, LLOYD Instruments Ltd., Hampshire, England) as per ASTM D882-91 Standard Method (ASTM, 1993b). Ten samples, 2.54 cm x 12 cm, were cut from each films. Initial grip separation and crosshead speed were set at 50 mm and 50 mm/min, respectively. Tensile strength was calculated by dividing the maximum force by the initial specimen cross-sectional area, and the percent elongation at break (ε) was calculated as follows:

$$\varepsilon = 100 \times (d_{after} - d_{before})/d_{before}$$

Where, d was the distance between grips holding the specimen before or after the break of the specimen.

8.5 Color

A CIE colorimeter (Hunter Associates Laboratory, Inc., VA, USA) was used to determine the film L*, a*, and b* color value [(L* = 0 (black) to 100 (white); a* = -60 (green) to +60 (red); and b* = -60 (blue) to +60 (yellow)]. The standard plate (calibration plate CX0384, L*= 92.82, a*= -1.24, and b*= 0.5) was used as a standard. Color (means of five measurements at different locations on each

specimen) was measured on 10 cm x 10 cm segment of film. Total color difference (ΔE^*_{ab}), hue angle (H), and chroma (C) were calculated using the following equation:

$\Delta L^* = L^*_{sample} - L^*_{standard}$, $\Delta a^* = a^*_{sample} - a^*_{standard}$, $\Delta b^* = b^*_{sample} - b^*_{standard}$

$\Delta E_{ab}^* = [(\Delta L^*)^2 + (\Delta a^*)^2 + (\Delta b^*)^2]^{0.5}$

$C = [(a^*)^2 + (b^*)^2]^{0.5}$

$H = \tan^{-1} (b^*/a^*)$ when $a^* > 0$ and $b^* > 0$

$H = 180^o + \tan^{-1} (b^*/a^*)$ when $a^* < 0$

$H = 360^o + \tan^{-1} (b^*/a^*)$ when $a^* > 0$ and $b^* < 0$

Prior to taking color measurements, film specimens were pre-conditioned at 60% RH and 27±2°C for 72 h.

8.6 Transparency

The transparency of films was determined using a UV-1601 spectrophotometer (Shimadzu, Kyoto, Japan). The film samples were cut into rectangles and placed on the internal side of the spectrophotometer cell. The transmittance of films was determined at 600 nm as described by Han and Floros (1997). The transparency of the films was calculated as follows:

$$\text{Transparency} = -\log (T_{600}/x)$$

Where T_{600} is the transmittance at 600 nm and x is the film thickness (mm).

8.7 Water Uptake

The kinetics of water absorption was determined for all the films. The dimension of specimens were 2 x 2 cm. The films were therefore supposed to be thin enough so that the molecular diffusion was considered to be one-dimensional. Sample were first dried overnight at 100°C. After weighing, they were condition at room temperature in desiccator containing sodium sulfate to ensure a RH ratio of 98%. The conditioning of samples in high moisture atmosphere was preferred to the classical technique of immersion in water because starch is very sensitive to liquid water and can partially dissolve after long time exposure to water. The samples were removed at

specific intervals and weighed using a four-digit balance. The water content or water uptake of the samples was calculated as follows:

$$\% \text{ Water uptake} = \frac{M_t - M_0}{M_0} \times 100$$

Where M_t is mass of sample at time t; M_0 the mass of sample at t=0.

8.8 Differential scanning calorimetry (DSC)

Thermal properties of native RS and RS films were analyzed with a Perkin-Elmer DSC-7 (Norwalk, Conn., U.S.A.) equipped with an intra-coolant Thermal Analysis Controller TAC7/DX (Perkin-Elmer). Samples (approx. 20 mg each, db) were weighed into stainless steel pans (Perkin-Elmer) designed to withstand high pressures. The stainless steel pan was sealed with an O-ring, and allowed to reach equilibrium of moisture for overnight. An empty DSC pan was used for a reference pan. The heating rate was programmed by holding at -50°C for 1 min, followed by ramping the temperature range of -50°C to 250°C at a rate of 20°C/min, and holding at 250°C for 1 min. Measurements were made at least in duplicate for each treatment.

8.9 Thermogravimetric analysis (TGA)

Thermogravimetric analysis was performed to study the degradation characteristic of the films. Thermal stability of each sample was determined using a (PerkinElmer, TGA7) with a heating rate of 10 ^{o}C/min in a nitrogen environment. It has a weighing capacity of 1.0 g. Samples were heated from room temperature to 500 ℃.

8.10 Dynamic mechanical thermal analysis (DMTA)

The small deformation analysis of the films was performed in tension in a dynamic mechanical thermal analyzer (Rheometric Scientific, DMTA V). The tested filmstrips were cut into small strips (20 × 5 mm) and clamped in the instrument with the initial grip separation 5.5 mm. The films were subjected to a sinusoidal strain on top of a static deformation. The testing was conducted at a constant frequency of 1 Hz and a strain of 0.02% and over a temperature range of 50 to 200 ^{o}C, at a heating

rate of 5 ^{o}C /min. The measurements of each experimental point were done at least in triplicates. When dynamic mechanical spectroscopy is employed within the linear viscoelastic regime to determine Tg, the storage and loss modulus (E' and E'') and loss tangent (tan $\delta = \Delta E'/E''$) are measured as a function of temperature at a constant frequency and a selected heating or cooling rate.

8.11 Fourier transform infrared (FTIR)

FTIR spectra of the fiber and the films were recorded using an attenuated total refraction (ATR) method in an IR spectrometer (Bruker, Equinox 55, Japan). The fiber and the films were applied directly onto the ZnSe ATR cell. For each spectrum, 128 consecutive scans at 4 cm^{-1} resolution were averaged.

8.12 X-ray diffraction

The crystallinity of the starch powder, palm pressed fiber (PPF), crystalline cellulose (CC), starch film and starch film reinforced with CC, were investigated by X-ray diffraction. The analysis was performed with a Philips X' Pert MPD, Natherlands, using copper radiation Kα at a voltage of 40 kV and 30 mA. The sample were scanned between 2θ = 3-40^{o} with a canning speed of 2^{o}/min. Prior to testing, the samples were dried and stored in a desiccator. The relative crystallinity index was calculated using equation 1 (Koksel *et al*., 1993; Muller *et al.*, 2009).

$$\%X_c = \frac{A_c}{A_t} = \frac{A_c}{A_c + A_a}$$

Where A_c is the crystalline area, A_a is the non-crystalline area and A_t is the total area.

9. Experimental design and statistical analysis

A completely randomized experimental design was used to characterize the composite films. Analysis of variance (ANOVA) was used to compare mean differences of the samples. If the differences in mean existed, multiple comparisons were performed using Duncan's Multiple Range Test (DMRT).

CHAPTER 3

RESULTS AND DISCUSSION

1. Characteristics of palm pressed fiber (PPF)

The color of unbleached pulp and bleached pulp had different value, the color of unbleached pulp was 68.56, 7.24 and 43.50 of L*, a* and b* value, for the color of bleached pulp was 87.39, 0.81 and 11.43 of L*, a* and b* value, respectively (Table 2).

Table 2. The color value of unbleached pulp and bleached pulp.

Pulp	color value		
	L*	a*	b*
Unbleached pulp	68.56±0.03	7.24±0.01	43.50±0.07
Bleached pulp	87.39±0.09	0.81±0.03	11.43±0.04

2. Compositional profile of materials

2.1 Compositional of palm pressed fiber (PPF)

The composition of unbleached pulp and bleached pulp were found to be 8.99, 45.97, 10.24, 3.50, 60.02 and 38.12% and 7.32, 55.61, 8.55, 2.93, 67.18 and 42.33% of moisture, cellulose, lignin, ash, acid detergent fiber and alpha cellulose, respectively (Table 3).

Table 3. Compositions of palm pressed fiber (PPF).

Compositions	Amount (%)	
	Unbleached pulp	Bleached pulp
Moisture	8.99±0.03	7.32±0.05
Cellulose	45.97±0.09	55.61±0.07
Lignin	10.24±0.02	8.55±0.06
Ash	3.50±0.08	2.93±0.13
Acid detergent fiber	60.02±0.01	67.18±0.02
Alpha cellulose	38.12±0.01	42.33±0.01

2.2 Compositional of starch

The composition of starch were found to be 10.65, 0.18, 0.34, 0.47 and 14.96% of moisture, ash, crude protein, crude fat and soluble amylose, respectively (Table 4).

Table 4. Compositions of starch.

Compositions	Amount (%)
Moisture	10.65±0.03
Ash	0.18±0.02
Protein	0.34±0.00
Fat	0.47±0.02
Soluble amylose	14.96±0.70

3. Effect of size and content of palm pressed fiber (PPF) on the properties of rice starch films

The thickness of resulted RS films were measured with a precision digital micrometer and the average thickness of RS films was approximate 0.085±0.01 mm. Mean thickness values of sample were calculated and used in tensile strength (TS), water vapor permeability (WVP) and transparency value of RS films.

3.1 Tensile strength (TS) and elongation at break (ε)

A biodegradable or edible film must withstand the normal stress encountered during its application and the subsequent shipping and handling of the food to maintain its integrity and barrier properties. Tensile strength (TS) is the maximum tensile stress sustained by the sample during the tension test. If maximum tensile stress occurs at either the yield point or the breaking point, it is designated tensile strength at yield or at break, respectively (ASTM, 1991). High TS is generally required, but deformation values must be adjusted according to the intended application of the films. That is, whether it is un-deformable material to provide structural integrity or reinforce structure of the food (Gontard *et al.*, 1992).

Elongation at break (ε) is an indication of films flexibility and stretch ability (extensibility), which is determined at point when the film breaks under tensile testing and is expressed as the percentage of change of the original length of the specimen between the grips of a film to stretch (extend). The TS and ε of the rice starch (RS) films reinforced with palm pressed fiber (PPF) or RS/PPF films is depicted in Figure 10. The TS of RS films were affected by size and content of PPF. The results demonstrated that the TS of RS films were enhanced as addition of PPF. This behavior was expected and was attributed to the resistance exerted by the fiber itself and due to 3D hydrogen bonds network formed between different components (Lu *et al.,* 2006). Furthermore, increasing of fillers content from 0 to 40% of starch resulted in an increase of TS (Figure 10A), indicated that a high compatibility occurs between starch matrix and PPF fillers and the performances (e.g., mechanical properties) Besides, at lower fiber content dispersion of fiber is very poor so that TS will not occur properly. Similar results were observed by Sreekumar *et al.* (2007) and Sangthong *et al.,* (2008). Size of PPF fillers also affected the TS of RS films, the result showed that, TS remarked increase as size of PPF fillers increase from 125 to 420 µm. According to the results, the maximum TS of RS films reinforced with 40% of starch at 420 µm (16.26 MPa) (Figure 10A). Regarding the tensile behavior of resole composites fiber size of 420 µm was found to be the optimum size for RS films. In the case of fibers smaller than this optimum size, the fibers will debond from the matrix resulting in weaker of composite. Besides, Dong *et al.* (1993) pointed out that short fiber act more like flaws in the structure of the matrix rather than long fiber as reinforcement agent, this could be the reason for the lower of tensile strength values. This result shows a reasonable agreement with experimental of Arbelaiz *et al.* (2006). Regarding the elongation at break (ε), size of PPF did not significantly affect on the ε but there was affected by the PPF content; results showed that increases in PPF fillers from 0 to 40% of starch provided decrease in ε from 40.54% to 1.69% (Figure 10B). The experiments showed that TS and ε of RS/PPF films is almost inversely related.

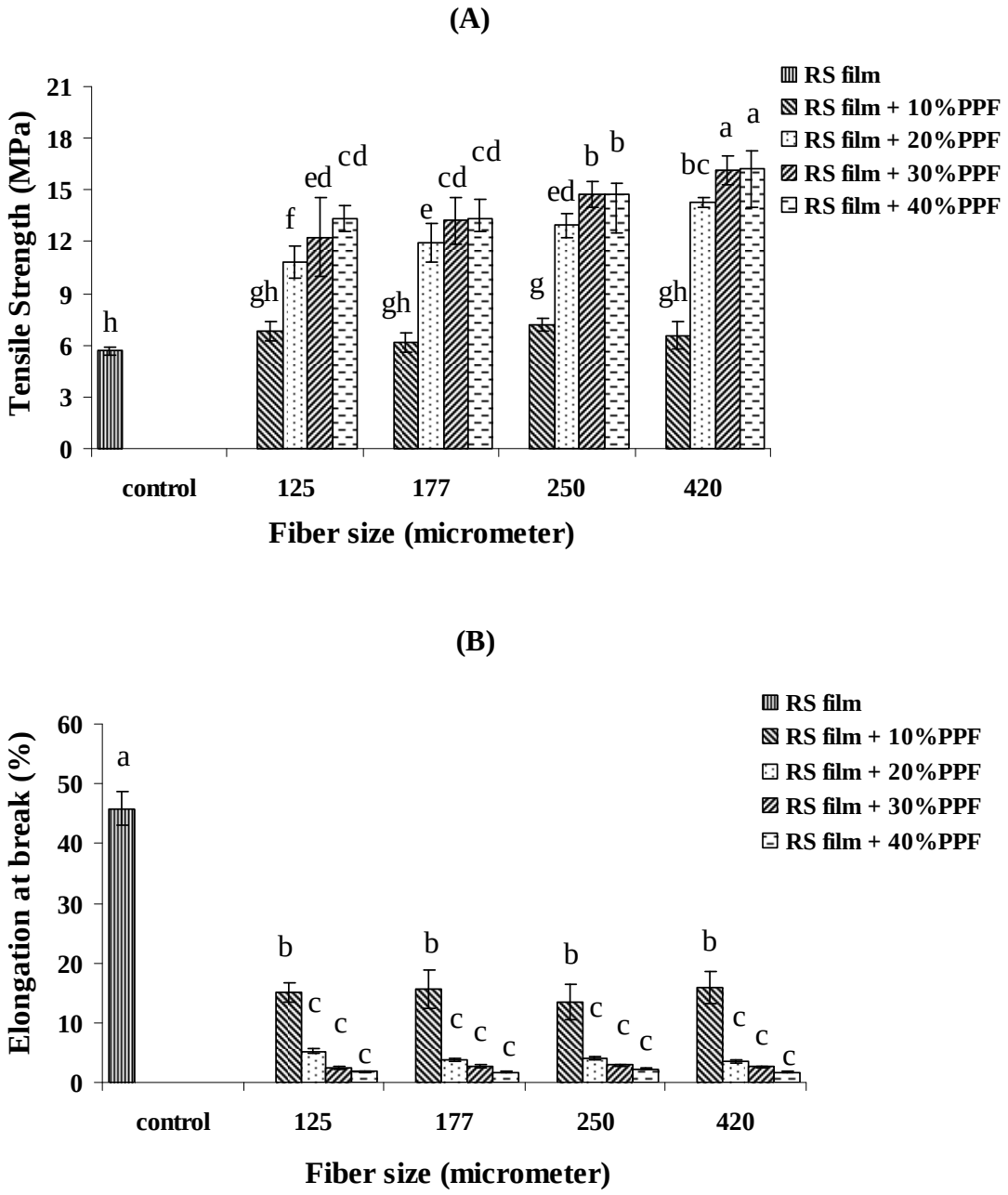

Figure 10. Effect of size and content of PPF on tensile strength (A) and elongation at break (B) of RS films. Mean values with different letter are significantly different ($p<0.05$).

3.2 Water vapor permeability (WVP)

As a food packaging, film is often required to avoid or at least to decrease moisture transfer between the food and the surrounding atmosphere, and water vapor permeability should be as low as possible (Ma *et al.*, 2008). The results demonstrated that RS films contained 40% PPF was broken during measuring the water vapor permeability, resulted from the occurring of brittle films. Hence, only 10-30% PPF was presented in this study. Water vapor permeability (WVP) of the RS films decreased with the addition of PPF, and the highest occurred when no fiber was added (14.15 g.mm/m^2.day.kPa) but the lowest value (4.27 g.mm/m^2.day.kPa) being obtained with addition of PPF (Figure 11), this results pointed out that water resistance of PPF was better than rice starch matrix. However, WVP of the RS films tended to increase as content of fibers increased (Figure 11). For example, WVP of the RS films increased from 4.33 g.mm/day.m^2.kPa to 10.60 g.mm/day.m^2.kPa when increasing the PPF content from 10 to 30% of starch at 420 µm of PPF (Figure 11). The addition of PPF probably introduced a tortuous path for water molecule to pass through (Kristo and Biliaderis, 2007). At a low content of filler, PPF dispersed well in the rice starch matrix, and blocked the water vapor. However, superfluous filler was easy to congregate and increased porous on films, which actually decreased the effective contents of fiber and facilitated the water vapor permeation (Ma *et al.*, 2008). Additionally, as the fiber content increased the water absorption also increased due to the increased hydrophilic nature of the fibers. Moreover, large number of porous tubular structures present in fiber accelerates the penetration of water by the so-called capillary action (Sreekumar *et al.*, 2007). Similar trend is observed in for the composites prepared by Espert *et al.* (2004). Size of PPF fillers also affected the WVP of RS films, the result showed that, WVP tended to increase as size of PPF fillers decrease from 420 to 125 µm, because the small size of PPF increased the surface for contact the water in surrounding atmosphere. Pinnavaia and Beall (2000) reported that the changes in WVP of composite films due to the effect of the filler added are highly dependent on the size and aspect ratio (width-to-height) of the filler. Besides, bigger size of fiber showed higher agglomerated and, probably, this fact diminished the effectiveness of fiber for WVP decrease.

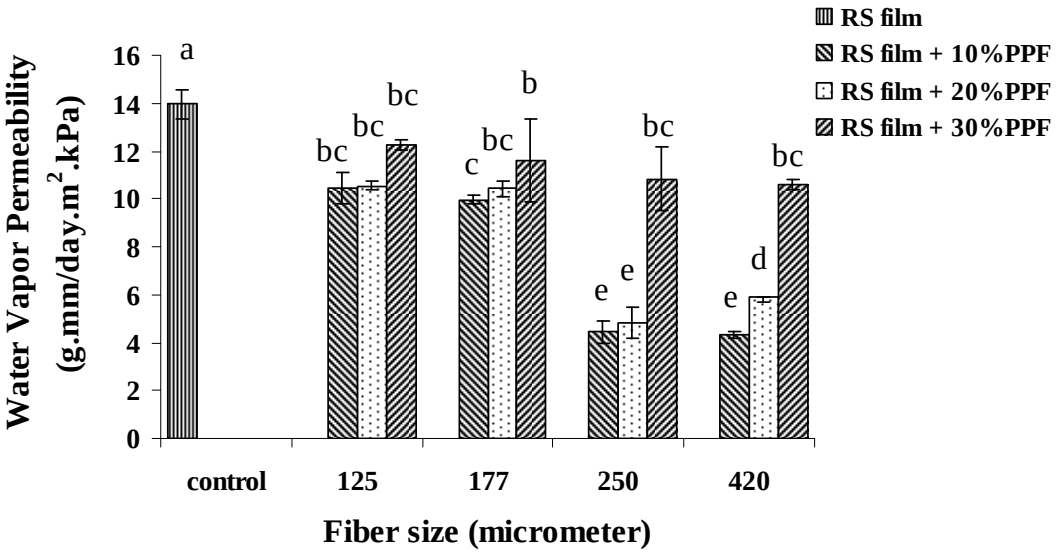

Figure 11. Effect of size and content of PPF on water vapor permeability of RS films. Mean values with different letter are significantly different ($p<0.05$).

3.3 Water Uptake

In sorption kinetics experiments, the mass of sorbed penetrant is measured as a function of time. The change in weight during conditioning at 98% RH is plotted against time in Figure 12 for RS films reinforced with PPF at different size (125-420 μm) and content (0-40%) of PPF. These swelling data are the results of several trials, and the measurement reliability was very good. We ascertained that each composition absorbed water during the experiment but behaved differently. Two well-separated zones are displayed in Figure 12(A-D). At lower time (zone I: $t < 2$ day or 48 h), the kinetics of absorption are fast, while the longtime kinetics of absorption are slow and lead to plateau (zone II). Similar results were observed by Demir *et al.* (2006). In zone I the water uptake for a given time is always as low as the cellulose content is high. In zone II the water uptake reaches a plateau whose value is always as low as the cellulose content is high. It corresponds to the weight percentage increase at equilibrium or the water uptake at equilibrium. Figure 12, the results demonstrated that the water uptake of RS films were significantly reduced as addition of PPF and decreased with increasing the PPF ($p<0.05$). This behavior was expected and was attributed to the resistance exerted by the 3D inter-wined cellulose network observed when mixed with gelatinized starch. The RS film processing by water

evaporation allows stabilization of this structure and reinforces it by the establishment of strong hydrogen bonds between cellulose during the evaporation step. This phenomenon is similar to the percolation of cellulose fibers in paper making (Batten and Nissan, 1987 by Dufresne *et al.*, 1999). Indeed, it is well established that the high mechanical properties of a paper sheet result from the hydrogen-bonding forces that hold the percolating network of the fibers. In our systems cellulose acts as a close network within the matrix and prevents the swelling of the starch material when exposed to water or moist atmosphere. In addition, favorable interactions probably exist between starch and cellulose that contribute to this phenomenon. Adding cellulose to the starchy matrix results in a decrease of water uptake (Dufresne *et al.*, 1999).

The water uptake of RS films was affected by size of PPF. The results demonstrated that the water uptake of RS films was significantly decreased with decreasing the size of PPF at the same content of PPF ($p<0.05$). Hedenqvist *et al.* (2006) and Xue *et al.* (2006) explained that the small size, the surface-to-volume ratio of the small particles is significantly greater than that of the corresponding great particles at the same mass content.

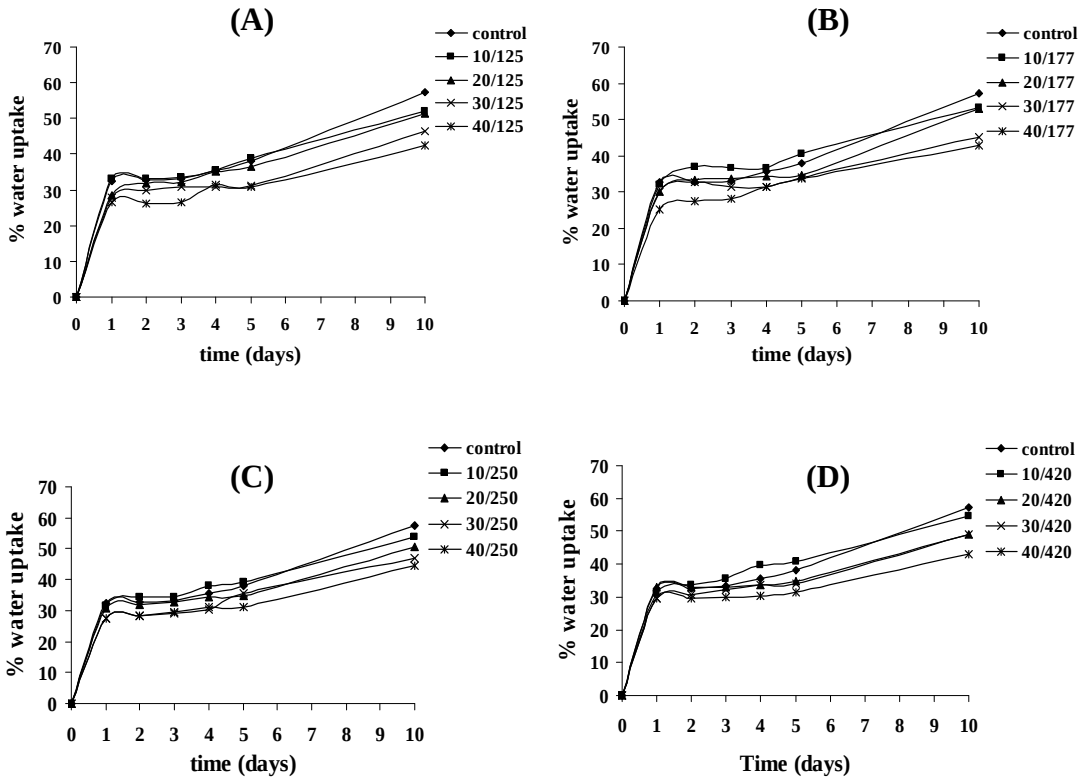

Figure 12. Effect of size and content of PPF at (A) 125 μm, (B) 177 μm, (C) 250 μm and (D) 420 μm on water uptake of RS films.

3.4 Color and transparency

Color of the packaging is an important factor in terms of general appearance and consumer acceptance (Srinivasa *et al.*, 2007). The results of the measurements performed on the RS film's color were expressed in accordance with CIELAB system and the rectangular coordinates (L*, a* and b*) and the total color difference (ΔE^*_{ab}), hue angle and chroma were calculated. Figure 13 and 14 depicted results from the effect of size and content of PPF fillers on color (L*, a*, b*, $\Delta E^*_{ab,}$ chroma and hue angle) of RS films. These results showed that the content of PPF fillers significantly affect the color of RS films. The b* chroma and ΔE^*_{ab} values increased as content of PPF fillers increased from 10 to 40% of starch concomitant with decreased in L*, a* and hue angle values. This indicated the decreasing lightness (L*) and increasing yellowness (b* and chroma) of RS film, possibly due to the PPF have white-yellowish color. Transparency of the films is also of importance in some instances, when used as packaging materials. Addition of PPF fiber into the RS films

resulted in decrease their transparency. Rice starch film without PPF fiber was the highest transparent. However, the lower transparency of the films was noticed when a greater amount of PPF was incorporated (Figure 15). The decrease in transparency could possibly arise from the light scattering from the retarding of light transmission of the PPF and RS/PPF films. At high level of PPF, the RS films demonstrated lower transparency than lesser PPF incorporation.

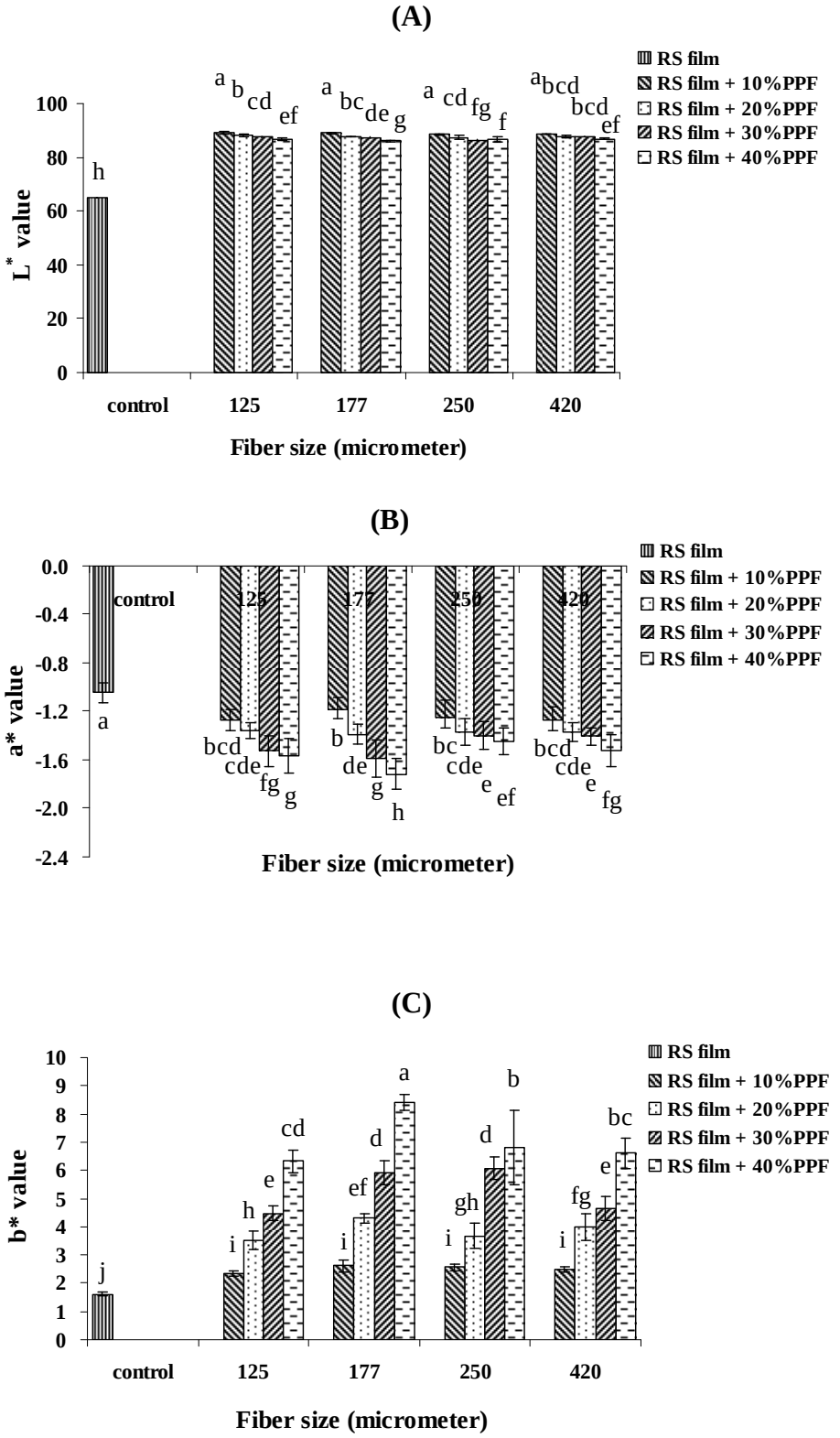

Figure 13. Effect of size and content of PPF on L* (A); a* (B) and b* (C) of RS films. Mean values with different letter are significantly different ($p<0.05$).

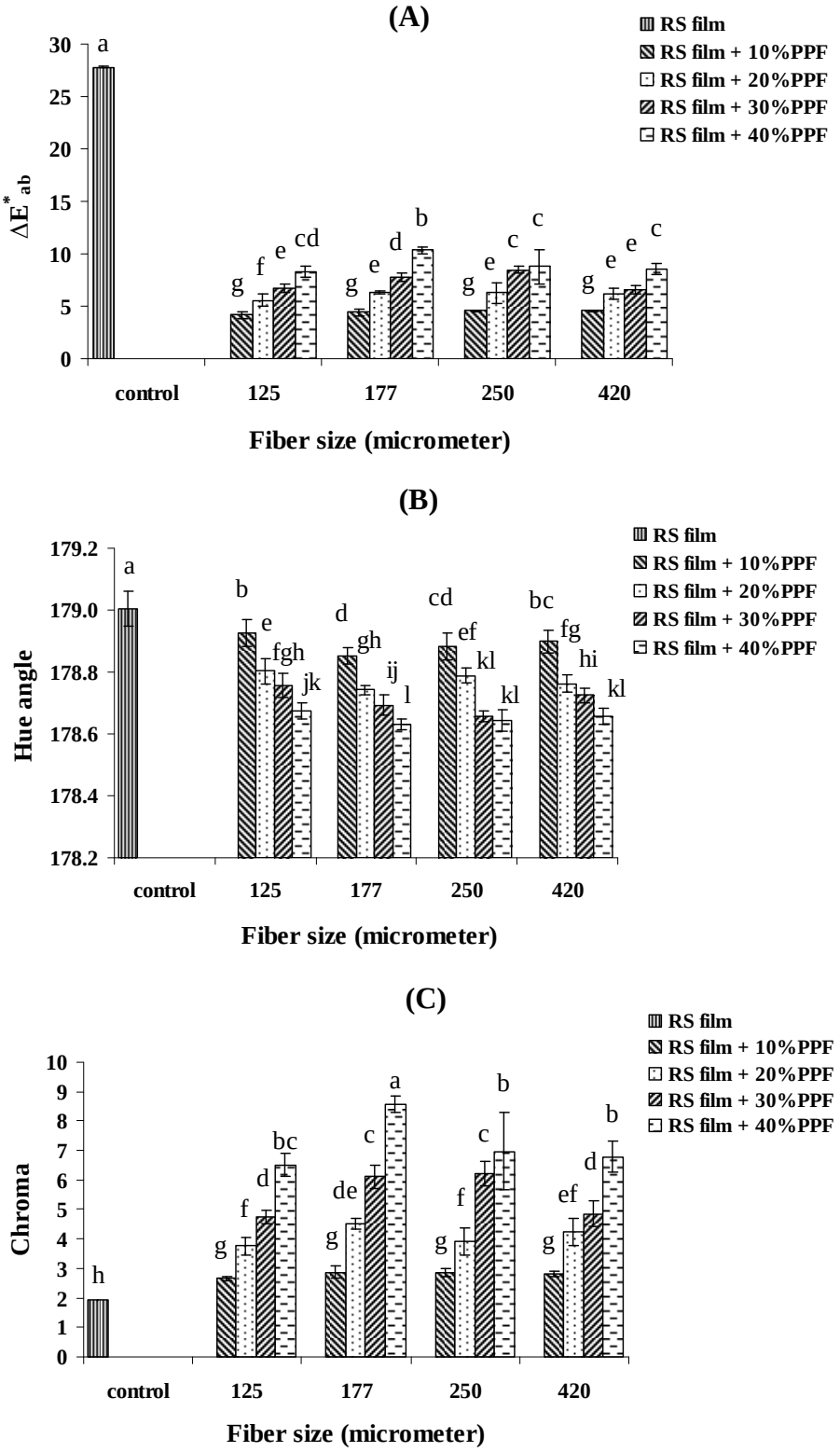

Figure 14. Effect of size and content of PPF on ΔE* (A); Hue angle (B) and Chroma (C) of RS films. Mean values with different letter are significantly different ($p<0.05$).

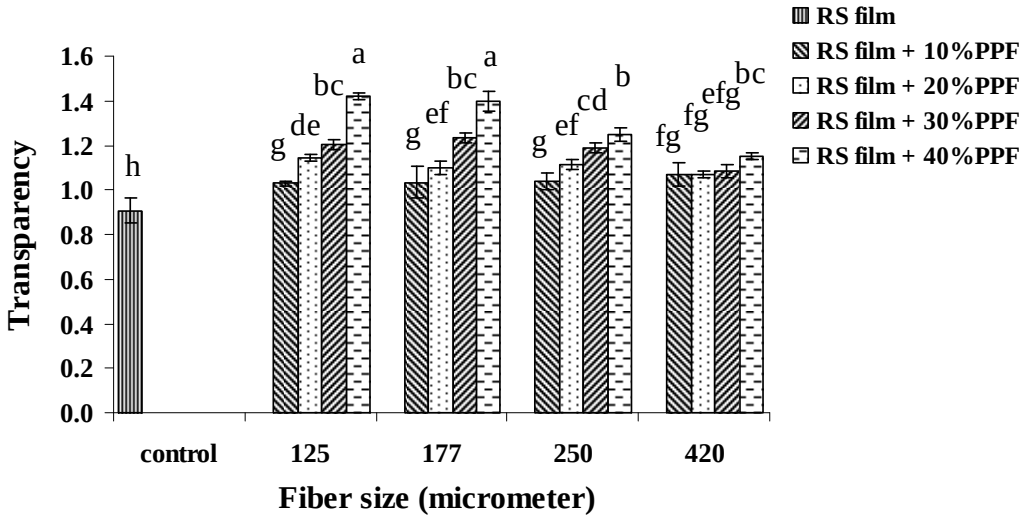

Figure 15. Effect of size and content of PPF on transparency of RS films. Mean values with different letter are significantly different ($p<0.05$).

3.5 Thermal properties

According to PPF at 420 μm yielded a good mechanical and barrier properties of RF films, hence thermal properties (thermogravimetric analysis, TGA, differential scanning calorimetry, DSC and dynamic mechanical thermal analysis, DMTA) of RS films reinforced with PPF at 420 μm for all PPF content were investigated.

3.5.1 Thermogravimetric analysis (TGA)

TGA thermograms and the char yields (500 ℃) of various samples under nitrogen are shown in Figure 16. The behavior of the char yield curves was similar in the composites (Figure 16). The fiber, even at low content (10% of starch, as shown in Figure 16), could improve thermal stability of RS films. The char yield of RS film was lesser (8.5%) than RS films reinforced with PPF (10.6-14.1%), resulting from the greater thermal stability of the PPF. By the reason of the mainly composition of PPF are cellulose that was strong structure. Therefore, addition of PPF into the RS films can be improved the thermal stability of RS films. It was found that the char yield of RS films was enhanced as PPF fillers content increased. For example, the char yield increased from 8.5 to 14.1% when increasing the PPF content from 0 to 40% of starch (Figure 16). These results indicated that fiber addition increased the

thermal stability of RS films, which is in agreement with the results reported by Ruseckaite and Jimenez (2003) for composites with sisal fibers and PCL matrix. The results revealed that the composites, the moisture content mainly contributed to mass loss at the onset temperature, while for pure RS films the moisture content and the addition of plasticizer resulted in the mass loss. This difference was due to the good adhesion between RS films and fiber. The fiber component decreased the mass loss of plasticizer, therefore, the thermal stability of RS films was improved.

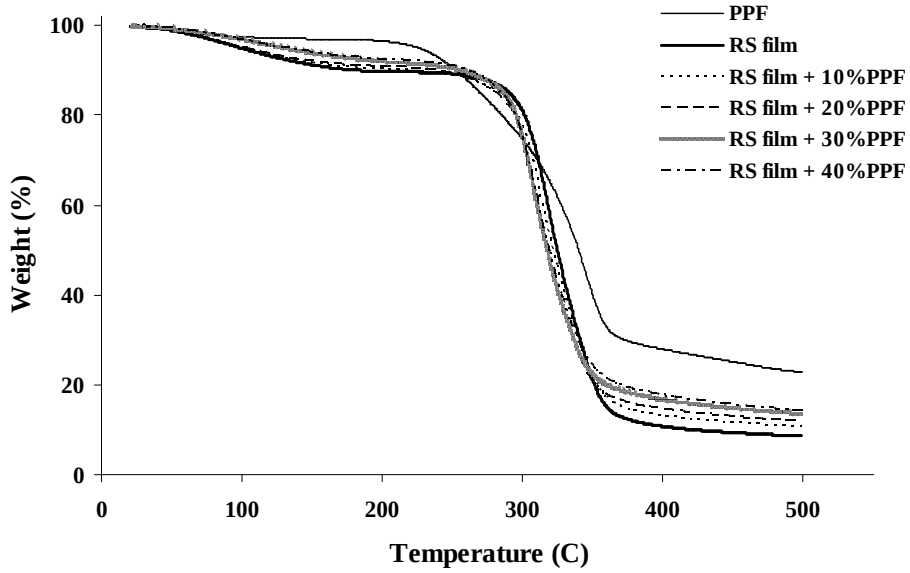

Figure 16. TGA thermograms of PPF, RS films and 10-40% of PPF (420 μm) reinforced RS films.

3.5.2 Differential scanning calorimetry (DSC)

The DSC results, which showed that the presence of PPF increases the T_g of the matrix, are in agreement with the water sorption experiments. Figure 17 shows the DSC curves in the temperature region of -50 to 220 ℃ of the RS films reinforced with PPF. No endothermic peaks, assigned to the glass transition temperature (T_g) of RS films. However, can be observed from the increasing endothermic heat flow when PPF was added into RS films. With the increase of PPF contents, the endothermic heat flow increased gradually, might be attributed to the occurrence of intermolecular interactions occurred between starch and PPF, which reduces the flexibility of molecular chains of starch (Lu *et al.*, 2006). This behavior

was already observed with different polysaccharides reinforced with cellulose fiber (Curvelo *et al.*, 2001; Ma *et al.*, 2005; Arbelaiz *et al.*, 2006).

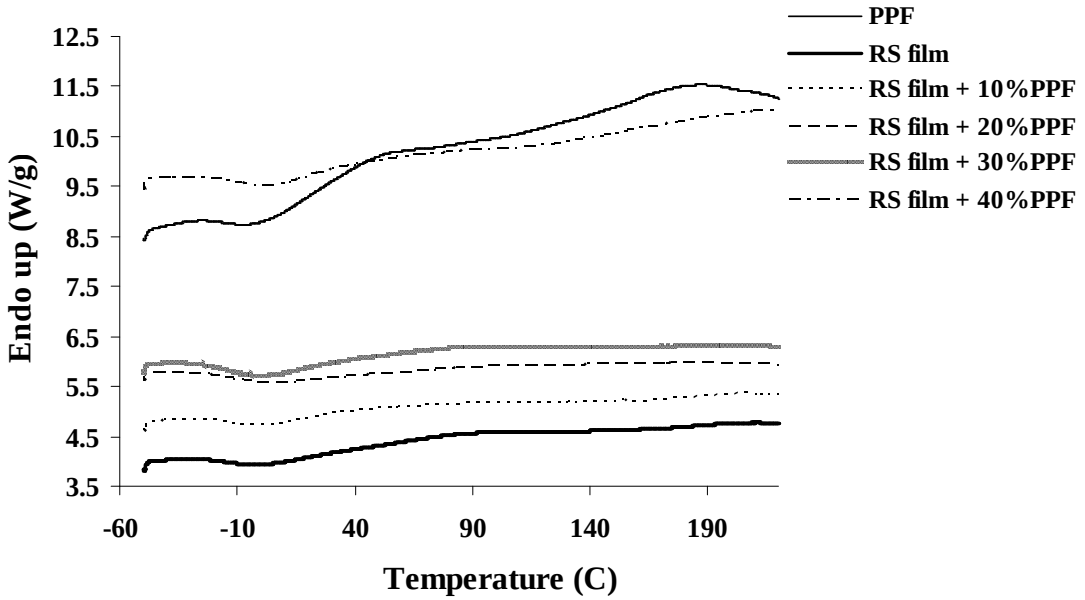

Figure 17. DSC curves of PPF, RS films and 10-40% of PPF (420 μm) reinforced RS films.

3.5.3 Dynamic mechanical thermal analysis (DMTA)

Figure 18 shows the temperature dependence of dynamic mechanical thermal analysis behaviors for the RS film and PPF/RS film. The storage modulus (E') of the RS film and PPF/RS films as a function of temperature is given in Figure 18A. The storage modulus of the films was increased with increasing PPF content compared to the pure RS film. By incorporating PPF fillers of 0 to 30% of starch, the thermal stability shifts to higher temperature. This can be attributed to the strong interfacial interactions through hydrogen bonding between large specific surface of PPF and starch matrix (Angles and Dufresne, 2001).

Figure 18B shows the tan δ curves of the RS film and PPF/RS films as a function of temperature. The glass transition temperatures were estimated from the tan δ peaks. The RS film exhibits a T_g transition at about 148 ℃. Additionally, the T_g of thermoplastic starch depends on the plasticizer content and humidity conditions as well as the composition of starch (Alemdar and Sain, 2007). With increasing the PPF

fillers content from 0 to 30% of starch, the tan δ peak shifts from 148 to 187 ℃, indicating that PPF fillers restrict molecular motions of starch, due to the strong interaction between starch and fillers (Park *et al.*, 2002).

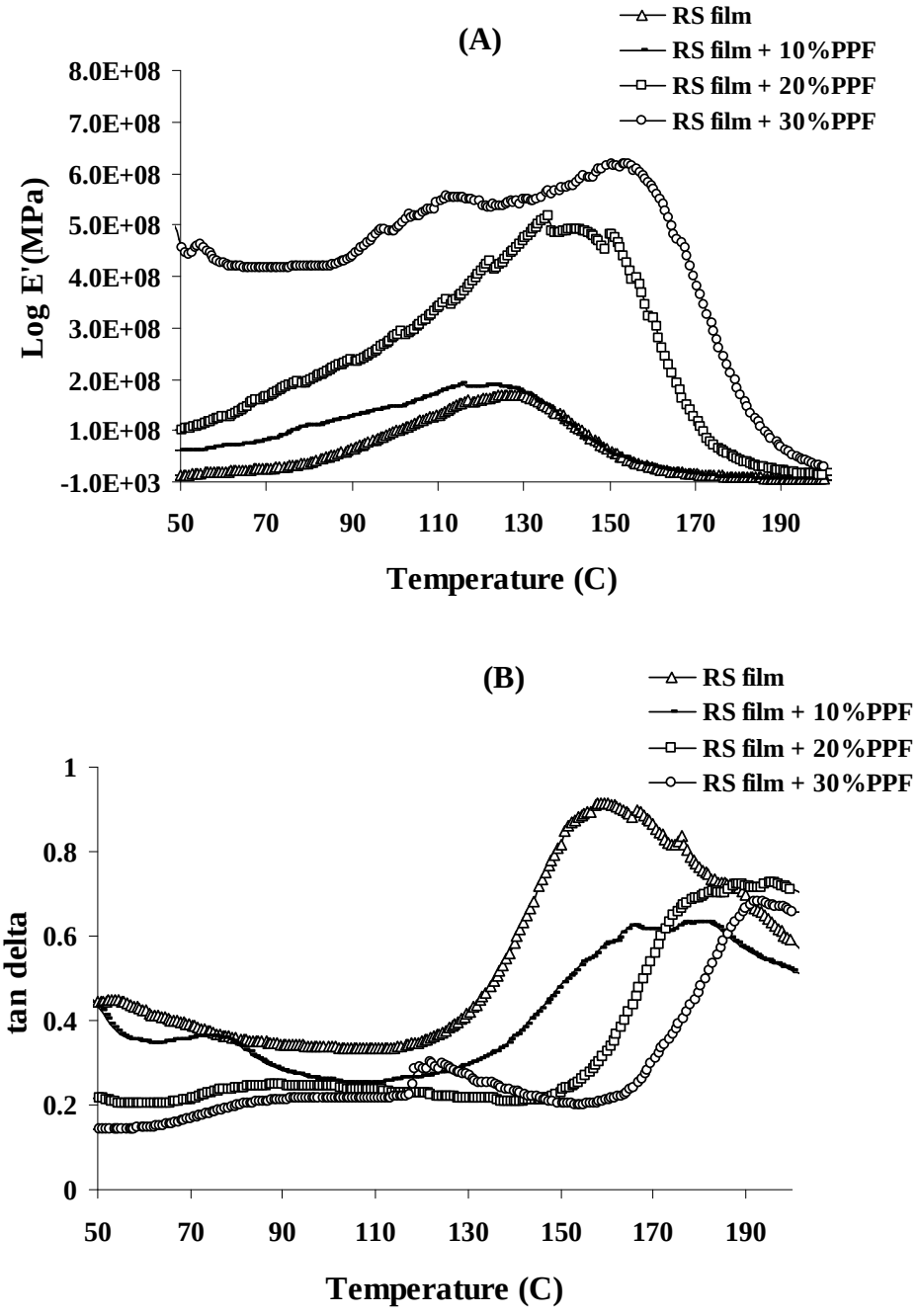

Figure 18. The dynamic mechanical behaviors of both (A) storage modulus (E') and (B) loss factor (tan δ) as a function of temperature for of PPF, RS films and 10-30% of PPF (420 μm) reinforced RS films.

3.6 Morphology of the films

Morphology of RS films reinforced with PPF (420 μm) at 10 - 40% of starch are depicted in Figure 19 and 20. At lower fiber content (10%) dispersion of fiber is poor than higher content (Figure 19). In the Figure 20 illustrates the morphology of RS films incorporated with 40% PPF at different size PPF (125, 177, 250 and 420 μm). The small fiber had length of fiber were shorter than the large fiber although the small size fiber had better dispersion than the large size fiber, the result had relationship with the TS of the RS films reinforced with PPF, TS remarked increase as size of PPF fillers increase from 125 to 420 μm because the long fiber had better mechanical properties than the short fiber such as the paper were manufactured from long fiber had the strong structure. Similarly, Pu *et al.* (2006), who reported the acrylic films reinforced with the longer acacia fiber had the higher TS than the acrylic films reinforced with the short acacia fiber.

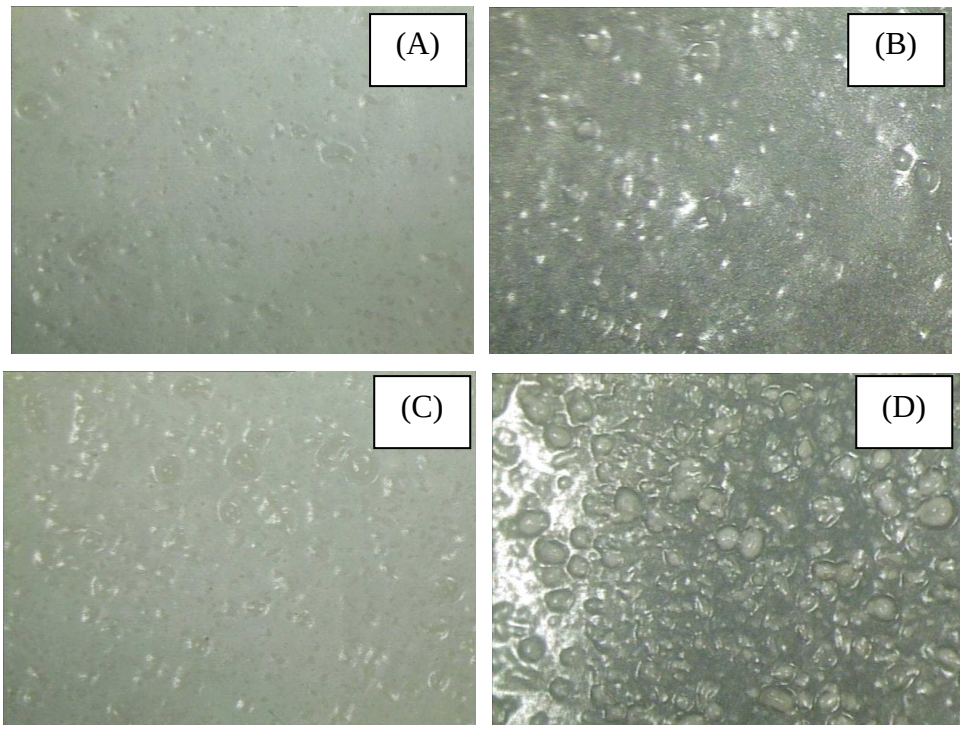

Figure 19. Surface (×10) of RS films reinforced with 420 μm PPF at (A) 10%, (B) 20%, (C) 30% and (D) 40%.

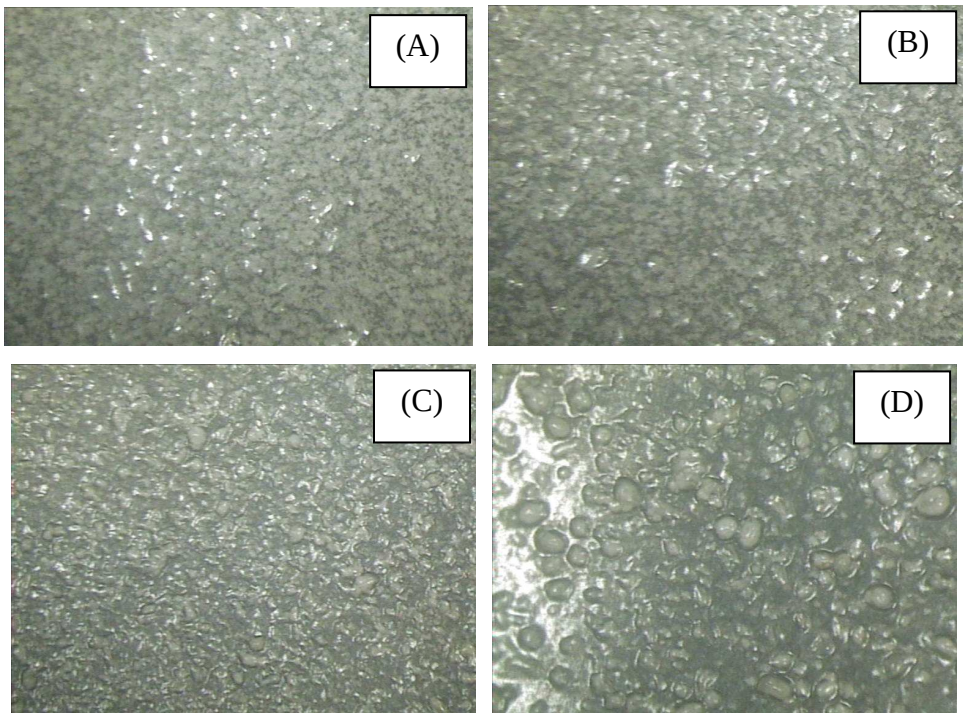

Figure 20. Surface (×10) of RS films reinforced with 40% PPF at (A) 125 μm, (B) 177 μm, (C) 250 μm and (D) 420 μm.

4. Effect of fiber surface treatment of palm pressed fiber (PPF) on the properties of rice starch films

Rice starch film were prepared and the influence of the fiber surface treatment (alkaline treatment and silane treatment) on the mechanical properties, water barrier properties and thermal properties of rice starch films were investigated. The PPF at 420 μm was selected according to mechanical, barrier properties and together with thermal properties. For this study, the effect fiber surface treatment of palm pressed fiber on the properties of rice starch films was investigated. The selected surface treatment of PPF on RS films properties included alkaline treatment and silane coupling agent treatment (glysidoxyproply trimethoxy silane) at various concentrations.

4.1 FTIR spectroscopy of untreated and treated PPF

FTIR spectra for the untreated PPF and silane treated PPF is shown in Figure 21, a strong and broad absorption was found at 3335 cm^{-1}. This implies the presence of –OH groups in the fibers and hydrogen bonding between those –OH groups. However, the absorption peak of –OH groups for the silane treated PPF was shifted to a higher wave number near 3400 cm^{-1}. This implies that the degree of hydrogen bonding between –OH groups was decreased, and the absorption peak of –OH groups was shifted to the position of free –OH groups (higher wave number) (Shih, 2006). Moreover, the characteristic absorption peaks of epoxide at 800 and 1272 cm^{-1} were found for silane coupling agent (glysidoxyproply trimethoxy silane). Furthermore, a slight increment in the broadness around 1000-1100 cm^{-1} was found for the silane treated PPF. This could be attributed to the presence of the asymmetric stretching of -Si-O-Si- and/or –Si-O-C- bonds. Which is in agreement with the results reported by Herrera-Franco and Valadez-Gonzalez (2005), the broad intense bands around 1200 was assigned to the stretching of the –Si-O-cellulose. The former bond is indicative of the existence of silica deposited on the fibers, whereas the latter would confirm the occurrence of a condensation reaction between the silane coupling agents and the fibers.

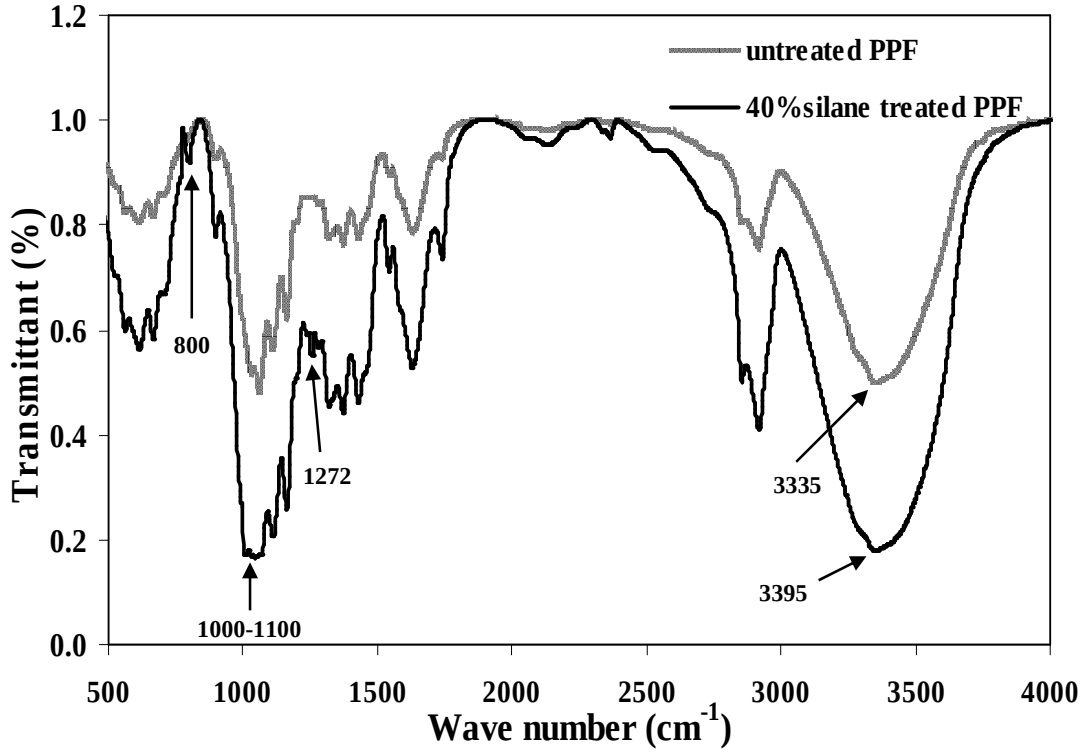

Figure 21. Fourier Transform Infrared (FTIR) spectra for the untreated PPF and 40% silane treated PPF.

4.2 Tensile strength (TS) and elongation at break (ε)

The mechanical properties of the rice starch (RS) films reinforced with treated palm pressed fiber (PPF) or RS/PPF biocomposite films, such as tensile strength (TS) and elongation at break (ε) is depicted in Figure 22. The importance of the treatment with coupling agent can be assessed by comparing the results of the untreated and treated PPF. Figure 22A illustrates the TS of RS films containing the untreated and treated PPF (10 - 40% silane coupling agents). Comparing with same amount of PPF fillers, the TS of the RS film reinforced with treated PPF showed higher than the RS film reinforced with untreated PPF. This is in agreement with the results reported by Herrera-Franco and Valadez-Gonzalez (2005) for composites with henequen fibers were treated with vinyltris silane and HDPE matrix. The results showed that, the TS of the RS film reinforced with untreated PPF and treated PPF increased as the PPF content increased. The result indicated that a high compatibility occurs between starch matrix and PPF fillers and the performances (e.g., mechanical properties) due to 3D hydrogen bonds network formed between different components (Lu *et al.*, 2006). However, increasing of fillers content from 0 to 30% of starch resulted in an increase of TS (Figure 22A), indicated that a high compatibility occurs between starch matrix and PPF fillers and the performances (e.g., mechanical properties). Similar results were observed by Sreekumar *et al.* (2007) and Sangthong *et al.* (2008). While the TS of RS films reinforced with 40% of treated PPF was decreased due to superfluous filler was easy to congregate and increased porous on the films. Similar results were observed by Pickering *et al.* (2003), reported that at the highest fiber percentages, an actual reduction in strength was observed. One explanation for the general reduction in the strength for the treated wood fiber as the PPF content increases could be related to fiber agglomeration, which would be more likely at higher fiber contents. Fiber – fiber interaction from hydrogen bonding is considered to be a significant to fiber dispersion (Matuana *et al.*, 1999).

Comparing between alkaline treatment and silane treatment of the fiber on the RS films properties. The result demonstrated that, the TS of RS film reinforced with alkaline treated PPF showed higher than RS film reinforced with silane treatment at the same content of PPF fillers. Bisanda *et al.* (1991) and Pickering *et al.* (2003) explained that, alkaline treatment results in an improvement in the interfacial bonding

by giving rise to additional sites of mechanical interlocking, hence promoting more fiber/matrix interpenetration at the interface. Herrera-Franco and Voladez-Gonzalez (2005) found that the TS of the high density polyethylene (HDPE) reinforced with alkaline treated short natural-fiber showed higher than HDPE composite reinforced with silane treated short natural-fiber.

Concentration of silane coupling agent also affected the TS of RS films, the result showed that, TS tended to increase as concentration of silane coupling agent increase from 10 to 40%. The increased in the TS with an increased of silane concentration can be explained by the better adhesion between the filler and the starch matrix. Without silane coupling agent, the only adhesion mechanism is inter-diffusion. Silane coupling agents yields to hydrogen and covalent bonding between hydroxyl groups of filler and polysiloxanes formed by hydrogenation of silanes providing better adhesion between the fiber and the starch matrix. Better adhesion improves stress transfer through fibers, therefore, increases the TS of RS films (Demir *et al.,* 2006). Abdelmouleh *et al.* (2004) pointed that the adsorption of silane onto the surface of fiber revealed that the same pre-hydrolysed silanes used were adsorbed onto the surface of cellulosic fibers. This adsorption followed a mono- and multi-layer processes depending on the ratio between the quantity of the silane and that of the substrate. This adsorption was essentially driven by the formation of hydrogen bonds between the hydroxyl groups at the end of the short aliphatic moiety of the silane structure also contributed to the adsorption process through specific interactions. Regarding the elongation at break (ε), fiber surface treatment and silane concentration did not significant effect on the ε of RS films but there was affected by the treated PPF content; results showed that increases both PPF fillers and silane concentration yielded decrease in ε (Figure 22B). The decrease in the ε due to the adhesion between fiber and matrix restricts deformation capacity of matrix in the elastic zone as well as the plastic zone (Demir *et al.,* 2006).The experiments showed that TS and ε of RS films is almost inversely related.

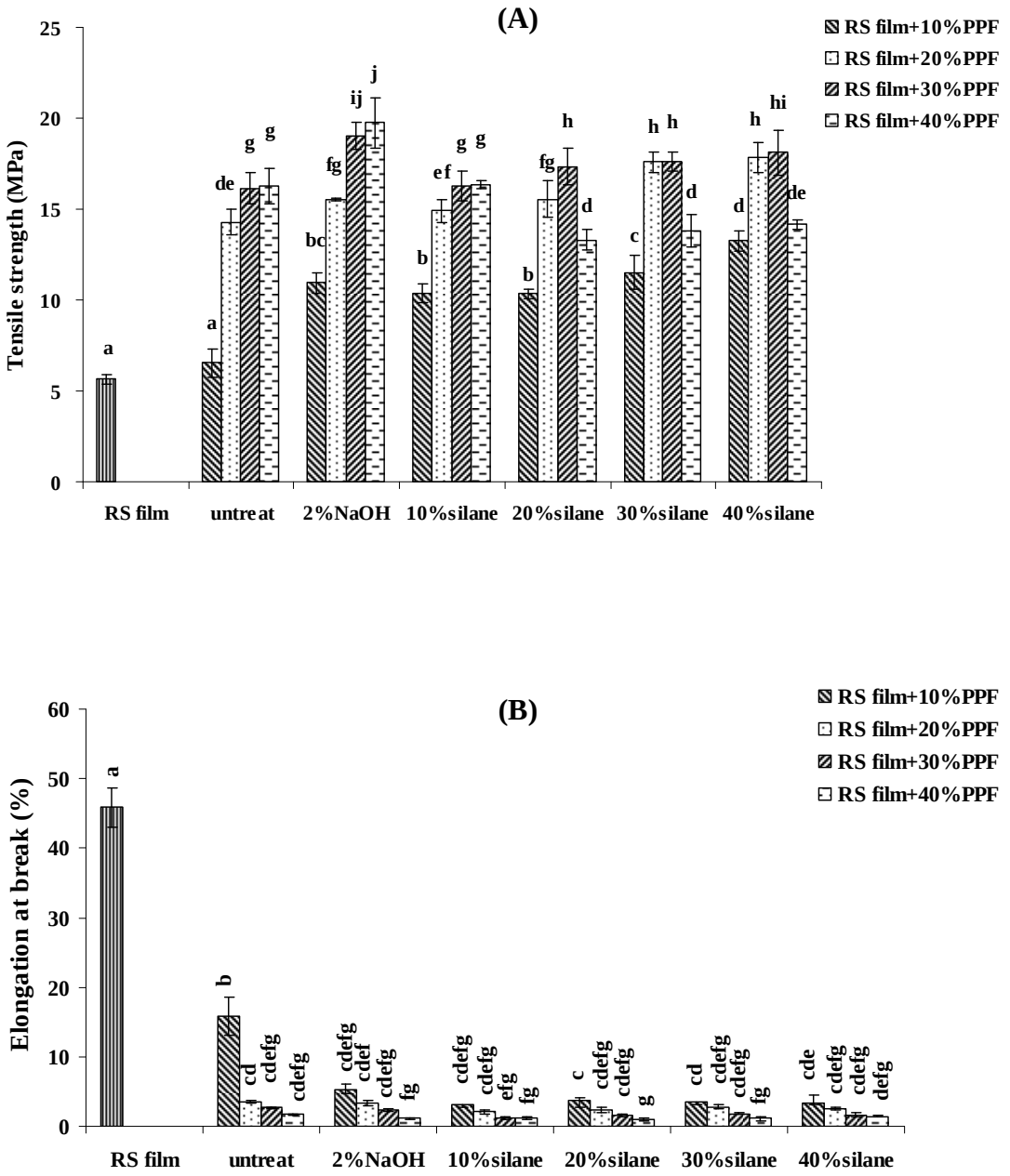

Figure 22. Effect of fiber surface treatment on tensile strength (A) and elongation at break (B) of RS films. Mean values with different letter are significantly different ($p<0.05$).

4.3 Water vapor permeability (WVP)

The WVP value of film or coating material should be taken into account when applying onto a moist product such as precooked beef patties. The films ability to retard moisture loss from the product (Wu, 2001) is an important characteristic that affects product quality. The results demonstrated that RS films contained 40% of untreated PPF and alkaline treated PPF were broken during measuring of water vapor permeability, resulted from the occurring of brittle films. Hence, 10-30% of untreated PPF and alkaline treated PPF were tested. The water vapor permeability (WVP) of the RS film decreased with the addition of both untreated and treated PPF, and the highest occurred when no fiber was added (14.15 g.mm/m^2.day.kPa) but the lowest value (4.27 g.mm/m^2.day.kPa) being obtained with addition of untreated PPF (Figure 23), this results pointed out that water resistance of PPF was better than rice starch matrix.

According to the effect of PPF content on the WVP, found that WVP of the RS films tended to increase as content of untreated and treated PPF increased (Figure 23). The addition of PPF probably introduced a tortuous path for water molecule to pass through (Kristo and Biliaderis, 2007). At a low content of filler, PPF dispersed well in the rice starch matrix, and blocked the water vapor. However, superfluous filler was easy to congregate and increased porous on films, which actually decreased the effective contents of fiber and facilitated the water vapor permeation (Ma *et al.,* 2008). Additionally, as the fiber content increased the water absorption also increased due to the increased hydrophilic nature of the fibers. Moreover, large number of porous tubular structures present in fiber accelerates the penetration of water by the so-called capillary action (Sreekumar *et al.,* 2007). Similar trend is observed in for the composites prepared by Espert *et al.* (2004).

Comparing of WVP between the RS films reinforced with alkaline treated PPF and the RS films reinforced with silane treated PPF. The results showed that, the WVP of RS film reinforced with silane treated PPF showed higher than RS film reinforced with alkaline treated PPF in the same amount of treated PPF fillers. Besides, concentration of silane coupling agent did not significant effect on the WVP of RS films reinforced with treated PPF. Water absorption in cellulose fibers is caused by hydrogen bonding between free hydroxyl groups on cellulose molecules and water

molecules. Silane coupling agents form hydrogen or covalent bonds with some of free hydroxyl groups of cellulose, which reduce the water absorption capacity of cellulose (Sreekala and Thomas, 2003; Demir *et al.*, 2006) but inversely in this research, WVP of the RS films increased with the addition of silane treated PPF compared the RS film reinforced with untreated PPF. It could be explained that R-group of silane coupling agents contained hydrophilic groups, and then could bonded with water resulted in increase water vapor permeability of resulted RS films. According to the alkaline treatment of PPF on the RS films, the processing of fiber surface treatment with alkaline treatment used the strong base solution (NaOH), when the PPF were immersed into the base, PPF occurred swelling and absorbed the water also resulted in increase WVP of RS films (Bledzki and Gassan, 1999).

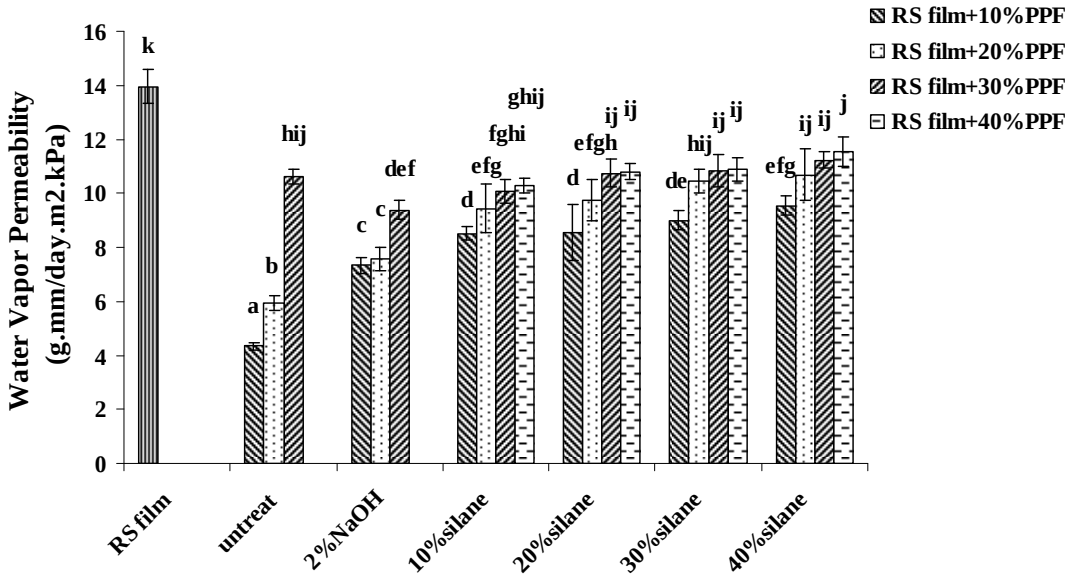

Figure 23. Effect of fiber surface treatment on the properties of RS films. Mean values with different letter are significantly different ($p<0.05$).

4.4 Water Uptake

Figure 24 shows the water uptake of RS films and RS films reinforced with treated PPF during conditioning in 98% RH as a function of time. The water uptake –t curves display two well-separated zones. At shorter times, t < 2 day or 48 h, the kinetics of absorption is very fast, whereas at longer times, t > 2 days, the kinetics of absorption is slow and leads to a plateau, corresponding to the water uptake at equilibrium. The water uptake at equilibrium were significantly decreased with increasing the content of PPF fillers for all treated PPF ($p<0.05$). By the reason of starch matrix in the RS films display a reduced swelling capacity (Lu *et al.,* 2006). Dufresne *et al.* (1999) reported that cellulose and starch act as a close network within the matrix and prevent the swelling of the starch material when exposed to water or moist atmosphere.

In Figure 25, all treatment of the RS films reinforced with 30% treated PPF were studied. The results showed that, at the lower silane concentration (10-20%), the water uptake of RS film reinforced with alkaline treated PPF showed significantly higher than RS film reinforced with silane treated PPF ($p<0.05$). However, water uptake of RS film reinforced with higher concentration silane treated PPF showed significantly higher than RS film reinforced with alkaline treated PPF ($p<0.05$). It could be explained that the R-group of silane coupling agents contained hydrophilic properties resulted in higher interaction with water in surrounding atmosphere.

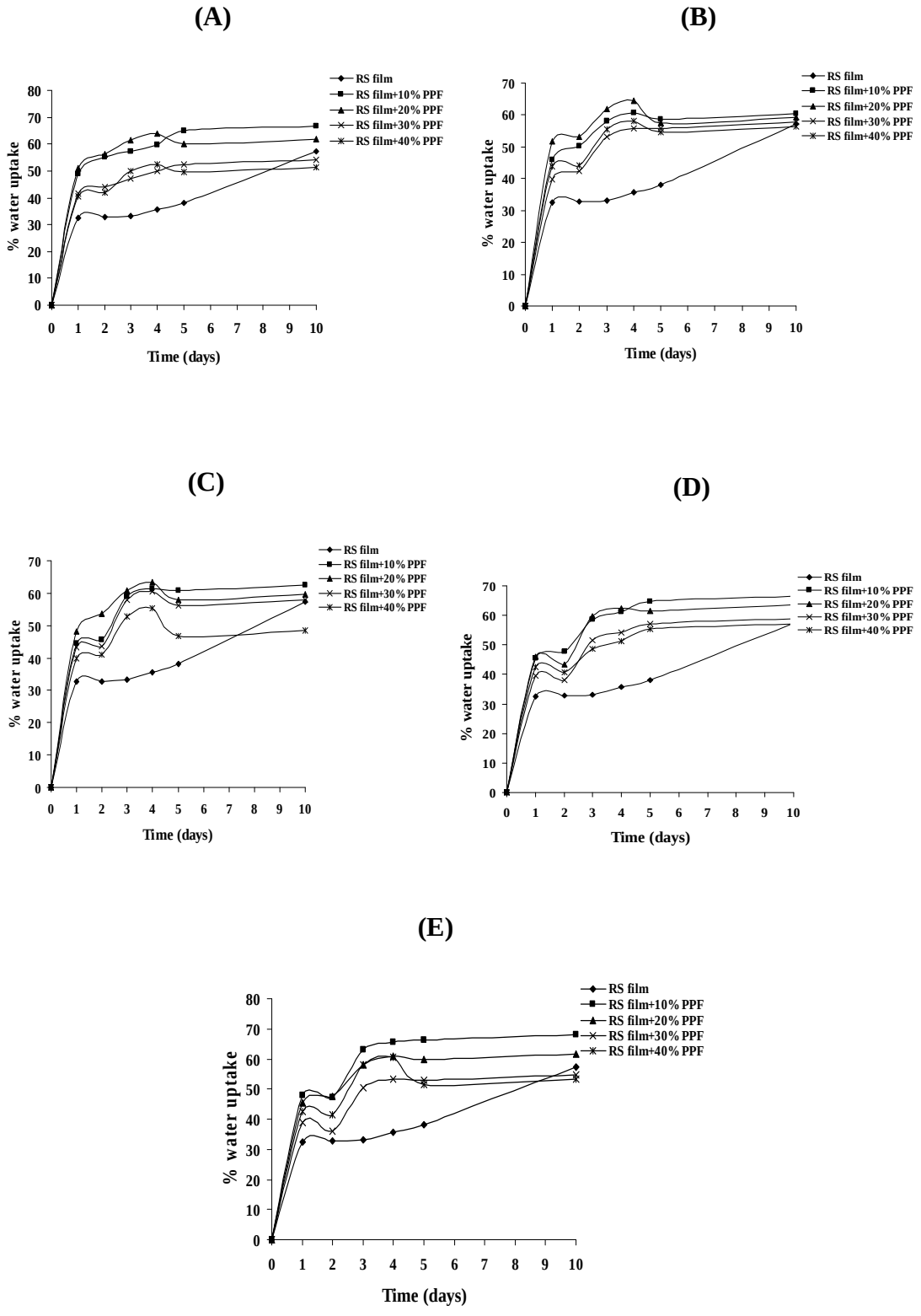

Figure 24. Effect of fiber surface treatment of PPF on water uptake of RS films: (A) 2%NaOH, (B) 10% Silane, (C) 20% Silane, (D) 30% Silane and (E) 40% Silane.

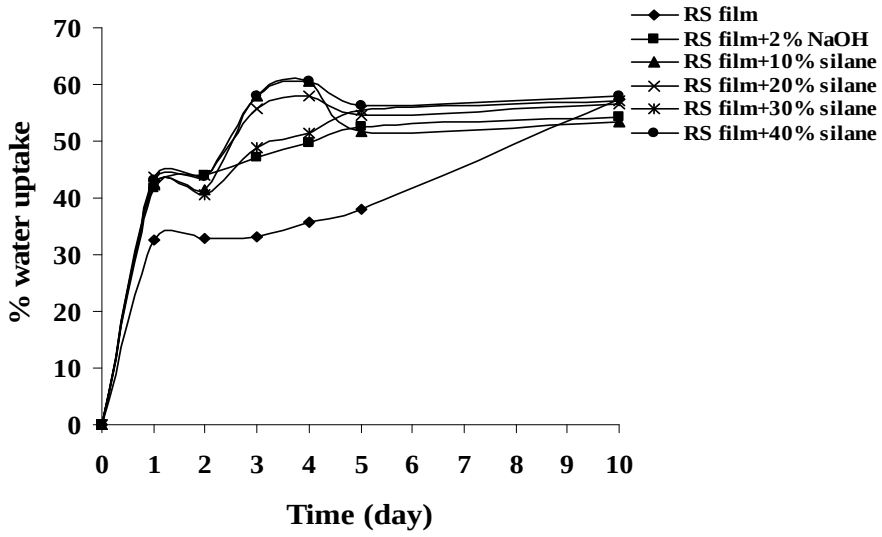

Figure 25. Effect of fiber surface treatment of 30% PPF content on water uptake of RS films.

4.5 Color and transparency

The results of the measurements performed on the RS film's color were expressed in accordance with CIELAB system and the rectangular coordinates (L*, a* and b*) and the total color difference (ΔE^*_{ab}), hue angle and chroma were calculated. Figure 26 and 27 depicted results from the effect of PPF surface treatment and content of PPF fillers on color (L*, a*, b*, $\Delta E^*_{ab,}$ chroma and hue angle) of RS films. The b* value and chroma of the RS films increased with the addition of silane treated PPF and alkaline treated PPF compared with untreated PPF. This elucidated that the increasing yellowness (b* and chroma) of film, possibly due to alkaline treated PPF and silane coupling agents have yellowish color, resulted in a yellowish of RS films. Comparing between alkaline and silane treated PPF on the color of RS films, found that both PPF surfaces treated did not significant different in L*, a*, $\Delta E^*_{ab,}$ and hue angle of RS films. The content of PPF fillers significant effect on the color of RS films. The b*, chroma and ΔE^*_{ab} values increased as content of both untreated and treated PPF increased from 10 to 40% concomitant with decreased in L*, a* and hue angle values. This indicated the decreasing lightness (L*) and increasing yellowness (b* and chroma) of film, possibly due to the white-yellowish color of PPF.

Addition of treated PPF into the RS films resulted in decrease their transparency. Rice starch film without PPF fiber was the highest transparent. However, the lower transparency of the RS films was noticed when a greater amount of PPF was incorporated (Figure 28). The decrease in transparency could possibly arise due to the light scattering from the retarding of light transmission of the PPF and RS/PPF films. At high level of PPF, the RS films demonstrated lower transparency than lesser PPF incorporation.

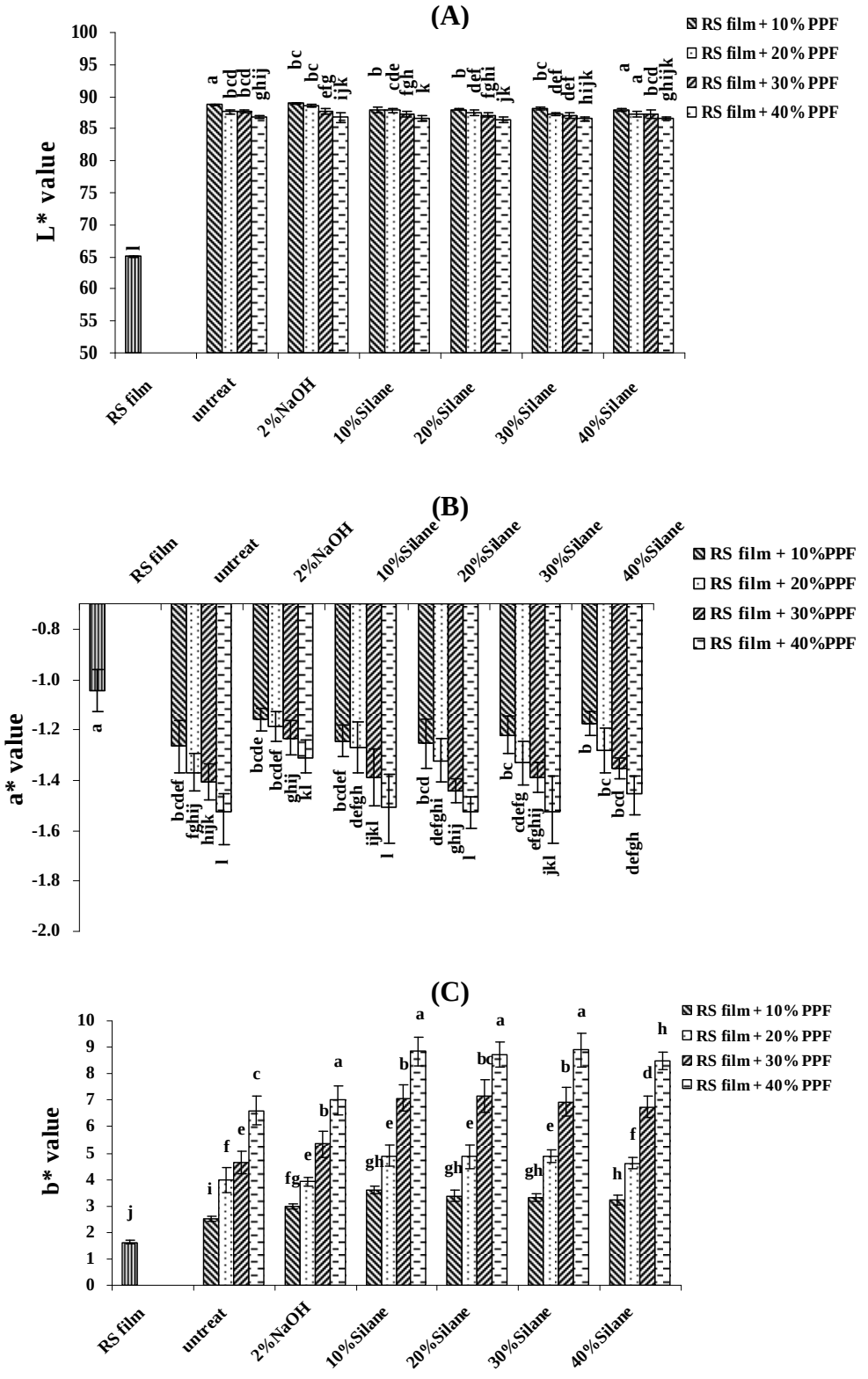

Figure 26. Effect of fiber surface treatment of PPF on L* (A); a* (B) and b* (C) of RS films. Mean values with different letter are significantly different ($p<0.05$).

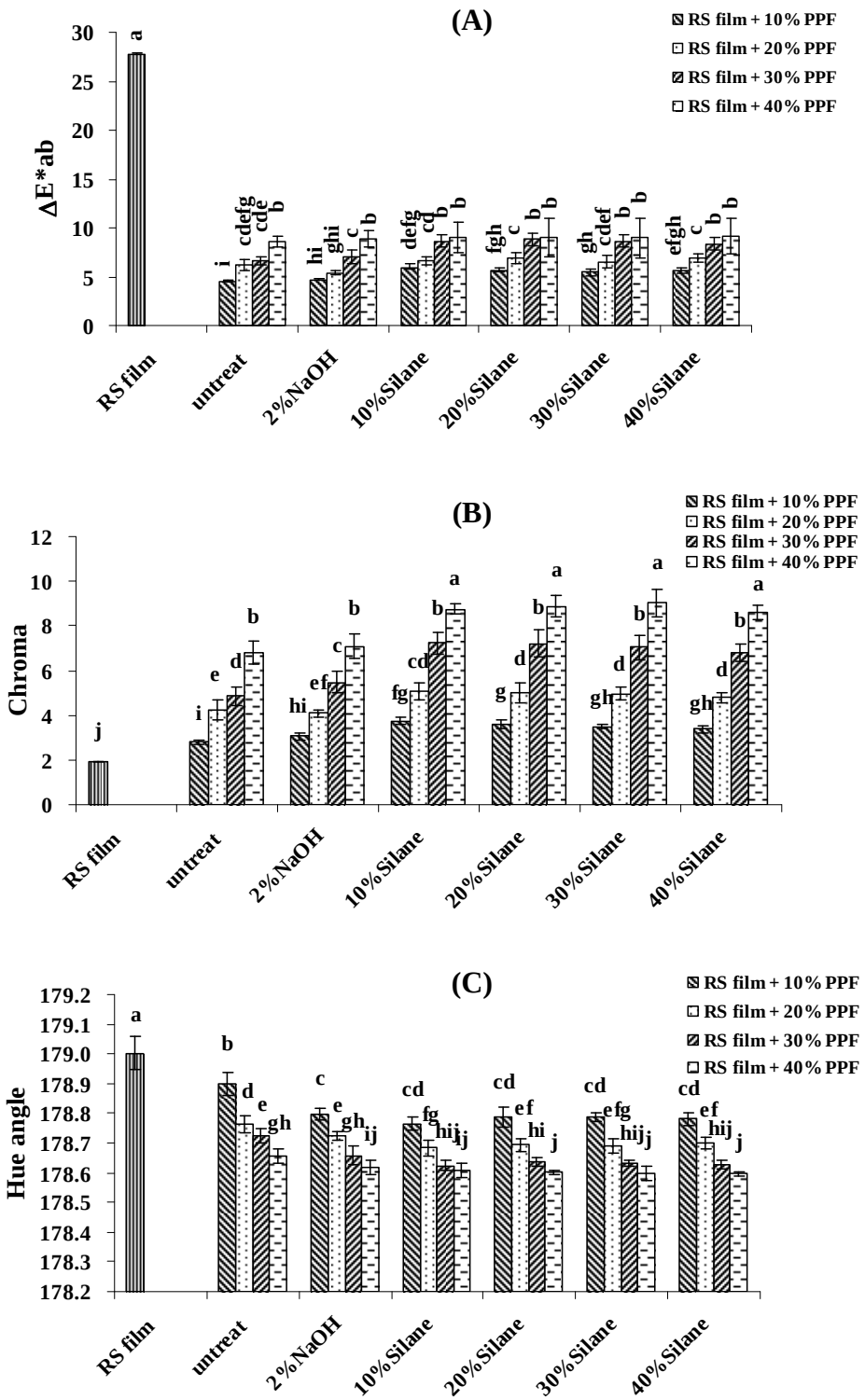

Figure 27. Effect of fiber surface treatment of PPF on ΔE* (A); Hue angle (B) and Chroma (C) of RS films. Mean values with different letter are significantly different ($p<0.05$).

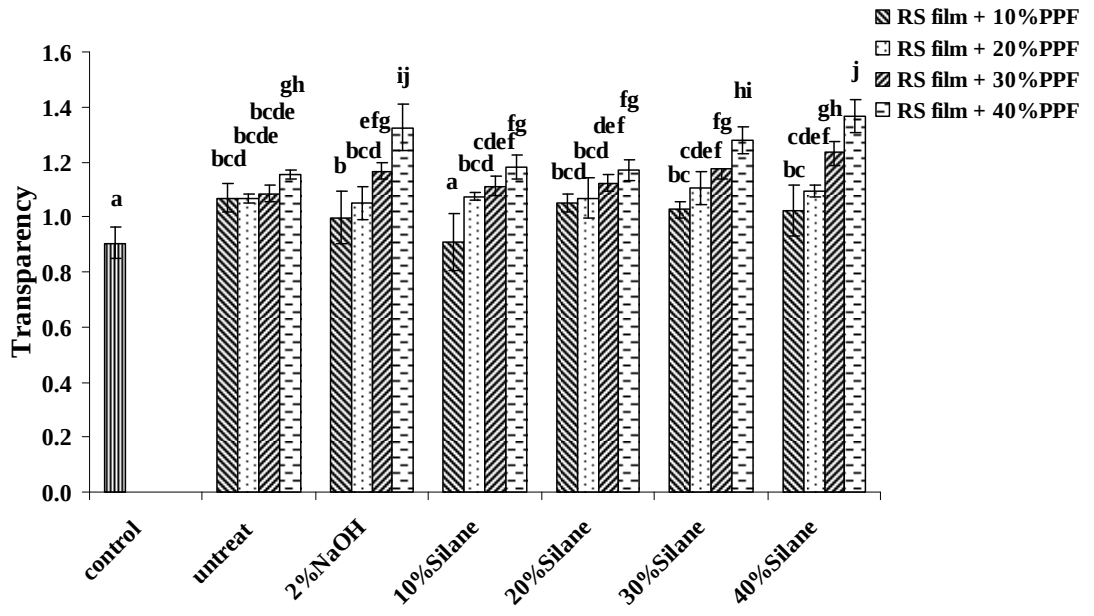

Figure 28. Effect of fiber surface treatment of PPF on transparency of RS films. Mean values with different letter are significantly different ($p<0.05$).

4.6 Thermal properties

According to the previous study addition of 30% treated PPF into RS films provided a good mechanical and barrier properties of resulted films. Hence, the RS films reinforced with treated PPF at 30% was selected for thermal properties investigation.

4.6.1 Thermogravimetric analysis (TGA)

TGA thermograms and the char yields (500 ℃) of various samples under nitrogen are shown in Figure 29. The behavior of the char yield curves was similar in the composites (Figure 29). The results demonstrated that addition of treated PPF showed little better thermal properties of RS films than untreated fiber. This difference was due to the good adhesion between RS films and fiber, the silane coupling agent like adhesive that increased adhesion between PPF and matrix (Park *et al.*, 2006). Similar trend was observed in the composites prepared by Shih (2006). For RS films reinforced with alkaline treated PPF had almost similar char yield with RS films reinforced with untreated PPF, by the reason of alkaline treated PPF had same composition and structure with the untreated PPF (Bledzki and Gassan, 1999). According to the results, found that the char yield of RS films was enhanced as PPF

content increased. Shih (2006) reported that the char yield is directly correlated to the potency of flame retardation for the polymers. Increasing char formation can limit the production of combustible gases, decreased the exo-thermicity of the pyrolysis reaction, and inhibit the thermal conductivity of the burning materials.

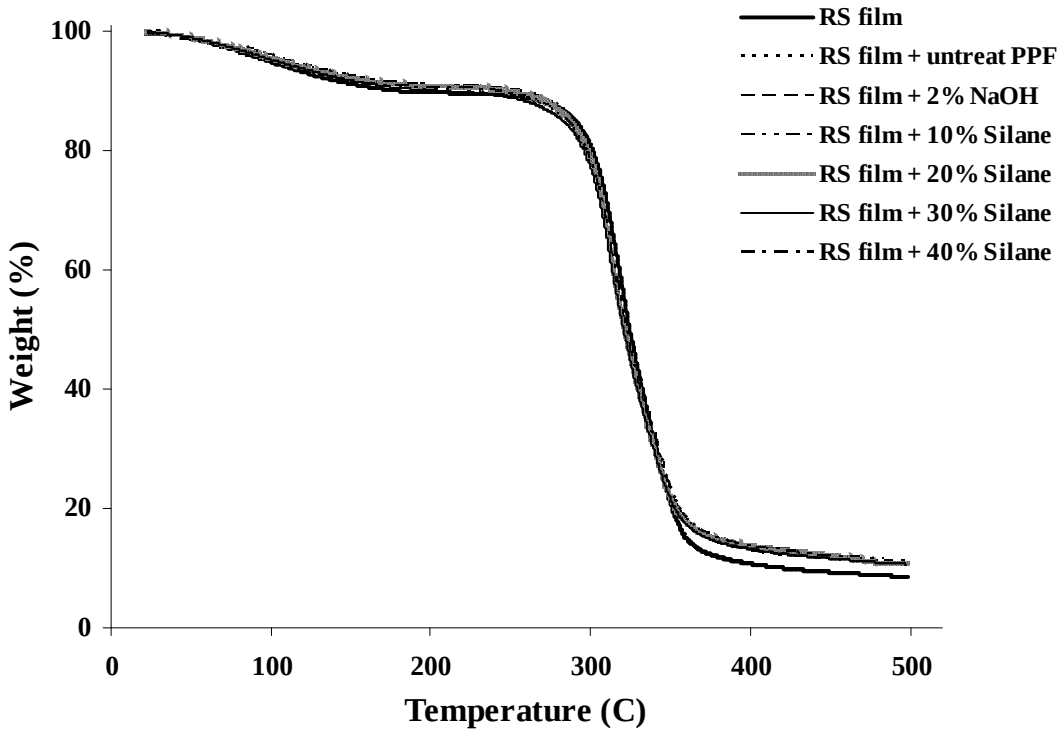

Figure 29. TGA thermograms of RS films, RS film reinforced with untreated PPF and treated PPF (30% of starch).

4.6.2 Differential scanning calorimetry (DSC)

Figure 30 shows the DSC curves RS films; RS film reinforced with untreated PPF and treated PPF. No endothermic peaks, assigned to the glass transition temperature (T_g) of RS films. However, it can be observed from the increasing of endothermic heat flow when PPF was added into RS films. The endothermic heat flows of RS films reinforced with treated PPF fibers was higher than RS films reinforced with untreated PPF. Comparing the effect of PPF surface treatment methods, the result showed that the endothermic heat flow of the RS films reinforced

with silane treated (20-40% concentration of silane) PPF showed higher than RS films reinforced with alkaline treated PPF, however RS films reinforced with 10% of silane concentrate treated PPF exhibited lower the endothermic heat flow than the RS films reinforced with alkaline treated PPF. For the silane concentration, when increasing concentration of silane treated PPF. It could be explained that the silane coupling agent could perform better compatibility between PPF fiber and starch matrix, which reduces the flexibility of molecular chains of starch (Lu *et al.,* 2006). In addition, silane coupling agent is the synthetic chemical, hence it was difficult to destroyed when received heat (Agrawal *et al.,* 2000).

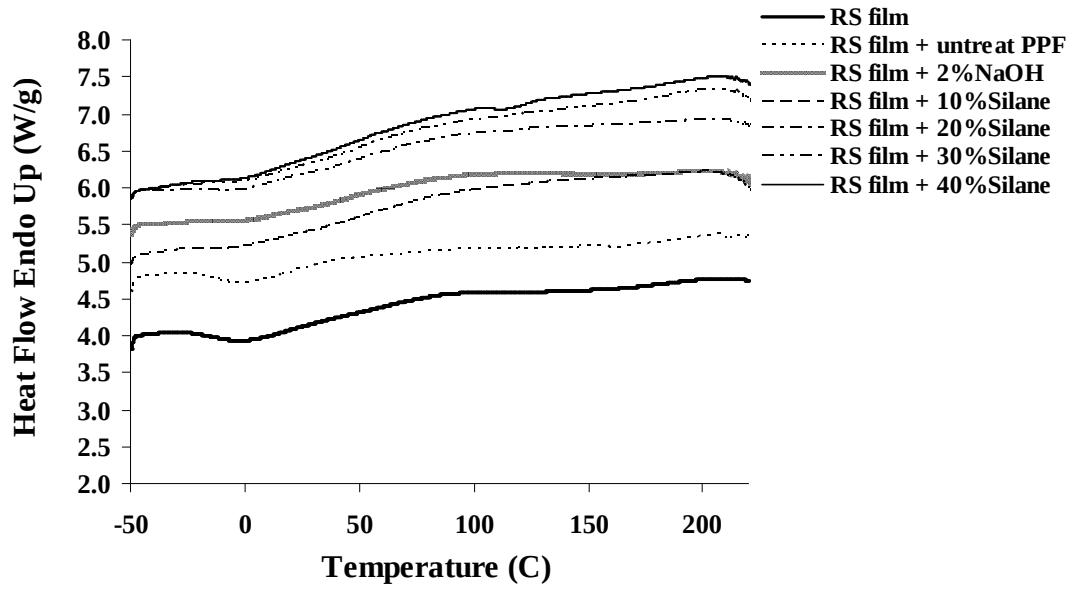

Figure 30. DSC curves of RS films; RS film reinforced with untreated PPF and treated PPF (30% of starch).

4.6.3 Dynamic mechanical thermal analysis (DMTA)

The dynamic mechanical thermal properties of the RS film and the RS reinforced with untreated and treated PPF were studied by DMTA measurements. DMTA is a very suitable tool to investigate the viscoelastic properties of materials in a wide range of temperatures and does not only provide fundamental information at the molecular level, but also correlates results with those obtained from tensile testing (Alemdar and Sain, 2007). In all the cases, a fiber loading of 30% have been used.

The storage modulus (E') of the RS film and the RS reinforced with untreated and treated PPF films as a function of temperature is given in Figure 31A. The peak of the storage modulus (E') value occurs at the temperature range around 110 ℃ to 140 ℃. The storage modulus of the films was increased when the treated PPF were added to RS film compared to the RS reinforced with untreated PPF films. Further the results showed that the storage modulus of the RS film reinforced with alkaline treated PPF showed lower than the RS films reinforced with silane treated PPF (20-40% of silane concentration). It could be explained that the change in the molecular structure of the starch polymer by interaction with the organo functional group of the silane treated fiber. The organo functional group of the silane forms interpenetrating polymer networks with the starch matrix that can be believed to cause the change in the polymer structure (Pothan and Thomas, 2003). The molecular structure of the polymer profoundly affects the T_g (Aklonis and MacKnight, 1983). The results pointed out that concentration of silane coupling agents also affected the E' of RS films, found that, E' tended to increase as silane concentration increase from 10 to 40% by the reason of silane coupling agents could be improved the thermal properties by the better adhesion between the filler and the matrix.

Figure 31B shows the tan δ curves of the RS film and RS film reinforced with treat and untreated PPF as function of temperature. The glass transition temperatures were estimated from the tan δ peaks. The results depicted that there is a broad peak in tan δ at around 148 ℃ of pure RS film and the T_g increased when untreated PPF was added into RS film. Additionally, the peak of tan delta of RS film reinforced with untreated shifted from 166 ℃ to 187 ℃ when reinforced with treated PPF. Similar results were observed by Agrawal *et al.* (2000). According to the results, increasing concentration of silane resulted in increased T_g of RS films. These results indicate that the fiber treated by coupling agents exhibited better compatibility with the starch matrices than the untreated fibers. Eklind and Maurer (2003) have reported on an interlayer model to simulate the dynamic mechanical properties of filled blends. The filler particles have been reported to be surrounded by an interlayer attached to the filler surface. This phenomenon could give rise to filler structure in the matrix able to alter the dynamic mechanical modulus (Ray *et al.,* 2001).

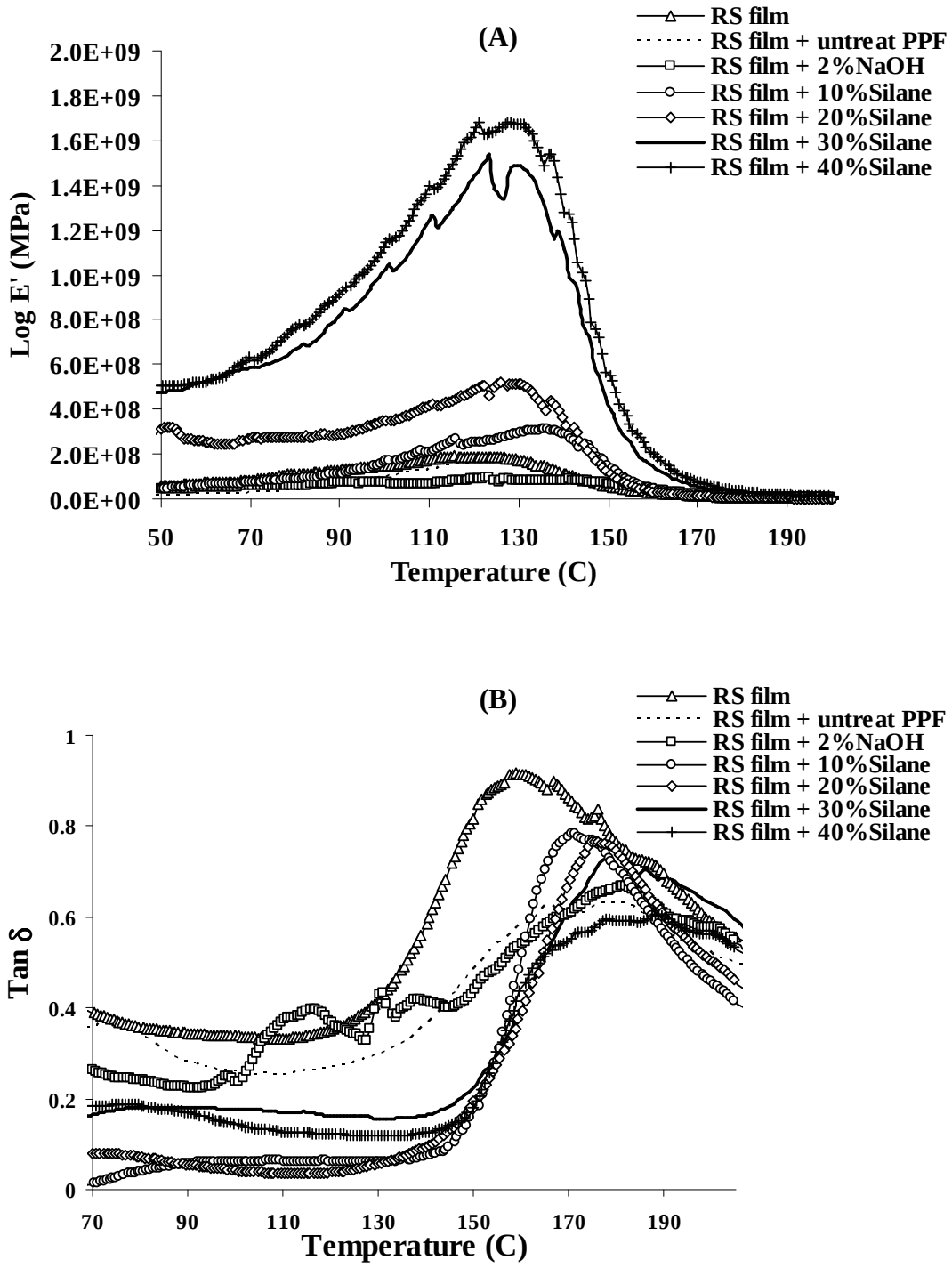

Figure 31. The dynamic mechanical behaviors of (A) storage modulus and (B) loss factor (tan δ) as a function of temperature for of RS films and RS films reinforced with treated and untreated PPF.

4.7 Morphology of the films

Morphology of RS films reinforced with untreated PPF and treated PPF at 30% PPF content is shown in Figure 32. The result showed that RS films reinforced with alkaline treated PPF demonstrated smaller particles and smoother than RS film reinforced with silane treated PPF (Figure 32A). Possible to the silane treated PPF were covered with the silane coupling agent (Figure 32C-F), and the silane coupling agent were increased binding between starch matrix and fiber.

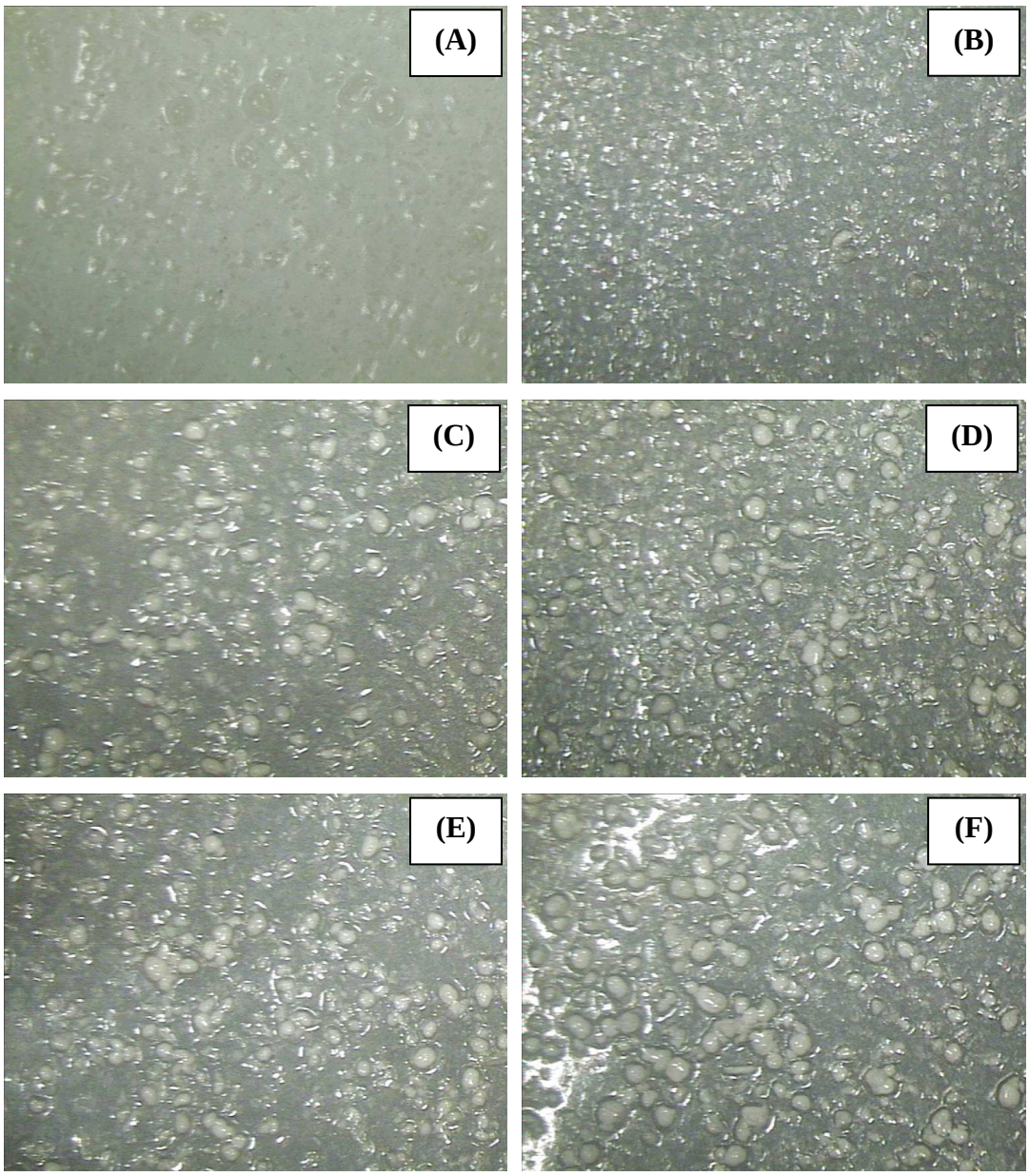

Figure 32. Surface (×10) of RS films reinforced with (A) untreated, (B) 2% NaOH, (C) 10% Silane, (D) 20% Silane, (E) 30% Silane and (F) 40% Silane PPF at 30% PPF fillers.

5. Effect of crystalline cellulose (CC) on the properties of rice starch films

5.1 Particle size distribution

Crystalline cellulose (CC) was prepared by acid hydrolysis of palm pressed fiber and the particle size was analyzed by Laser Particle Size Analyzer (LPSA). The results showed that the most presence (60-70%) of particle size distribution in the nanometer scale (90±0.051nm) (data not shown).

5.2 X-ray diffraction

X-ray diffraction was used to determine the crystallinity of the materials. The crystallinity of the starch powder, cellulose powder (PPF), crystalline cellulose (CC) and RS films are shown in Figure 33 and Figure 34. As observed, the rice starch powder showed a trypical A-type diffraction pattern with strong reflection at 17 and 17.5 degree. This result shows a reasonable agreement with experimental of Bourtoom and Chinnan (2008). The diffraction peak of PPF powder was founded at 17 and 22.5 degree. Similar results were observed by Alemdar and Sain (2007). The results showed that diffraction peak of CC were sharper than the diffraction peak of PPF powder The sharper diffraction peak is an indication of higher crystallinity value in the structure of the cellulose powder (PPF). The crystallinity values were estimated as 69.67% and 94.60%, for the PPF and CC, respectively. The increase in the crystallinity of the CC is due to partial removal of the hemicellulose, lignin which was amorphous phase during the extracted CC processing (Alemdar and Sain, 2007). The dried regular rice starch films, after gelatinization, had different structures. The amorphous structure was observed in the rice starch film and the crystallinity value was estimated as 25.91%. When the CC was added into RS films, the results showed that the crystallinity was increased. Furthermore, increasing of CC content from 10 to 40% of starch resulted in an increase of crystallinity value. These results suggest that CC increased the crystallinity of the RS films, as has been reported by other authors, who attributed this phenomenon to the more crystalline nature of cellulose fiber (Amash and Zugenmaier, 2000; Ma *et al.*, 2005).

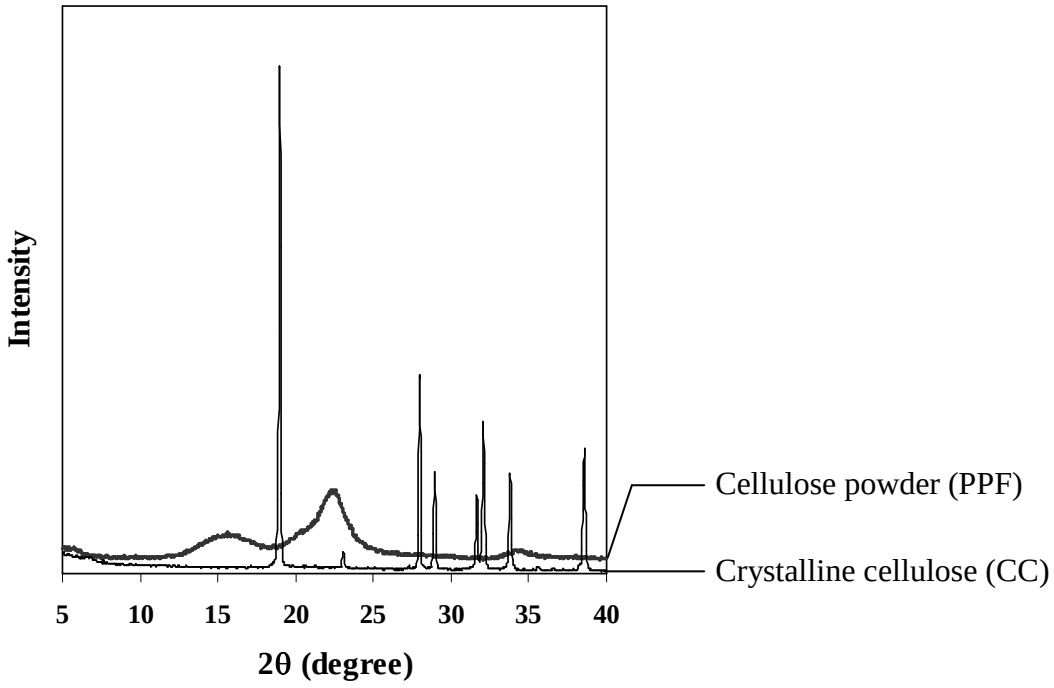

Figure 33. X-ray diffractograms of PPF powder (PPF) and crystalline cellulose(CC).

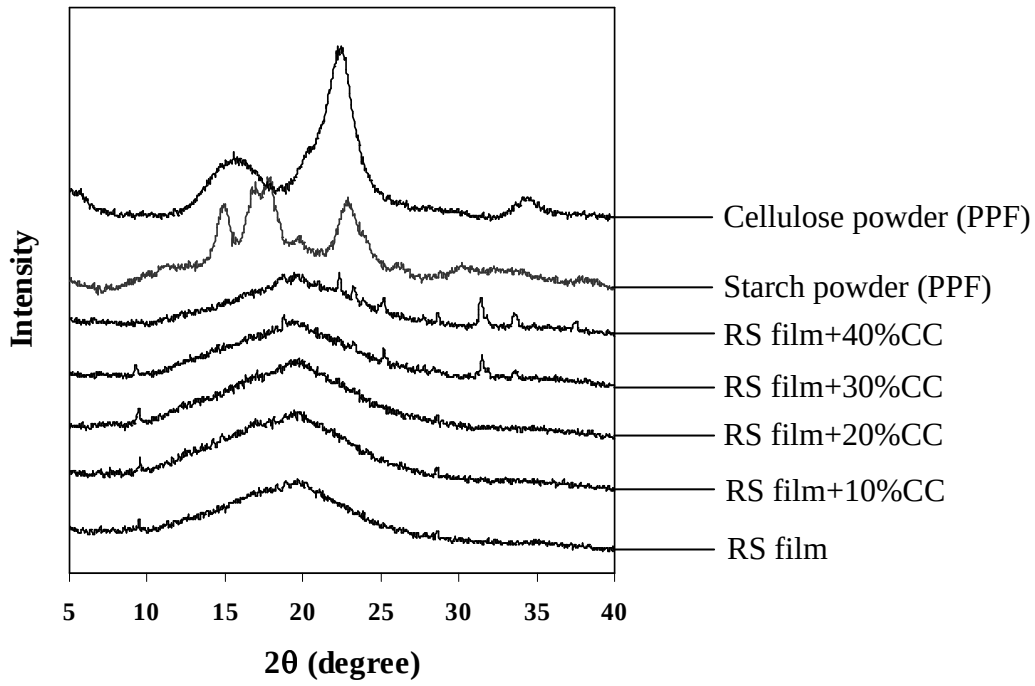

Figure 34. X-ray diffractograms of starch powder, cellulose powder, RS film and RS films reinforced with CC at various content.

5.3 Tensile strength (TS) and elongation at break (ε)

Biopolymer materials, such as films, may be subjected to various kinds of stress during use; the determination of the mechanical properties involves not only scientific but also technological and practical aspects (Cagri *et al*., 2001). Tensile strength (TS), elongation at break (ε) are parameter that relate mechanical properties of films to their chemical structure (McHugh and Krochta, 1994) TS expresses the maximum stress developed in a film during tensile testing (Gennadios, 1994). The TS and ε of the RS films reinforced with crystalline cellulose (CC) from PPF is depicted in Figure 35. This figure clearly demonstrates the reinforcing effect of CC fillers. The TS of the RS films increased from 5.66 MPa to 18.52 MPa when increasing the CC fillers content from 0 to 20% (Figure 35A). This was due to the remarkabled instrinsic adhesion of the filler-matrix interface caused by the chemical similarity (polysaccharide structure) of starch and CC (Ma *et al.,* 2008). The existence of such interaction, related to the contents of CC, has already been confirmed by Averous *et al.* (2001). Moreover, Suryanegara *et al.* (2009) reported that when the content of crystallinity (X_c) increased resulted in increase of TS of composites films, due to the crystallite structure of the CC makes the composites were strength. Similar results were observed by Angles and Dufresne (2001), Lu *et al.* (2006), Pu *et al.* (2006), Alemdar and Sain (2007) and Muller *et al.* (2009). However, the addition of CC at 30-40% could induce the conglomeration, as indicated by SEM (Figure 44), which actually decreased the effective contents of CC. Thus, RS films reinforced with 30-40% CC contents exhibited lower tensile strength (TS) than that with 10-20%.

Regarding the ε, results showed that increasing of CC fillers from 10-20% provided an increase in ε from 10.42% to 15.51%. However, addition of CC fillers higher than 20% resulted in decreased elongation at break (Figure 35B). It is possibly due to the presence of high content of CC fillers might contribute to retarding the intermolecular interaction of the starch films. This induces the development of a heterogeneous film structure, featuring discontinuities, resulting in the decrease in ε of the films. In addition, CC fillers could not fully homogeneous and form small aggregates when 30-40% of CC fillers were filled. The results showed that addition of CC fillers provided the better mechanical properties of RS films in this work and they

are similar to those of biocomposites of plasticized starch reinforced with crystalline cellulose from cottonseed linter (Lu *et al*, 2005).

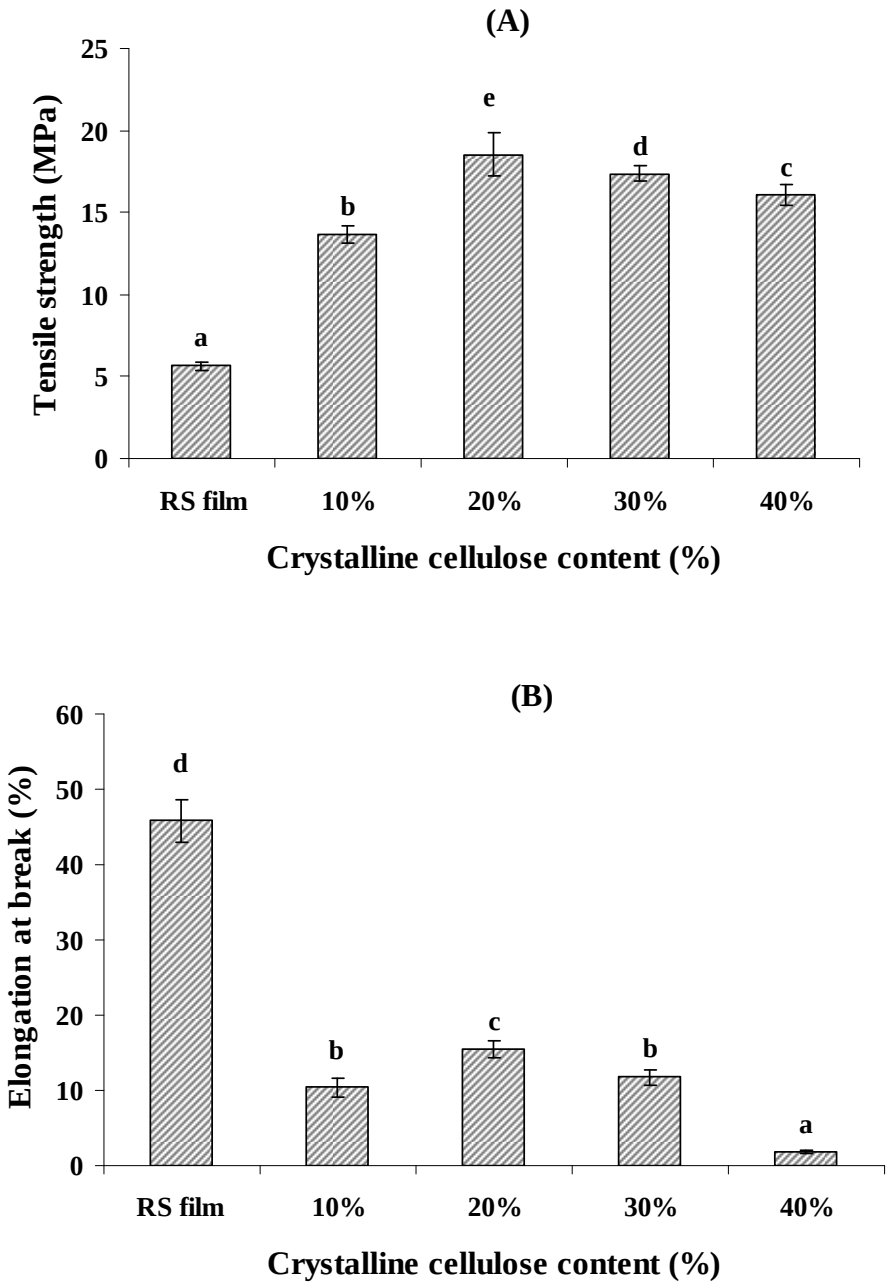

Figure 35. Effect of content of crystalline cellulose (CC) on tensile strength (A) and elongation at break (B) of RS films. Mean values with different letter are significantly different ($p<0.05$)

5.4 Water vapor permeability (WVP)

Water vapor permeability is proportionality constant assumed to be independent of the water vapor pressure gradient applied across the films. However, hydrophillic (edible or nonedible) materials, such as strach films, derivative from this ideal behavior due to interactions of permeating water molecules with polar groups in the films structure (Hagenmaier and Shaw, 1990). Deviation from the ideal behavior can also be induced by temperature effects on materials (Myers *et al*., 1962). Since a main function of an edible films or coatings are often to impede moisture transfer between food and the surrounding atmosphere, or between two components of a heterogeneous food products, water vapor permeability should be low as possible. The WVP of rice starch films with different CC were determined at a vapor pressure difference of 0/60% across films. The effect of content of CC fillers on water vapor permeability (WVP) of the rice starch films is shown in Figure 36. The WVP of rice starch films decreased as the content of CC fillers increased. For example, the WVP of the films decreased from 13.96 g.mm/m^2.day.kPa to 3.74 g.mm/m^2.day.kPa when increasing the CC fillers content from 0 to 40% (Figure 36). The improvement of the WVP of the RS films can be attributed to the formation of a rigid hydrogen-bonded network of cellulose in the RS composite films that is governed by percolation mechanism (Pu *et al.*, 2006). These considerations and the importance of the CC fillers aspect ratio are undoubtedly contributing factors to the mechanical and physical properties of the RS films reinforced with CC reported in this study. Moreover, comparing of WVP between the RS films reinforced with PPF in the previous study and RS films reinforced with CC at the same content of fillers, found that the RS films reinforced with CC had better water vapor barrier than the RS films reinforced with PPF, by the reason of the hydrophobic crystalline of CC led to the reduction of permeability (Ma *et al.*, 2008).

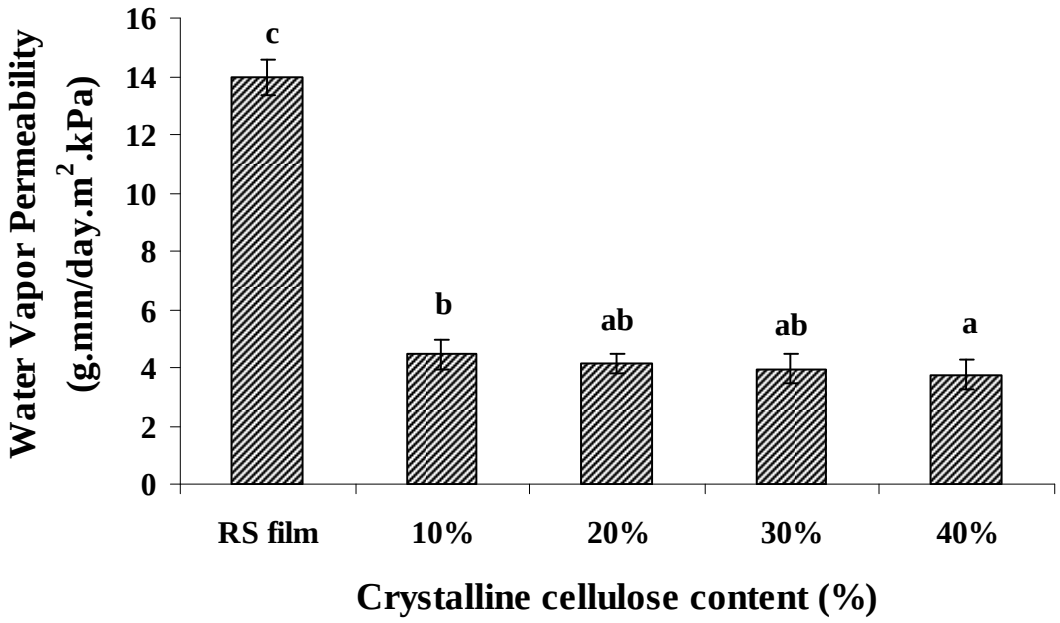

Figure 36. Effect of content of crystalline cellulose (CC) on water vapor permeability of RS films. Mean values with different letter are significantly different ($p<0.05$).

5.5 Water uptake

Water sensitivity is another important criterion for many practical applications of RS films. Figure 37 shows the water uptake of RS film and RS films reinforced with different content of CC fillers during conditioning in 98% RH as a function of time. The water uptake –t curves display two well-separated zones. At shorter times, t < 2 day or 48 h, the kinetics of absorption is very fast, whereas at longer times, t > 2 days, the kinetics of absorption is slow and leads to a plateau, corresponding to the water uptake at equilibrium. The water uptake at equilibrium were significantly decreased with increasing the content of CC fillers ($p<0.05$) because the biocomposite RS films display a reduced swelling capacity (Lu *et al.*, 2006). Svagen *et al.* (2009) reported that the moisture uptake decreased with increasing content of cellulose. Cellulose nanofibers are less hygroscopic than starch due to the higher degree of molecular order and the cellulose nanofiber network is reducing the swelling and thereby the moisture uptake.

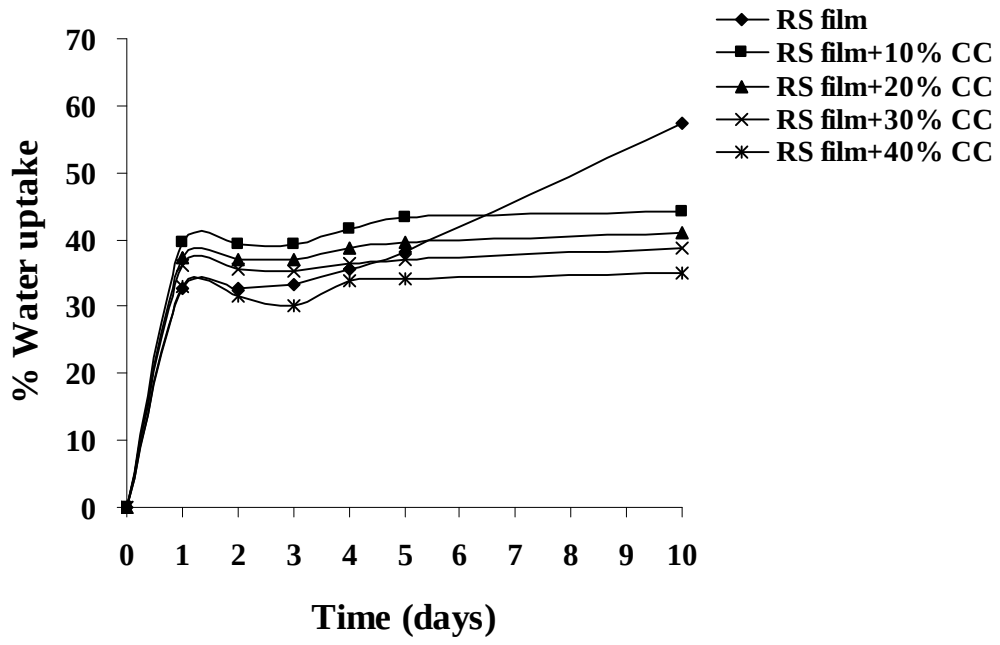

Figure 37. Effect of content of crystalline cellulose (CC) on water uptake of RS films.

5.6 Color and transparency

Figure 38 and Figure 39 shows the results from the effect of content of CC fillers on color (L*, a*, b*,$\Delta E^*_{ab,}$ chroma and hue angle) of rice starch films. The result showed that the content of CC fillers significant effect on the color of RS films. Rice starch films became more darker as evidenced by the decrease L*, a* and hue angle values as the content of CC filled rice starch increased from 10 - 40% concomitant with decreased in b*, ΔE^*_{ab} values and chroma. This indicated the decreasing lightness (L*) and increasing yellowness (b* and chroma) of the RS films, possibly due to the white-yellowish color of the CC. Figure 40 shows the results from the effect of content of CC fillers on transparency of the RS films. Addition of CC into the RS films resulted in decrease their transparency. Rice starch film with out CC fiber was the highest transparent. However, the lower transparency of the films was noticed when a greater amount of CC was incorporated (Figure 40). The decrease in transparency could possibly arise from the light scattering from the retarding of light transmission of the CC and RS/CC films. At high level of CC, the RS films demonstrated lower transparency than lesser CC incorporation.

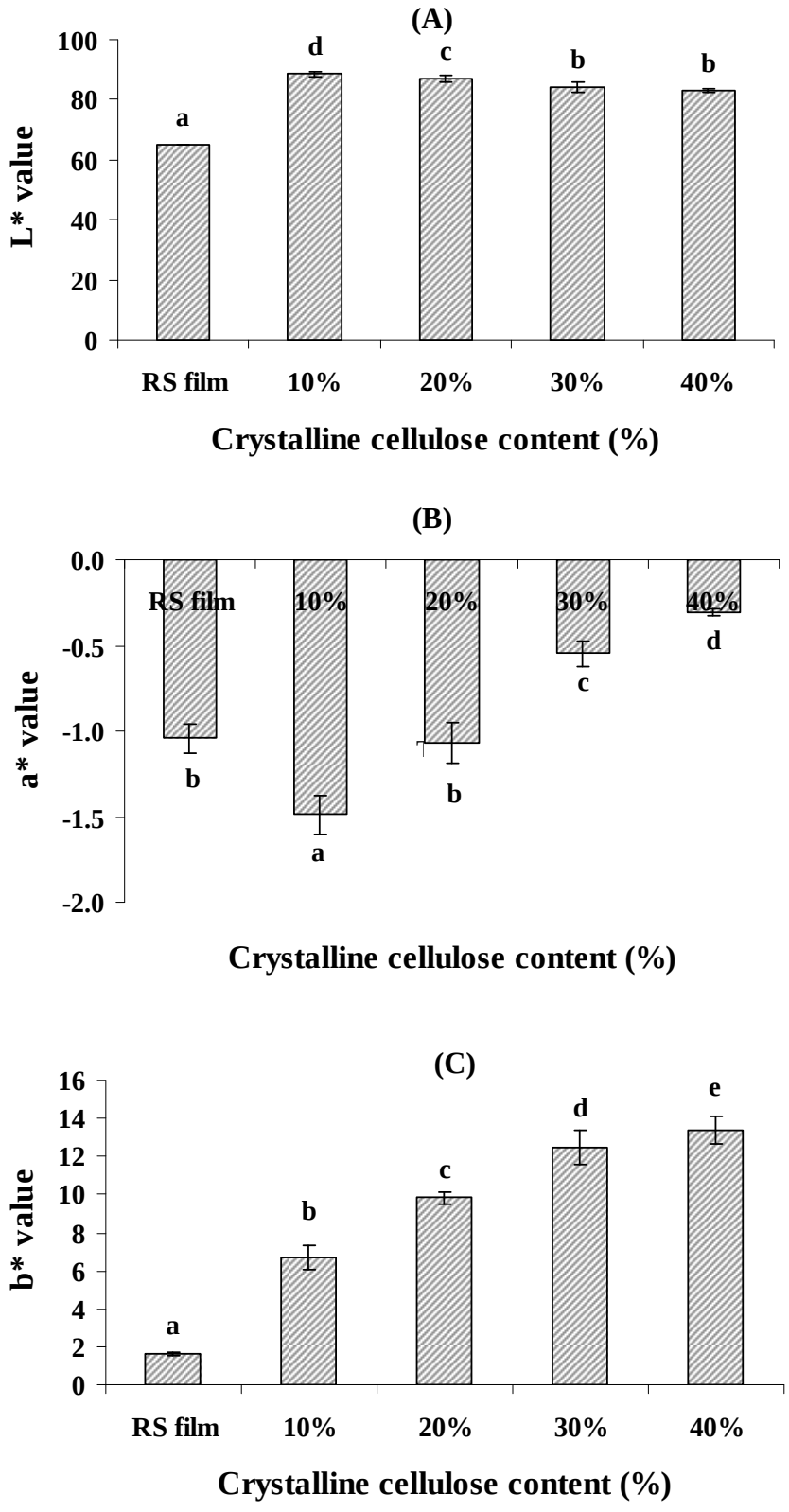

Figure 38. Effect of content of CC on L* (A); a* (B) and b* (C) of RS films. Mean values with different letter are significantly different ($p<0.05$).

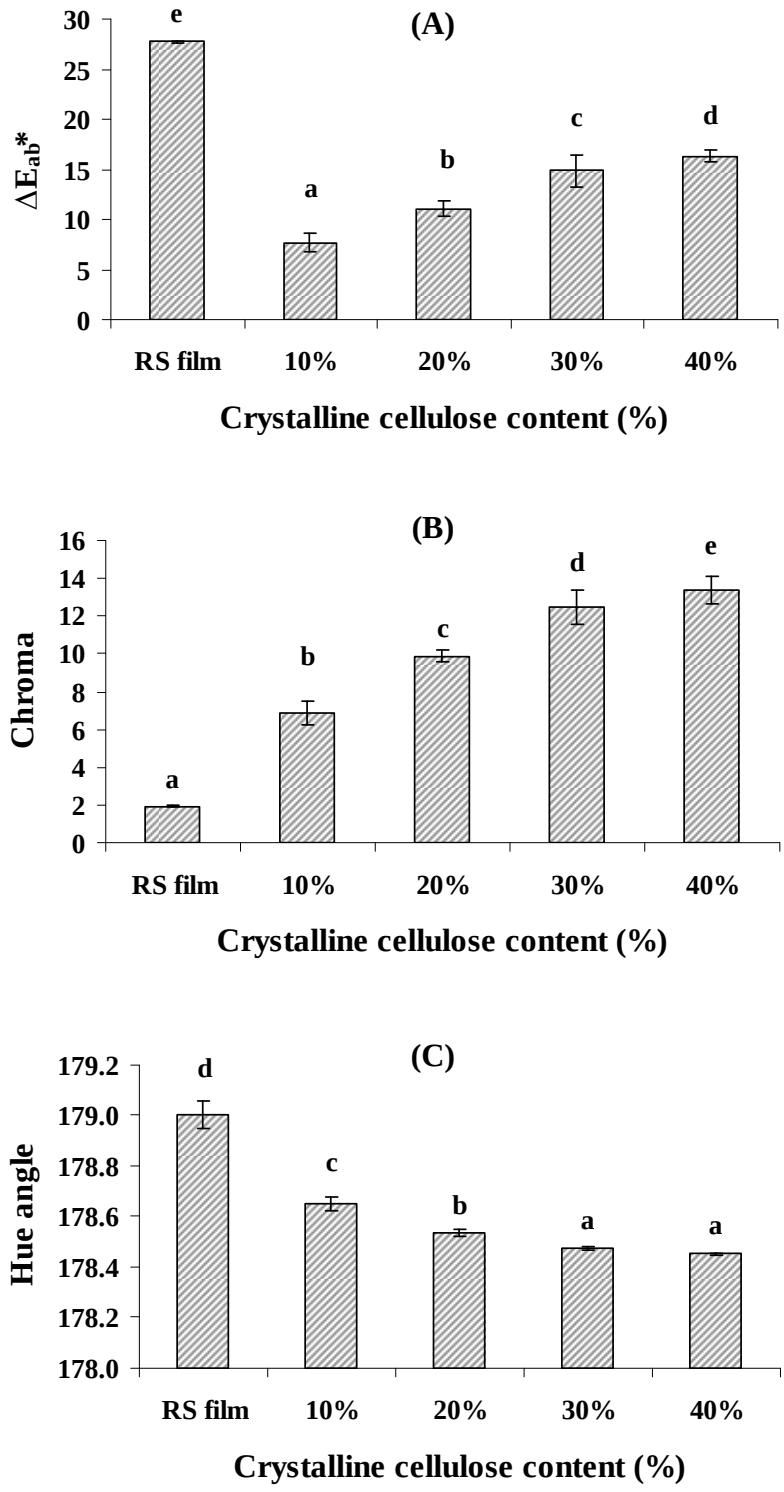

Figure 39. Effect of content of CC on ΔE* (A); Hue angle (B) and Chroma (C) of RS films. Mean values with different letter are significantly different ($p<0.05$).

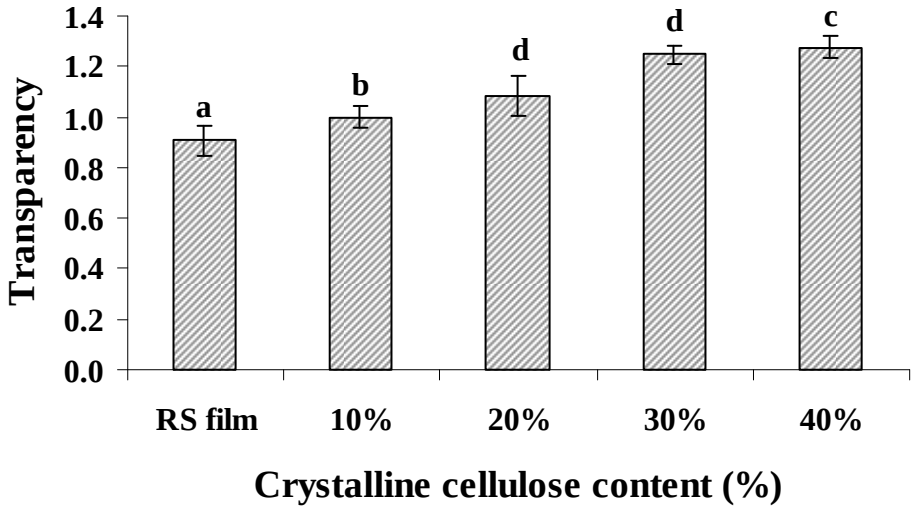

Figure 40. Effect of content of CC on transparency of RS films. Mean values with different letter are significantly different ($p<0.05$).

5.7 Thermal properties

5.7.1 Thermogravimetric analysis (TGA)

Thermogravimetric analysis (TGA) was performed for the composites, where the mass loss due to the volatilization of the degradation products was monitored as a function of temperature. Figure 41 shows the TGA thermograms of the RS film, CC and RS films reinforced with 10-40% of CC fillers content. It was found that the RS film starts to degrade at around 73.44, 89.98, 91.03, 95.64 and 97.15°C for the RS films reinforced with CC at 0-40%, respectively. The decline on the weight loss of the RS film and RS films reinforced with CC is due to evaporation of the plasticizer or sorbitol (Alemdar and Sain, 2007; Ma *et al.,* 2008). TGA thermograms show that the degradation temperature of the polymer matrix and the biocomposite films are close to each other and smaller than that of each component. These results are on agreement with Averos and Boquillon's work (2004) where they showed that the degradation temperature variations between thermoplastic starch and the composite filled with lignocellulosic fibers are rather low. The char yield of RS film was lesser (8.50%) than RS films reinforced with CC (19.66-27.76%), resulting from the greater thermal stability of the CC. By the reason of the mainly composition of CC contains high crystalline that is strong structure and the char yield of the CC was

90.95%. Therefore, addition of CC into the RS films can be improved the thermal stability of RS films. It was found that the char yield of RS films was enhanced as CC fillers content increased. The result showed that the CC was related to the good thermal stability of crystalline structure and the good interaction between CC and starch matrix (Ma *et al.*, 2008).

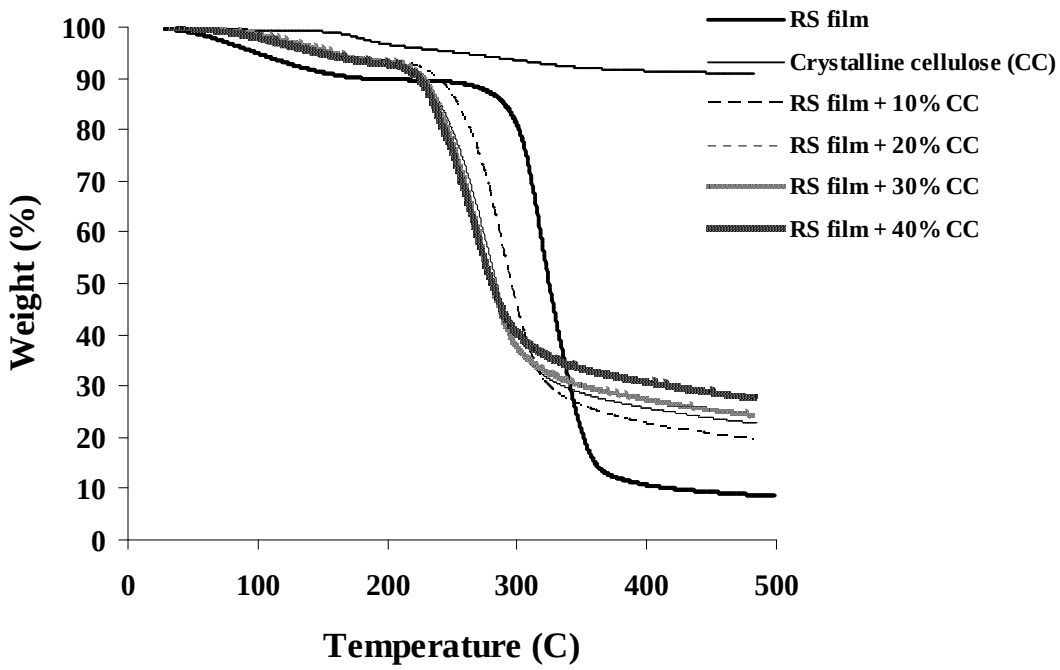

Figure 41. TGA thermograms of CC, RS films and 10-40% of CC reinforced RS films.

5.7.2 Differential scanning calorimetry (DSC)

Typical DSC thermograms of the RS film and RS films reinforced with 10-40% of CC fillers are depicted in Figure 42. No endothermic peaks, assigned to the glass transition temperature (T_g) of RS films. However, the increasing of endothermic heat flow was observed when CC was added into RS films. With the increase of CC contents, the endothermic heat flow increased gradually, might be attributed to the occurrence of intermolecular interactions occurred between starch and stiff crystallites of CC, which reduces the flexibility of molecular chains of starch (Lu *et al.*, 2006) and the CC was related to the good thermal stability of crystalline structure and the good interaction between CC and starch matrix (Ma *et al.*, 2008). This behavior was

already observed with different polysaccharides reinforced with cellulose fiber (Curvelo *et al.*, 2001; Ma *et al.*, 2005; Arbelaiz *et al.*, 2006).

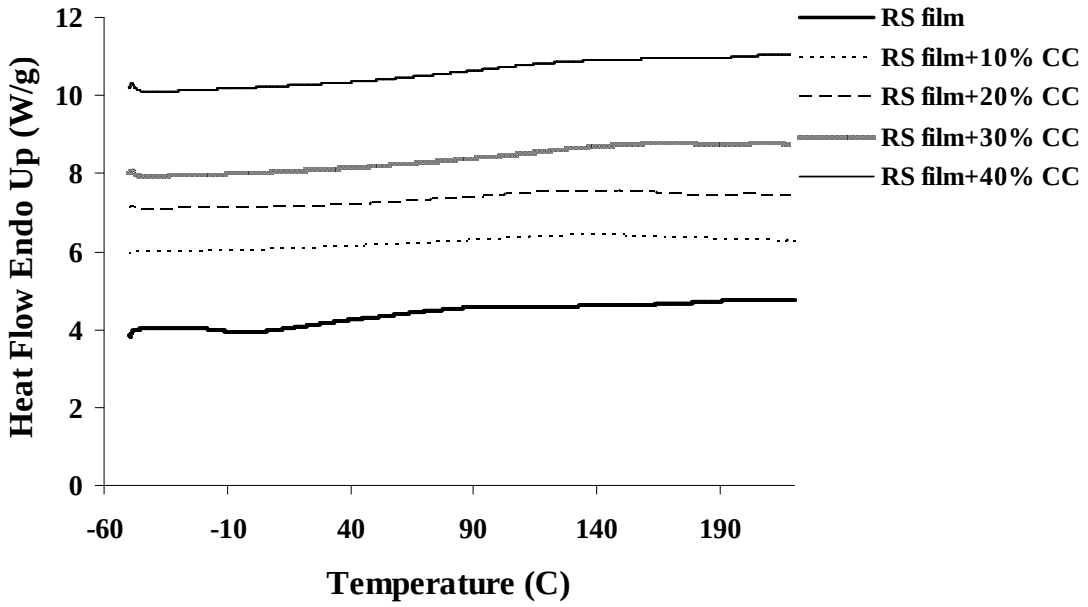

Figure 42. DSC curves of RS films and 10-40% of CC reinforced RS films.

5.7.3 Dynamic mechanical thermal analysis (DMTA)

Figure 43 shows the temperature dependence of dynamic mechanical thermal analysis behaviors for the RS film and RS films reinforced with 10-40% of CC. The results demonstrated that RS films contained 40% CC was broken during measuring the DMTA, resulted from the occurring of brittle films. Hence, only 10-30% CC was presented in this study. The storage modulus (E') of the RS film and RS films reinforced with CC as a function of temperature is given in Figure 43A. The storage modulus of the RS films increased with increasing CC content compared to the pure RS film. By incorporating CC fillers of 0 to 30% of starch, the thermal stability shifts to higher temperature. Iwatake *et al.* (2008) reported that the storage modulus of PLA reinforced with 20% nanofibers showed higher glass transition temperature (T_g) than pure PLA, that is, from 70°C to 120°C, resulting from the cellulose fiber network interconnected by hydrogen bonds resists the applied stress independently of the softening of PLA. Similar results by Ma *et al.* (2008), the storage

modulus of the nanocomposites was increased with increasing wheat straw nanofibers content compared to the pure thermoplastic starch.

Figure 43B shows the tan δ curves of the RS film and RS films reinforced with 10-30% CC fillers as a function of temperature. The glass transition temperatures were estimated from the tan δ peaks. The RS films exhibited a T_g at about 148 ℃. Alemdar and Sain (2007) reported that T_g of thermoplastic starch depends on the plasticizer content and humidity conditions as well as the composition of starch. The result demonstrated that increasing of CC content from 0 to 30% of starch resulted in increase in tan δ peak from 148 to 199 ℃, indicating that CC fillers affected the segmental motions of the RS films and decrease of the molecular mobility at the glass transition.

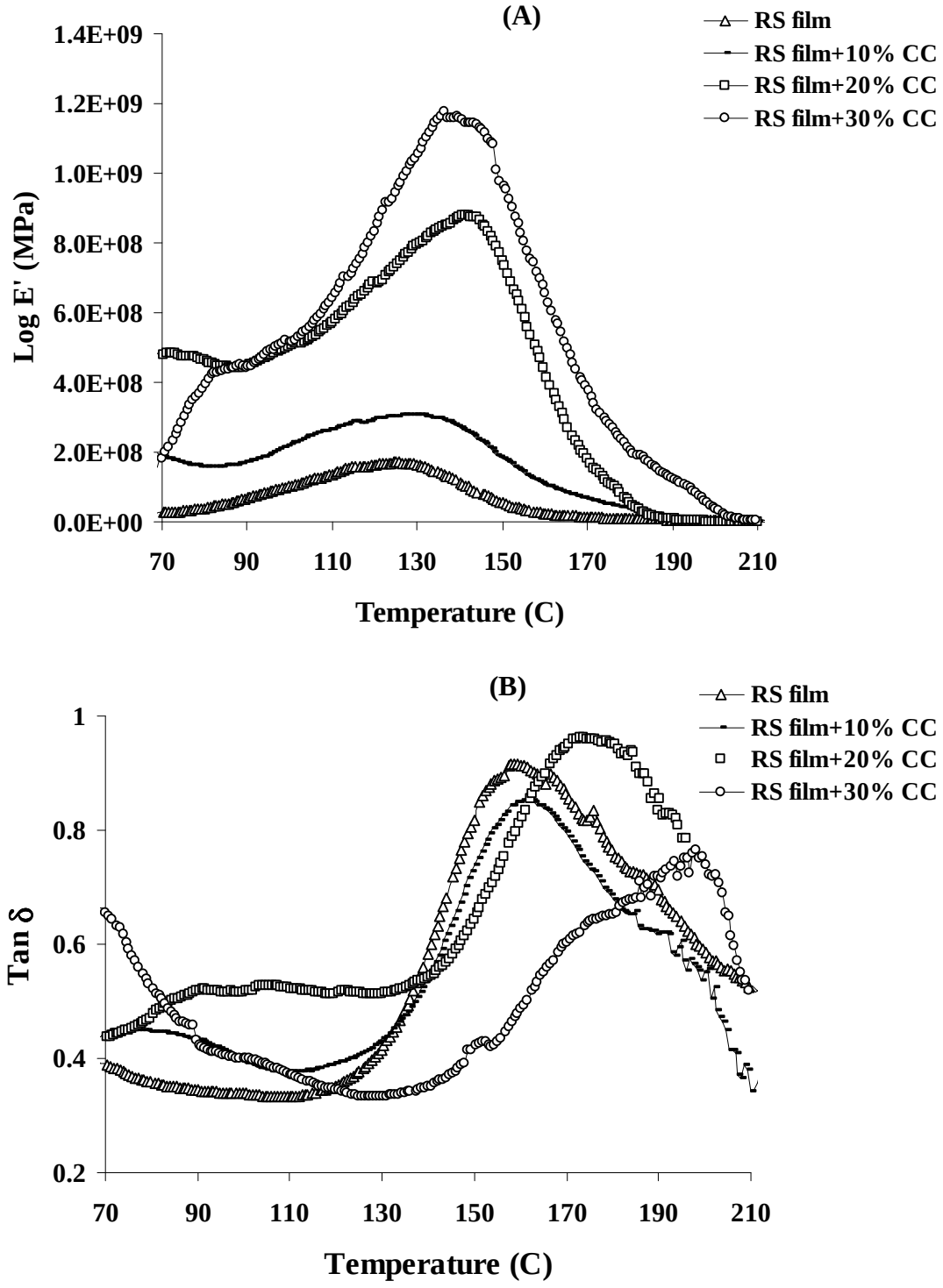

Figure 43. The dynamic mechanical behaviors of both (A) storage modulus (E') and (B) loss factor (tan δ) as a function of temperature for of RS film and 10-30% of CC reinforced RS films.

5.8 Morphology of the films

The morphology of the RS films was identified by Scanning electron microscopy (SEM). Figure 44 shows the surface of unfilled CC fillers (0%) and RS films reinforced with 10-40% of CC fillers. The rice starch film shows a relative smooth morphology. Compared with rice starch film, the surface morphology of the existence of the CC in the rice starch matrix can be easily observed in the composite films. However, it is difficult to distinguish the individual CC filler dispersion due to its small size. Some CC fillers appear as white domains at the surface of the sample (Figure 44). This should correspond to the CC filler in the perpendicular plane of the biocomposite film. By comparing the distribution of CC fillers into the rice starch films as affected by the CC content, the results showed that addition of CC fillers are more or less evenly distributed within the rice starch films. However some CC fillers are not fully individualized and form small aggregates (30- 40% of CC), which indicates some porosity, the results were relationship with the decreasing of tensile strength on RS films at high content of CC fillers.

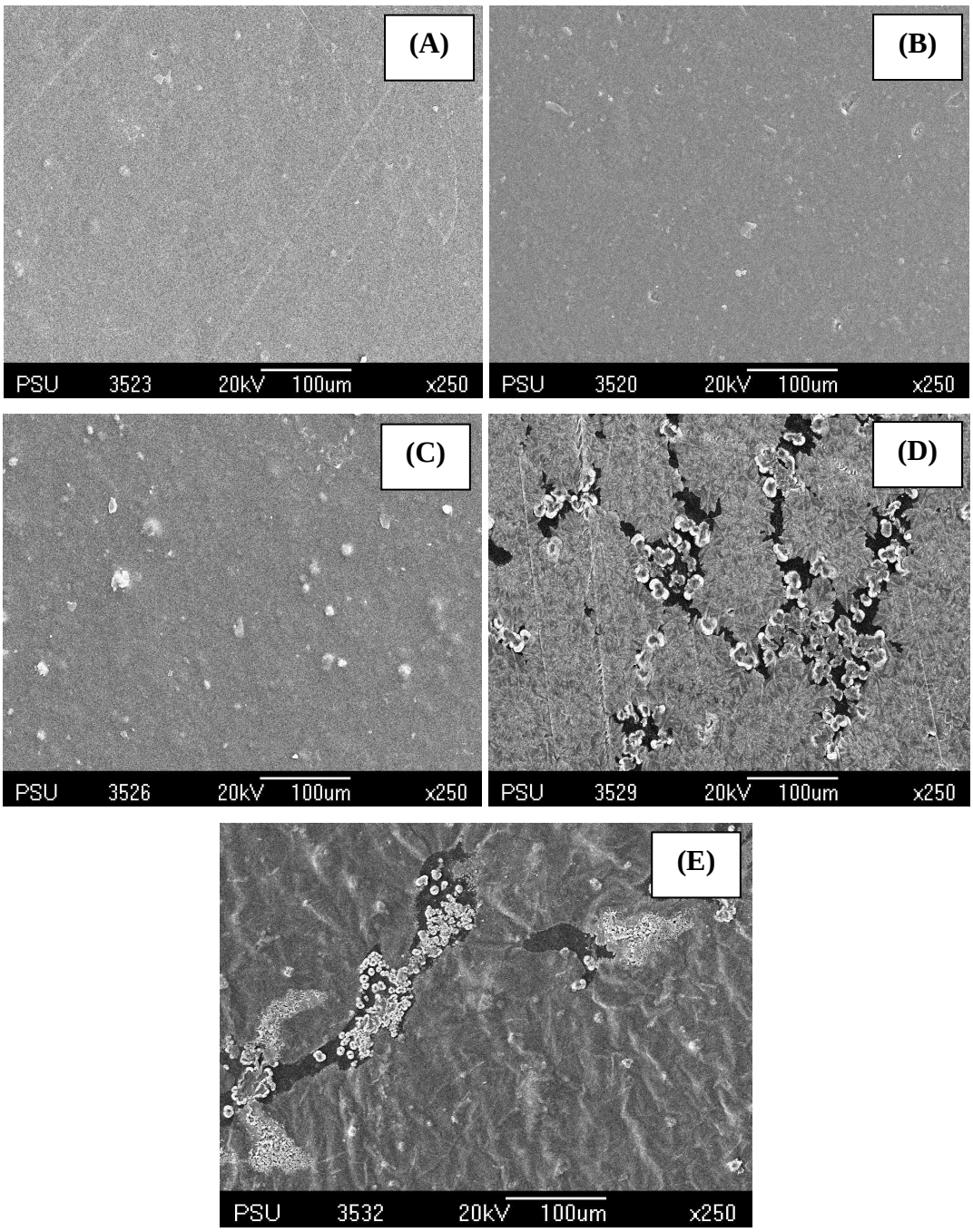

Figure 44. Scanning electron micrograph (SEM) (×250) of the RS films reinforced with (A) 0%, (B) 10%, (C) 20%, (D) 30% and (D) 40% of CC fillers.

6. Effect of moisture sorption on properties of rice starch film

Moisture sorption curves of RS films, RS films reinforced with 40% of PPF fillers, RS films reinforced with 40% of NaOH treated PPF, RS films reinforced with 30% of 40% Silane treated PPF and RS films reinforced with 20% crystalline cellulose (CC) were determined. Moisture adsorption was more rapid in the initial stages of moisture adsorption and a lesser amount of moisture was adsorbed as adsorption time increased. Then, the moisture content of RS films reached a plateau. Moisture equilibration time was mainly influenced by storage relative humidity. Films stored at higher relative humidity required more time to reach their equilibrium (data not presented). The sorption isotherm curves for equilibrium moisture content (EMC) (db) obtained from different type of fillers are shown in Figure 45. The moisture adsorption of RS films were significantly increased with increasing the relative humidity ($p<0.05$) and higher moisture adsorption rate was observed when higher relative humidity was used. Considering the type of fillers, the moisture absorption of the unfilled RS film was significantly the highest and the RS films reinforced with 20% CC was significantly the lowest at all relative humidities ($p<0.05$). By the reason of the hydrophobic crystalline of CC led to the reduction of permeability and adsorption the water (Ma *et al.,* 2008). Svagen *et al.* (2009) reported that, cellulose nanofibers are less hygroscopic than starch due to the higher degree of molecular order and the cellulose nanofiber network is reducing the swelling and thereby the moisture uptake. According to the RS films reinforced with both treated PPF, the results shows the moisture adsorption at EMC were significantly higher than the RS films reinforced with 40% PPF and 20% CC, resulted from both of surface treatments increased the site groups, which could interaction with the moisture, although almost of site groups were interaction with starch matrix. The result showed that moisture adsorption was related with the tensile strength of RS films. Figure 46 shows the tensile strength of biocomposite films at different relative humidities. The results demonstrated that the TS of the RS films and RS films reinforced with cellulose fillers were decreased as the relative humidity increased. The RS films were strongly sensitive to the moisture content. This phenomenon is ascribed to the starch being in the rubbery state at room temperature. The reinforcing effect of the cellulose

filler is therefore strongly diminished. Dufresne *et al.* (1999) reported that starch is more hydrophilic than cellulose, in moist conditions it absorbs most of the water. The cellulosic network is therefore surrounded by a soft phase. The interactions between the filler and the matrix are strongly reduced, and the TS remains practically constant, whatever the composition may be. However, 50% Relative humidity was the best relative humidity for the film condition.

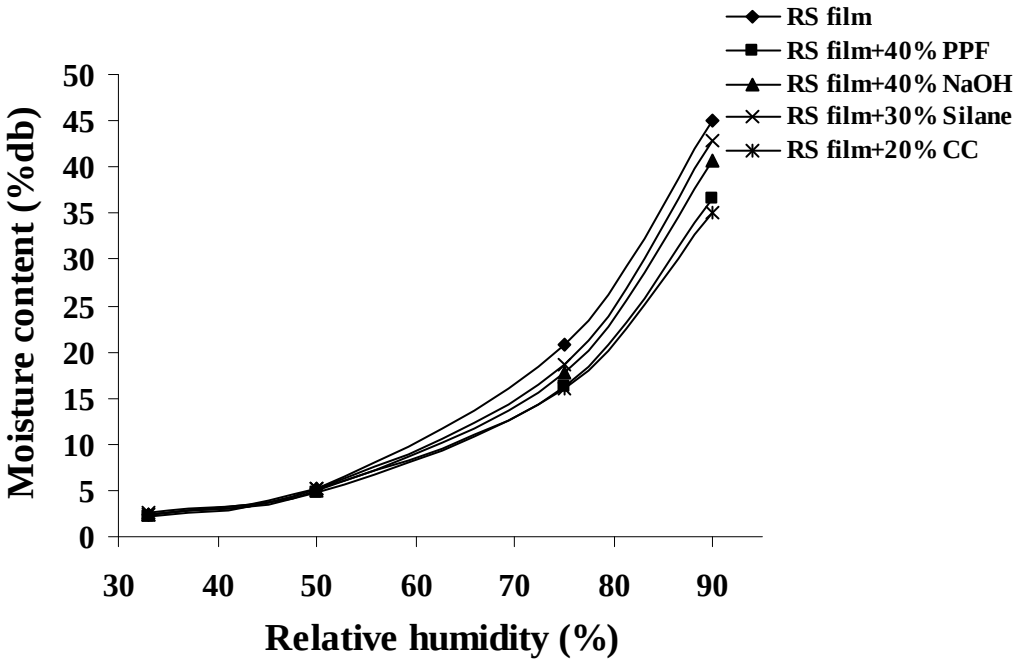

Figure 45. Moisture sorption isotherm curves of RS film and RS film reinforced with cellulose fillers at various relative humidities (27±2°C).

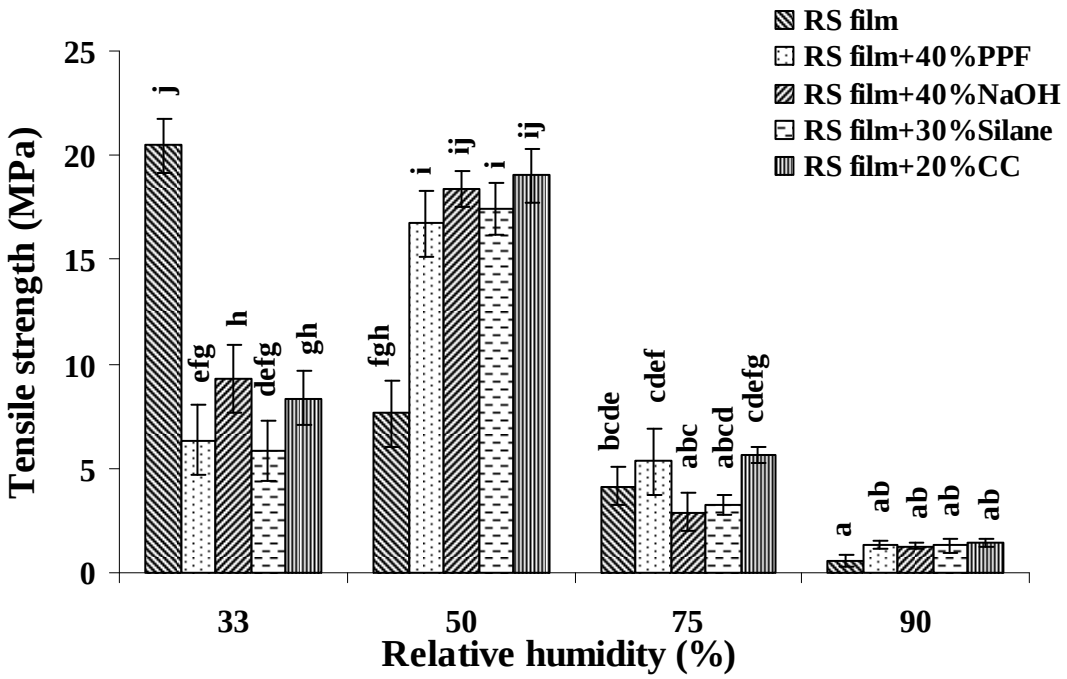

Figure 46. The tensile strength of the RS film and RS films reinforced with different fillers conditioned at different relative humidity. Mean values with different letter are significantly different ($p<0.05$).

CHAPTER 4

CONCLUSIONS

1. Palm pressed fibers were prepared by acid treatment and bleaching the produced pulp using the sodium chloride bleaching method. The proximate composition of unbleached PPF and bleached PPF were found to be 8.99, 45.97, 10.24, 3.50, 60.02 and 38.12% and 7.32, 55.61, 8.55, 2.93, 67.18 and 42.33% of moisture, cellulose, lignin, ash, acid detergent fiber and alpha cellulose, respectively

2. Palm Pressed Fiber (PPF) was used as a reinforced for RS film. The impact of PPF content was more significant, overall the RS films properties than size of PPF. The tensile strength, water vapor permeability, the water uptake and thermal properties of RS films increased with increasing PPF content; however elongation at break and transparency showed inversely. The improvement properties of the films can be attributed to the formation of rigid hydrogen bonded network of cellulose in the composite that is governed by percolation mechanism. The results demonstrated that addition of 420 μm of PPF showed better properties including mechanical, water barrier and thermal properties as well as physical properties than 250, 177 and 125 μm.

3. The tensile strength of RS film reinforced with alkaline treated PPF showed higher than RS film reinforced with silane treated PPF but lower in water vapor permeability, water uptake and thermal properties. Increasing concentration of silane and content of treated PPF resulted in increased tensile strength, water vapor permeability and thermal properties, but decreased elongation at break. The maximum improvement in the mechanical and thermal properties of RS films was obtained when 40% of glysidoxypropyltrimethoxy silane was applied.

4. A suspension of crystalline cellulose from palm pressed fiber (CC), having an average length about 90 ± 0.051 nm, and the crystallinity value was estimated as 94.60%. The tensile strength, thermal properties and crystallinity value (X_c) of the RS film reinforced with CC increased but decreased in elongation at the break, water vapor permeability and water uptake when increasing the CC content from 0-40 % CC. The morphology of the existence of CC in the rice starch film can

be easily observed in the composite films. When more than 20% of CC was used, the larger agglomerates was noticed, which indicates some porosity.

5. Moisture adsorption was more rapidly in the initial stages of moisture adsorption and a little of moisture was adsorbed when adsorption time increased. The moisture adsorption data of RS biocomposite films were increase with increasing the relative humidity and higher moisture adsorption rate was observed when higher relative humidity was used. Moreover, the tensile strength of RS biocomposite films was decrease at high relative humidity. The optimum relative humidity for conditioning the RS biocomposite films should be 50% RH.

Suggestions

For further study, the application in food products and production cost are needed to be determined before transfer this technology to selected industry.

REFFERENCES

Abdelmouleh, M., Boufi, S., Belgacem, M.N., Duarte, A.P., Salah, A.B. and Gandini, A. 2004. Modification of cellulosic fibers with functionalized silanes: development of surface properties. Int. J. Adhes. Adhes. 24: 43-54.

Agrawal, R., Saxena, N. S., Sharma, K. B., Thomas, S. and Sreekala, M. S. 2000. Activation energy and crystallization kinetics of untreated and treated oil palm fiber reinforced phenol formaldehyde composites. Mater. Sci. Eng. A. 277: 77-82.

Aklonis, J. J. and Macknight, W. J. 1983. Introduction to polymer viscoelasticity. John Wiley. London.

Alemdar, A. and Sain, M. 2007. Biocomposites from wheat straw nanofibers: Morphology, thermal and mechanical properties. Compos. Sci. Technol: In press.

Allen, L., Nelson, A. I., Steinberg, M. P. and McGill, J. N. 1963. Edible corn-carbohydrate food coatings. Food Technol. 17: 1437-1452.

Amash, A. and Zugenmaier, P. 2000. Morphology and properties of isotropic and oriented samples of cellulose fibres-polypropylene composites. Polymer. 41: 1589-1596.

Angles, M. N. and Dufresne, A. 2000. Plasticized/tunicin whiskers nanocomposites. 1. Structural analysis. Macromolecules. 33: 8344-8353.

Angles, M. N. and Dufresne, A. 2001. Plasticized/tunicin whiskers nanocomposites materials. 2. Mechanical behaviour. Macromolecules. 34: 2921-2931.

Arbelaiz, A., Fernandez, B., Valea, A. and Mondragon, I. 2006. Mechanical properties of short flax fiber bundle/poly (3-caprolactone) composites: Influence of matrix modification and fiber content. Carbohydr. Polym. 64: 224–232.

Arvanitoyannis, I., Psomiadou, E., Nakayama, A., Aiba, S. and Yamamoto, N. 1997. Edible films made from gelatin, soluble starch and polyols, part 3. Food Chem. 60: 593-604.

ASTM. 1993a. Standard practice for conditioning plastics and electrical insulating materials for testing: D618-61 (Reproved 1990). *In* ASTM. Annual book of American Standard Testing Methods. Vol. 8.01: P. 146-148. Philadelphia, PA.

ASTM. 1993b. Standard test method for water vapor transmission rate through plastic film and sheeting using a modulated infrared sensor: D1249-90. *In* ASTM. Annual book of American Standard Testing Methods. Vol. 15.09. P. 1168-1172. Philadelphia, PA.

ASTM. 1995. Standard test methods for tensile properties of thin plastics sheeting D882-91. *In* ASTM Annual Book of American Standard Testing Methods. Vol 8.01: P. 182-190. West Conshohochem, PA.

Averous, L. and Boquillon, N. 2004. Biocomposites based on plasticized starch: thermal and mechanical behaviors. Cabohydr. Polym. 56: 111-122.

Aziz, A. A., Das, K., Husin, M. and Mokhtar, A. 2002. Effects of physical and chemical pre-treatment on xylose and glucose production from oil palm press fibre. J. Oil Palm Res. 14: 10-17.

Balasubramanium, V. M., Chinnan, M. S., Mallikajunan, P. and Phillips, R. D. 1997. The effect of edible film on oil uptake and moisture retention of a deep-fried poultry product. J. Food Process. Eng. 20: 17-29.

Banker, G. S. 1966. Film coating theory and practice. J. Pharmacol. 55: 81-89.

Battista, O. A. 1975. Microcrystal polymer science. McGraw-Hill Book Company. New York.

Beakou, A., Ntenga, R., Lepetit, J., Ateba, J. A. and Ayina, L. O. 2008. Physico-chemical and microstructural characterization of “Rhectophyllum camerunense” plant fiber. Compos. Part A. 39: 67-74.

Bigg, D. M., Hiscock, D. F., Preston, J. R. and Bradbury, E. J. 1988. Thermoplastic matrix sheet composite. Polym. Compos. 9: 222-228.

Bisanda, E. T. N. and Anell, M. P. 1991. The effect of silane treatment on the mechanical and physical properties of sisal-epoxy composites. Compos. Sci. Technol. 41: 165-178.

Bismarck, A., Mishra, S. and Lampke, T. 2005. Natural fibres, biopolymers and biocomposites. CRC Press. New York.

Bledzki, A. K. and Gassan, J. 1999. Composites reinforced with cellulose based fibres. Prog. Polym. Sci. 24: 221-274.

Bourtoom T, and Chinnan, M. S. 2008. Preparation and properties of rice starch-chitosan blend biodegradable film. LWT. 41: 1633-1641.

Bushuk, W. and Wrigley, C. W. 1974. Protein: composition, structure and function. In G. E. Inglett (ed.), Wheat: Production and Utilization. p. 119-145. Westport, CT: Avi Publishing.

Cagri, A., Ustunol, Z. and Ryser, E. T. 2001. Antimicrobial, mechanical, and moisture barrier properties of low pH whey protein-based edible films containing p-Amminobenzoic or sorbic acid. J. Food Sci. 66: 865–870.

Curvelo, A. A. S., De Carvalho, A. J. F. and Agnelli, J. A. M. 2001. Thermoplastic starch-cellulosic fibers composites: Preliminary results. Carbohydr. Polym. 45: 183-188.

De Carvalho, A. J. F., Curvelo, A. A. S. and Agnelli, J. A. M. 2002. Wood pulp reinforced thermoplastic starch composites. Int. J. Polym. Mater. 51, 647-660.

Debeaufort, F., Martin-Polo, M. and Voilley, A. 1993. Polarity homogeneity and structure affect water vapor permeability of model edible films. J. Food Sci. 58: 426-434.

Demir, H., Atikler, U., Balkose, D. and Tihminlioglu, F. 2006. The effect of fiber surface treatments on the tensile and water sorption properties of polypropylene- luffa fiber composites. Compos. Part A. 37: 447-456.

Dong, S., Sapieha, S. and Schreiber, H. P. 1993. Mechanical properties of corona-modified cellulose/polyethylene composites. Polym. Eng. Sci. 33: 343–346.

Donhowe, I. G. and Fennema, O. R. 1993. The effects of plasticizers on crystallinity, permeability, and mechanical properties of methylcellulose films. J. Food Proc. Preserv. 17: 247-257.

Dufresne, A., Dupeyre, D. and Vignon, M. R. 2000. Cellulose microfibrils from potato tuber cells: processing and characterization of starch-cellulose microfibril composites. J. Appl. Polym. Sci. 76: 2080-2092.

Dufresne, A. and Vignon, M. R. 1998. Improvement of starch film performances using cellulose microfibrils. Macromolecules. 31: 2693-2696.

Eichhorn, S. J., Baillie, C. A., Zafeiropoulos, N., Mwaikambo, L. Y., Ansell, M. P. and Dufresne, A. 2001. Current international research into cellulosic fibres and composites. J. Mater. Sci. 36: 2107-2131.

Eklind, H., Maurer, F. H. J. and Steeman, P. A. M. 1997. Micromechanical and microdielectric transitions in P (S-g-EO) modified PPO/PMMA blends. Polymer. 38:1047-1055.

Espert, A., Vilaplana, F. and Karlsson, S. (2004). Comparison of water absorption in natural cellulosic fibres from wood and one-year crops in polypropylene composites and its influence on their mechanical properties. Compos. Part A. 35: 1267–1276.

Favier, V., Chanzy, H. and Cavialle, J. Y. 1996. Polymer nanocomposites reinforced by cellulose whiskers. Macromolecules. 28: 6365-6367.

Feuge, R. O., Vicknair, E. J. and Lovegren, N. V. 1953. Modification of vegetable oils. Some additional; properties of acetostearin products. JAOCS. 30 : 283.

Fishman, M. L., Coffin, D. R. and Konstance, R. P. 2000. Extrusioon of pectin/starch blends plasticizered with glycerol. Carbohydr. Polym. 41: 317-325.

Funke, U., Bergthaller, W. and Lindhauer, M. G. 1998. Processing and characterization of biodegradable products based on starch. Polym. Degrad. Stab. 59: 293-296.

Garcia, M. A., Martino, M. N. and Zaritzky, N. E. 1999. Edible starch films and coatings characterization: scanning electron microscopy, water vapor transmission and gas permeabilities. Scanning. 21: 348-353.

Gennadios, A., Brandenburg, A. H., Weller, C. L. and Testin, R. F. 1993. Effect of pH on properties of wheat gluten and soy protein isolate films. J. Agric. Food Chem. 41: 1835-1839.

Gennadios, A., McHugh, T. H., Weller, C. L. and Krochta, J. M. 1994. Edible coating and films based on protein. In Krochta, J. M., Balwin, E. A. and Niperos-Carriedo, M. O. (eds.). Edible Coatings and Films to Improve Food Quality. p. 201-277. Lancaster. Basel: Technomic Publishing.

Goda, K., Sreekala, M. S., Gomes, A., Kaji, T. and Ohgi, J. 2006. Improvement of plant based natural fibers for toughening green composites-Effect of load application during mercerization of ramie fibers. Compos. Part A. 37: 2213-2220.

Gontard, N., Guilbert, S. and Cuq, J. L. 1992. Edible wheat gluten film: influence of the main process variable on film properties using response surface methodology. J. Food Sci. 57: 190-195.

Greener, I. K. and Fennema, O. 1989a. Barrier properties and surface characteristics of edible bilayer films. J. Food Sci. 54: 1393-1399.

Greener, I. K. and Fennema, O. 1989b. Evaluation of edible, bilayer films for use as moisture barrier for food. J. Food Sci. 54: 1400-1406.

Guilbert, S. 1986. Technology and application of edible protective films. In Food packaging and preservation: Theory and practice. London. Elsevier Appl. Sci. Publis. Co.. p. 371-393.

Gurmit, S. 1994. Management and utilization of oil palm by-products. In Proceedings of the Third National Seminar on Utilization of Oil Palm Tree and Other Palms. 27-29 September 1994. Kuala Lumpur. P. 19-48.

Hagenmaier, R. D. and Shaw, P. E. 1990. Moisture permeability of edible films made with fatty acid and (hydroxypropyl) methylcellulose. J. of Food Agri. and Food Chem. 38: 1799-1803.

Han, J. H. and Floros, J. D. 1997. Casting antimicrobial packaging films and measuring their physical properties and antimicrobial activity. J. Plastic Film Sheet. 13: 287-298.

Hanlon, J. F. 1992. Films and foils. In Handbook of Package Engineering, 2nd ed. p. 1-59. Lancaster, PA: Tecnomic Publishing.

Hedenqvist, M. S., Backman, A., Gallstedt, M., Boyd, R. H. and Gedde, U. W. 2006. Morphology and diffusion properties of whey/montmorillonite nanocomposites. Compos. Sci. Technol. 66: 2350-2359.

Hernandez, E. 1994. Edible coating from lipids and resins. In Krochta, J. M. Balwin, E. A. and Niperos-Carriedo, M. O. (Eds.). Edible Coatings and Films to Improve Food Quality. p. 279-303. Lancaster. Basel: Technomic Publishing.

Herrera-Franco, P.J. and Valadez-Gonzalez, A. 2005. A study of the mechanical properties of short natural-fiber reinforced composites. Compos. Part B Eng. 36: 597-608.

Ishikawa, A., Okano, T. and Sujiyama, J. 1997. Fine structure and tensile properties of ramie fibers in the crystalline form of cellulose I, II, III. Polymer. 38: 463-468.

Iwatake, A., Nogi, M. and Yano, H. 2008. Cellulose nanofiber-reinforced polylactic acid. Compos. Sci. Technol. 68: 2103-2106.

Jackson, F. L. and Lutton, E. S. 1952. The polymorphism of 1-stearyl and 1-palmityldiacetin-dibutyrin,-dicaproin and 1-stearyldipropionin. J. Am. Chem. Soc. 74: 4827-4831.

Jayaraman, K. 2003. Manufacturing sisal-polypropylene composites with minimum fibre degradation. Compos. Sci. Technol. 63: 367-374.

Jokay, L., Nelso, G. E. and Powell, E. L. 1967. Development of edible amylaceous coatings for foods. Food Technol. 21: 1064.

John, M. J. and Thomas, S. 2008. Biofibres and biocomposites. Carbohydr Polym. 71: 343-364.

Joseph, K., De Carvalho, L. H. 2000. Jute/cotton woven fabric reinforced polyester composites: effect of hybridization. Embrapa Agricultural Instrumentation. Brasil.

Kamper, S. L. and Fennema, O. N. 1985. Use of an edible film to maintain water vapor gradients in food. J. Food Sci. 50: 382-384.

Kester, J. J. and Fennema, O. R. 1986. Edible films and coatings: a review. Food Technol. 40: 47-59.

Koelsch, C. M. and Labuza, I. P. 1992. Functional, physical and morphological properties of methyl cellulose and fatty acid-based edible film barriers. LWT. 25: 404-411.

Koksel, H., Sahbaz, F. and Ozboy, O. 1993. Influence of wheat-drying temperatures on the birefringence and X-ray diffraction patterns of wet-harvested wheat starch. Cereal Chem. 70: 481-483.

Kristo, E. and Biliaderis, C. G. 2007. Physical properties of starch nanocrystal-reinforced pullulan films. Carbohydr. Polym. 68: 146-148.

Krochta, J. M. and Mulder-Johnston, J. 1997. Edible and biodegradable polymer films: challenges and opportunities. Food Technol. 51: 61-74.

Krumel, K. L. and Lindsay, T. A. 1976. Nonionic cellulose ethers. Food Technol. 30: 36-43.

Kunanopparat, T., Menut, P., Morel, M. H. and Guilbert, S. 2008. Reinforcement of plasticized wheat gluten with natural fibers: From mechanical improvement to deplasticizing effect. Compos. Part A. 39: 777-785

Kvien, I. and Oksman, K. 2007. Orientation of cellulose nanowhiskers in polyvinyl alcohol. Appl. Phys. A: Mater. Sci. Process. 87: 641-643.

Lawton, J. W. 1996. Effect of starch type on the properties of starch containing films. Carbohydr. Polym. 29: 203-208.

Lee, S-H. and Wang, S. 2006. Biodegradable polymers/bamboo fiber biocomposite with bio-based coupling agent. Compos. Part A. 37: 80-91.

Lourdin, D., Vaiie, G. and Colonna, P. 1995. Della influence of amylase content on starch films and foams. Carbohydr. Polym. 27: 275-280.

Low, I. M., McGrath, M., Lawrence, D., Schmidt, P., Lane, J., Latella, B. A. and Sim, K. S. 2007. Mechanical and fracture properties of cellulose-fiber-reinforced epoxy laminates. Compos. Part A. 38: 963-974.

Lu, Y., Weng, L. and Cao, X. 2005. Biocomposites from plastizied starch and cellulose crystallites from cottonseed Linter. Macromolecular Biosci. 68: 251-260.

Lu, Y., Weng, L. and Cao, X. 2006. Morphological,thermal and mechanical properties of ramie crystallites reinforced plasticized strach biocomposites. Carbohydr. Polym. 63: 1-7.

Ma, X., Chang, P. R. and Yu, J. 2008. Properties of biodegradable thermoplastic pea starch/carboxymethyl cellulose and pea starch/microcrystalline cellulose composites. Carbohydr. Polym. 72: 369-375.

Ma, X., Yu J., and Kennedy, J. 2005. Studies on the properties of natural fibers-reinforced thermoplastic starch composites. Carbohydr. Polym. 62: 19-24.

Mali, S. and Grossmann, M. V. E. 2003. Effects of yam starch films on storability and quality of fresh strawberries. J. Agric. Food Chem. 7005-7011.

Mark, A. M., Roth, W. B., Mehltretter, C. L. and Rist, C. E. 1966. Oxygen permeability of amylomaize starch films. Food Technol. 20: 75-78.

Matuana, L. M., Balatinecz, J. J., Park, C. B. and Sodhi, R. N. S. 1999. X-ray photoelectron spectroscopy study of silane-treated newsprint-fibers. Wood Sci. Technol. 33: 259-270.

McHugh, T. H., Aujard, J. F. and Krochta, J. M. 1994. Plasticized whey protein edible films: water vapor permeabilities. J. Food Sci. 59: 416-420.

McHugh, T. H. and Krochta, J. M. 1994. Water vapor permeability properties of edible whey protein-lipid emulsion films. J.Amer. Oil Chem. Soc. 71: 307-312.

Michell, A. J. 1989. Wood cellulose-organic polymer composites. Compos. Asia Pac. 89: 23-34.

Milewski, J. V. 1992. Whiskers and short fiber technology. Polym. Compos. 13: 223-236.

Mohanty, A. K., Drzal, L. T. and Misra, M. 2002. Engineered natural fiber reinforced polypropylene composites: Influence of surface modifications and novel powder impregnation processing. J. Adhes. Sci. Technol. 16: 999-1015.

Mohanty, A. K., Misra, M. and Drzal, L. T. 2001. Surface modifications of natural fibers and performance of the resulting biocomposites: an overview. Comp. Interfaces. 8: 313-343.

Mohanty, A. K., Misra, M. and Hinrichsen, G. 2000. Biofibres, biodegradable polymers and biocomposites: An overview. Macromol. Mater. Eng. 276: 1-24.

Morrison, R. T. and Boyd, R. N. 1959. Organic Chemistry. Allyn and Bacon: Boston.

Muller, C. M. O., Laurindo, J. B. and Yamashita, F. 2009. Effect of cellulose fibers on the crystallinity and mechanical properties of starch based films at different relative humidity values. Carbohydr. Polym: In press.

Murphy, P. 1999. Handbook of hydrocolloids. 2nd Ed. Woodhead Publishing Ltd. Cambride. UK.

Murray, D. G., Luft, L. and Low, D. E. 1973. Corn starch hydrolysates. Food Technol. 27: 32-39.

Myers, A.W., Meyer, J.A., Roger, C.E., Stannett, V. and Szwarc, M. 1962. The permeation if water vapor. In M. Kouris (Eds). Permeability of plastic Films and Coated Paper to Gases and Vapors, pp 62-77. Technical Pulp and Paper Industry. New York.

Nelson, K. L. and Fennema, O. R. 1991. Methylcellulose films to prevent lipid migration in confectionery products. J. Food Sci. 56: 504-509.

Nevell, T. P. and Zeronian, S. H. 1985. Cellulose chemistry and its applications. Wiley. New York.

Noishiki, Y., Nishiyama, Y., Wada, M., Kuga, S. and Magoshi, J. 2002. Mechanical properties of silk fibroin-microcrystalline cellulose composite films. J. Appl. Polym. Sci. 86: 3425-3429.

Ohkita, T. and Lee, S-H. 2006. Thermal degradation and biodegradability of poly(lactic acid)/corn starch biocomposites. J. Appl. Polym. Sci. 100: 3009-3017.

Olesen, P. O. and Plackett, D. V. 1999. Perspectives on the performance of natural plant fibres presented at natural fibres performance forum (Online). Available. http://www.ienica.net/fibreseminar/olesen.pdf/ (22 December 2008)

Panthalakkal, S. and Sain, M. 2007. Injection-molded short hemp fiber/glass fiber-reinforced polypropylene hybrid composites-Mechanical, water absorption and thermal properties. J. Appl. Polym. Sci. 103: 2432-2441.

Park, H. M., Li, X., Jin, C. Z., Park, C. Y., Cho, W. J. and Ha, C. S. 2002. Preparation and properties of biodegradable thermoplastic starch/clay hybrids. Macromol. Mater. Eng. 287: 553-558.

Park, J. M., Quang, S. T., Hwang, B. S. and Devries, K. L. 2006. Interfacial evaluation of modified Jute and Hemp fibers/polypropylene (PP)-maleic anhydride polypropylene copolymers (PP-MAPP) composites using micromechanical technique and nondestructive acoustic emission. Compos. Sci. Technol. 66: 2686-2699.

Park, J. W., Testin, R. F., Vergano, P. J., Park, H. J. and Weller, C. L. 1994. Fatty acid concentration effect on tensile strength, elongation and water vapor permeability of laminated edible films. J. Food. Sci. 59: 916-919.

Pickering, K. L., Abdalla, A., Ji, C., McDonald, A. G. and Franich, R. A. 2003. The effect of silane coupling agents on radiate pine fibre for use in thermoplastic matrix composites. Compos. Part A. 34: 915-926.

Plackett, D., Andersen, T. L., Pedersen, W. B. and Nielsen, L. 2003. Biodegradable composites based on L-polylactide and jute fibres. Compos. Sci. Technol. 63: 1287-1296.

Pothan, L.A. and Thomas, S. 2003. Polarity parameters and dynamic mechanical behaviour of chemically modified banana fiber reinforced polyester composites. Compos. Sci. Technol. 63: 1231-1240.

Pu, Y., Zhang, J., Elder,T., Deng, Y., Gatenholm, P. and Ragauskas, A. J. 2006. Investigation into nanocellulosics versus acacia reinforced acrylic films. Compos. Part B Eng: In press.

Rankin, J. C., Wolf, I. A., Davis, H. A. and Rist, C. E. 1958. Permeability of amylose film to moisture vapor, selected organic vapors, and common gases. Ind. Eng. Chem. 3: 120-124.

Ray, D., Sarkar, B. K., Rana, A. K. and Bose, N. R. 2001. The mechanical properties of vinylester resin matrix composite reinforced with alkali treated jute fibers. Compos. Part A. 32: 119-127.

Roth, W. B. and Mehltretter, C. L. 1967. Some properties of hydroxypropylated amylomaize starch films. Food Technol. 21: 72-74.

Rozman, H. D., Kumar, R. N., Abdul Khalil, H. P. S., Abusamah, A., Lim, P. P. and Ismail, H. 1996. Preparation and properties of oil palm frond composite based on methacrylic silane and glycidyl methacrylate. J. Eur. Polym. 33: 225-230.

Rodriguez, M., Oses, J., Ziani, K. and Mate, J. I. 2006. Combined effect of plasticizers and surfactants on the physical properties of starch based edible films. Food Res. Int. 39: 840-846.

Ruseckaite, R. A. and Jimenez, A. 2003. Thermal degradation of mixtures of polycaprolactone with cellulose derivates. Polym. Degrad. Stab. 81: 353–358.

Salame, M. 1986. Barrier polymers. In M. Bakker (ed.), The Wiley Encyclopedia of Packaging Technology. p. 48-54. New York.

Sangthong, S., Pongprayoon, T. and Yanumet, N. 2008. Mechanical property improvement of unsaturated polyester composite reinforced with admicellar-treated sisal fibers. Compos. Part A: In press.

Santayanon, R. and Wootthikanokkhan, J. 2003. Modification of cassava starch by using propionic anhydride and properties of the starch-based composite foams. Carbohydr. Polym. 51: 17-24.

Satyanarayana, K. G., Gregorio, G. C. Arizaga, F. W. 2008. Biodegradable composites based on lignocellulosic fibers -an overview. Prog. Polym. Sci.: In press.

Satyanarayana, K. G., Guimaraes, J. L. and Wypych, F. 2007. Studies on lignocellulosic fibers of Brazil: Part I- Source, production, morphology, properties and application. Compos. Part A. 38: 1694-1709.

Satyanarayana, K. G. Ravikumar, K. K., Sukumaran, K., Mukherjee, P. S., Pillai, S. G. K. and Kulkarni, A.K. 1986. Structure and properties of some vegetable fibres. Part 3. Talipot and palmyrah fibres. J. Mater. Sci. 21: 57-61.

Shih, Y. F. 2006. Mechanical and thermal properties of waste water bamboo husk fiber reinforced epoxy composites. Mater. Sci. Eng. A: In press.

Soykeabkaew, N., Supaphol, P. and Rujiravanit, R. 2004. Preparation and characterization of jute-and flax-reinforced starch-based composite foams. Carbohydr. Polym. 58: 53-63.

Sreekala, M. S. and Thomas, S. 2003. Effect of fiber surface modification on water-sorption characteristics of oil palm fibres. Compos. Sci. Technol. 63: 861-869.

Sreekumar, P. A., Joseph, K., Unnikrishnan, G. and Thomas S. 2007. A comparative study on mechanical property of sisal leaf fibre reinforced polyester composites prepared by resin transfer and compression moulding techniques. Compos. Sci. Technol. 67(3-4): 453-461.

Srinivasa, P. C., Ramesh, M. N. and Tharanathan, R. N. 2007. Effect of plasticizers and fatty acids on mechanical and permeability characteristics of chitosan films. Food Hydrocolloids. 21: 1113-1122.

Suryanegara, L., Nakagaito, A. N. and Yano, H. 2009. The effect of crystallization of PLA on the thermal and mechanical properties of microfibrillated cellulose-reinforced PLA composites. Compos. Sci. Technol: In press.

Svagen, A. J., Hedenqvist, M. S. and Berglund, L. 2009. Reduced water vapour sorption in cellulose nanocomposites with starch matrix. Compos. Sci. Technol. 69: 500-506.

Wolf, I. A., Davis, H. A., Cluskey, J. E., Gundrum, L. J. and Rist, C. E. 1951. Preparation of films from amylose. Ind. Eng. Chem. 43: 915-920.

Wollerdorfer, M. and Bader, H. 1998. Influence of natural fibers on the mechanical properties of biodegradable polymers. J. Industr. Crops Prod. 8: 105-112.

Wu, Y., Weller, C. L., Hamouz, F., Cuppett, S. and Schnepf, M. 2001. Moisture loss and lipid oxidation for precooked ground-beef patties packaged in edible starch-alginate-based composite films. J. Food Sci. 66: 486–493.

Xiaodong, C., Hua, D. and Chang, M. L. 2007. New nanocoposite materials reinforced with flax cellulose nanocrystals in waterborne polyurethane. Biomacromolecules. 8: 899-904.

Xu, X. Y., Kim, K. M., Hanna, M. A. and Nag, D. 2005. Chitosan-starch composite film: preparation and characterization. J. Industr. Crops Prod. 21: 185-192.

Xue, L., Borodin, O. and Smith, G. D. 2006. Modelling of enhanced penetrant diffusion in nanoparticle-polymer composite membranes. J. membr. Sci. 286: 293-300.

Yam, K. L., Gogoi, B. K., Lai, C. C. and Selke, S. E. 1990. Composites from compounding wood fibers with recycled high density polyethylene. Polym. Eng. Sci. 30: 693-699.

APPENDIX

ANALYTICAL METHODS

1. Moisture content (AOAC, 1999)

Method

1. Dry the empty dish and lid in the oven at 105°C for 30 min and transfer to desiccator to cool (30 min). Weigh the empty dish and lid.
2. Weigh about 5 g of sample to the dish. Spread the sample with spatula.
3. Place the dish with sample in the oven. Dry for 16 h or overnight at 105°C.
4. After drying, transfer the dish with partially covered lid to the desiccator to cool. Reweigh the dish and its dried content.

Calculation

$$\% \text{ Moisture} = \frac{(W_1 - W_2)}{W_1} \times 100$$

Where W_1 = weight (g) of sample before drying

W_2 = weight (g) of sample after drying

2. Fat (AOAC, 1999)

Reagent

- Petroleum ether

Method

1. Place the bottle and lid in the incubator at 105°C overnight to ensure that weight of bottle is stable.
2. Weigh about 3-5 g of sample to paper filter and wrap.
3. Take the sample into extraction thimble and transfer into soxhlet.
4. Fill petroleum ether about 250 ml into the bottle and take it on the heating mantle.
5. Connect the soxhlet apparatus and turn on the water to cool them and then switch on the heating mantle.
6. Heat the sample about 14 h (heat rate of 150 drop/min).
7. Evaporate the solvent by using the vacuum condenser.
8. Incubate the bottle at 80-90°C until solvent is completely evaporate and bottle is completely dry.
9. After drying, transfer the bottle with partially covered lid to the desiccator to cool. Reweigh the bottle and its dried content.

Calculation

$$\% \text{ Fat content} = \frac{\text{Weight of fat}}{\text{Weight of sample}} \times 100$$

3. Ash (AOAC, 1999)

Method

1. The crucible and lid is firstly placed in the furnace at 550°C overnight to ensure that impurities on the surface of crucible is burned off. The crucible is then cool in the desiccator (30 min).
2. Weigh the crucible and lid to 3 decimal places.
3. Weigh about 5 g sample into the crucible. Heat over low Bunsen flame with lid haft covered. When fumes are no longer produced, place crucible and lid in furnace.
4. Heat at 550°C overnight. During heating, do not cover the lid. Place the lid after complete heating to prevent loss of fluffy ash. Cool down in the desiccator.
5. Weigh the ash with crucible and lid when the sample turns to gray. If not, return the crucible and lid to the furnace for the further ashing.

Calculation

$$\% \text{ Ash content} = \frac{\text{Weight of ash}}{\text{Weight of sample}} \times 100$$

4. Protein (AOAC, 1999)

Reagents

- Kjedahl catalyst: Mix 9 part of potassium sulphate (K_2SO_4) anhydrous, nitrogen free with 1 part of copper sulphate ($CuSO_4$)
- Sulfuric acid (H_2SO_4)
- 40% NaOH solution (w/v)
- 0.2 N HCl solution
- 4% H_3BO_3
- Indicator solution: Mix 100 ml of 0.1% methyl red (in 95% ethanol) with 200 ml of 0.2% bromocresol green (in 95% ethanol)

Method

1. Place sample (0.5-1.0 g) in digestion flask.
2. Add 5 g Kjeldahl catalyst, and 200 ml of conc. H_2SO_4.
3. Prepare a tube containing the above chemical except sample as blank. Place flasks in inclined position and heat gently unit frothing ceases. Boil briskly until solution clears.
4. Cool and add 60 ml distilled water cautiously.
5. Immediately connect flask to digestion bulb on condenser, and with tip of condenser immersed in standard acid and 5-7 indicator in receiver. Rotate flask to mix content thoroughly; then heat until all NH_3 is distilled.
6. Remove receiver, wash tip of condenser, and titrate excess standard acid distilled with standard NaOH solution.

Calculation

$$\% \text{ Protein} = \frac{(A-B) \times N \times 1.4007 \times 5.95}{W}$$

Where:

A = volume (ml) of 0.2 N HCl used sample titration

B = volume (ml) of 0.2 N HCl used in blank titration

N = Normality of HCl

W = weight (g) of sample

14.007 = atomic weight of nitrogen

5.95 = the protein-nitrogen conversion factor for starch and its by-products

5. Cellulose and lignin (AOAC, 1999)

Reagents

- Acetone
- 72% H_2SO_4 solution
- Decahydronapthalene
- Acid detergent solution: Add 20 g of CTAB (Cetyl Trimethyl Ammonium Bromide) to 1 L 1.0 N H_2SO_4

Method

1. Weigh 1 g sample (S) ground to pass 1 mm screen, into beaker (600 ml). Add 100 ml acid detergent solution.
2. Heat to boiling in 5-10 min, reduce heat to avoid foaming as boiling begins. Reflux 60 min from onset of boiling, adjusting boiling to slow, even level.
3. Remove container, swirl, and filter thru weighed (W_1) fritted glass crucible, using min suction. Break up filtered mat with rod and fill crucible 2/3 full with hot (90-100°C) water. Stir and let soak 15-30 sec. Dry with vacuum and repeat water washing, rising sides of crucible. Wash twice similarly with acetone and remove residual acetone with vacuum.
4. Dry 3 h or overnight in 100°C oven and weigh (W_2).
5. Cover contents of crucible with cooled (15°C) 72% H_2SO_4 and stir with glass rod to smooth paste. Fill crucible about half-way with acid and stir, refill with 72% H_2SO_4 and stir hourly as acid drains.
6. After 3 h, filter as completely as possible with vacuum, and wash with hot water until acid-free to pH paper.
7. Dry crucible in 100°C oven, cool in desiccator and weigh (W_3).
8. Ignite crucible in 500°C furnace 2 h or until C-free. Transfer to desiccator, cool, and weigh (W_4).

Calculation

$$ADF = \frac{(W_2-W_1) \times 100}{S}$$

$$L = \frac{(W_3-W_4) \times 100}{S}$$

$$C = ADF - L$$

Where:

ADF = Acid detergent content (%)

L = Lignin content (%)

C = Cellulose content (%)

W_1 = weight (g) of crucible

W_2 = weight (g) of crucible and sample after passed acid detergent

W_3 = weight (g) of crucible and sample after passed 72% H2SO4

W_4 = weight (g) of crucible and sample after ignited

S = weight (g) of sample

VITAE

Name Miss Phattaraporn Thongsane

Student ID 5011020022

Educational Attainment

Degree	Name of Institution	Year of Graduation
Bachelor of Science (Material Product Technology)	Prince of Songkla University	2006

List of Publication and Proceedings

Thongsane, P. and Bourtoom, T. 2007. Nanocomposites of rice starch film reinforced with nanocrystalline cellulose from palm pressed fiber. In Proceedings of The 10th Asean Food Conference 2007: Food for Mankind-Contribution of Science and Technology. Kuala Lumpur, Malaysia. 21-23 August 2007. P. 239-242.

Thongsane, P., Sridach, W. and Bourtoom. T. 2009. Processing and characterization of edible rice starch films reinforced with palm pressed fibers. In Proceedings of The 10th Annual Conference of Thai Society of Agricultural Engineering. Suranaree University of Technology, Thailand. 1-3 April 2009. P. 247-250.